C_1-C_4 Hydrocarbon Oxidation Mechanism

DISSERTATION

submitted to the

Faculty of Chemistry

of the Rupertus Carola University of Heidelberg, Germany

for the degree of

Doctor of Natural Sciences

presented by

Crina I. Heghes, Chem. Eng.

born in Sebeş, Romania

Supervisor: Prof.Dr.Dr.h.c. Jürgen Warnatz

Heidelberg, September 2006

Interdisziplinäres Zentrum für Wissenschaftliches Rechnen
Ruprecht-Karls-Universität Heidelberg
2006

C_1-C_4 Hydrocarbon Oxidation Mechanism

Crina I. Heghes

Heidelberg, September 2006

Abstract

Detailed mechanisms with hundreds of elementary reactions and species are now available for the combustion of alkanes as a result of the consistent pursuit of mechanism development over several decades. The chemical reaction scheme presented in this work was developed on the basis of a previously available one, V. Karbach (2006), and includes the oxidation reactions of high-temperature combustion of H_2, CO, CH_4, C_2H_6, C_3H_8 and C_4H_{10}. The mechanism consists of 412 elementary reactions and 61 species and is based on a rate-data compilation by Baulch et al. (2005). It is documented by Hegheş et al. (2005) and Warnatz and Hegheş (2006). The approximate temperature range is from 900 K to 2500 K. To test the validity of the mechanism, for each fuel considered, premixed laminar flame velocities and ignition delay times have been calculated. The results were compared to experiments for the largest possible conditions range (initial temperature, pressure, equivalence ratio).

The flame velocity is a function of fuel concentration, temperature and pressure of the unburnt mixture. The flame calculations are performed using the Mixfla code (J. Warnatz, Ber. Bunsenges. Phys. Chem. **82**, 1978). The flame modelling was used for two purposes: to test the validity of experimental methods and to calculate flame velocities for comparison to experimental results.

The ignition delay time is a characteristic quantity of the fuel and also depends on initial temperature, pressure and mixture composition. Homogenous simulations were performed using the code Homrea (U.Mass, Dissertation, University Heidelberg, 1988). Calculation of the dependence of the ignition delay time on temperature and reactant composition provides a powerful tool for modelling and understanding the combustion mechanism of a given fuel, in special at lower temperatures.

It is known that the rates of elementary reactions in combustion processes differ greatly. For sensitive reactions, values for the rate coefficients have to be well-known. Sensitivity analysis has been performed in order to identify the rate-limiting reactions and to understand the behavior of the chemical system under different conditions. Furthermore, reaction flow analysis has been conducted to elucidate the important chemical pathways over a wide range of conditions.

To demonstrate the capabilities of the mechanism proposed in this work, a comparison between experimental data and simulations of flame velocities and ignition delay times is presented.

In summary, a detailed kinetic mechanism has been developed to simulate the oxidation of hydrocarbons up to C_4 species under high-temperature conditions. The calculated ignition delay times and flame velocities are in a good agreement with experimental data for all hydrocarbon fuels studied in this work, except for the ignition delay time in case of acetylene, where our calculations show shorter ignition delay time at comparable conditions.

Kurzfassung

Heutzutage stehen für die Verbrennung von Alkanen detaillierte Mechanismen mit Hunderten von Elementarreaktionen und Spezies zur Verfügung – als Ergebnis zahlreicher zielstrebiger Forschungsarbeiten zur Mechanismus Entwicklung in den vergangenen Jahrzehnten. Das in der vorliegenden Arbeit vorgestellte chemische Reaktionsschema ist ausgehend von einem bereits vorhandenen, V. Karbach (2006), entwickelt worden und beinhaltet die Oxidationsreaktionen der Hochtemperaturverbrennung von H_2, CO, CH_4, C_2H_6, C_3H_8 und C_4H_{10}. Der Mechanismus besteht aus 412 Elementarreaktionen und 61 Spezies und beruht auf einer Kompilierung der Daten für die Geschwindigkeitskoeffizienten nach Baulch *et al.* (2005). Er ist dokumentiert von Heghes *et al.* (2005) und Warnatz und Heghes (2005). Der angenäherte Temperaturbereich erstreckt sich von 900 K bis 2500 K. Zur Validierung des Mechanismus sind die entsprechenden vorgemischten laminaren Flammengeschwindigkeiten und Zündverzugszeiten berechnet worden. Die Ergebnisse sind mit Experimenten unter ähnlichen Bedingungen (Anfangstemperatur, Druck, Äquivalenzverhältnis) verglichen worden.

Die Flammengeschwindigkeit hängt von Brennstoffkonzentration, Temperatur und Druck der unverbrannten Mischung ab. Die Flammenberechnungen erfolgten unter Verwendung des Mixfla-Codes (J. Warnatz, Ber. Bunsenges. Phys. Chem. **82**, 1978). Das Flammenmodellieren hatte zwei Zwecke: das Testen der Gültigkeit experimenteller Methoden und die Berechnung der Flammengeschwindigkeiten für den Vergleich mit experimentellen Ergebnissen.

Die Zündverzugszeit ist ein Brennstoffcharakteristikum und hängt ebenfalls von Anfangstemperatur, Druck und Mischungszusammensetzung ab. Homogene Simulationen sind unter Verwendung des HOMREA-Codes (U. Mass, Dissertation, Universität Heidelberg, 1988) durchgeführt worden. Die Berechnung der Abhängigkeit der Zündverzugszeit von Temperatur und Zusammensetzung des Reaktanden ist wichtig für das Modellieren und für das Verständnis des entsprechenden Verbrennungsmechanismus.

Die Geschwindigkeiten der Elementarreaktionen in Verbrennungsprozessen schwanken bekanntermaßen sehr stark. Für sensitive Reaktionen müssen die Werte der Geschwindigkeitskoeffizienten bekannt sein. Die durchgeführten Sensitivitätsanalysen dient zur Identifizierung der geschwindigkeitsbestimmenden Reaktionen und dem Verständnis des Verhaltens des chemischen Systems unter verschiedenen Bedingungen. Ferner sind zur Aufklärung der wichtigen chemischen Pfade für zahlreiche Bedingungen Reaktionsflussanalysen vorgenommen worden.

Um das Potential des in dieser Arbeit vorgeschlagenen Mechanismus zu veranschaulichen, wird ein Vergleich zwischen experimentellen Daten und Simulationen der Flammengeschwindigkeiten und der Zündverzugszeiten vorgestellt.

Insgesamt ist für die Simulation der Oxidation von Kohlenwasserstoffen bis zu C_4 im Hochtemperaturbereich ein detaillierter kinetischer Mechanismus entwickelt worden. Die berechneten Zündverzugszeiten und Flammengeschwindigkeiten stimmen für alle untersuchten Brennstoffe sehr gut mit experimentellen Werten überein.

Acknowledgements

Like any other Dissertation, the one presented here also has only one author but could not have been produced without the help and support of many other people: staff and colleagues at IWR and the REAFLOW research group and also friends and family. I would like to thank Prof. J. Warnatz for his contribution as supervisor. The work reported here owes much to him, as does my development in what when I started was an entirely new field for me. Similar words could be used to refer to Prof. Uwe Riedel, for whose help and advice I am very grateful. Support from the IWR staff (Ingrid Hellwig, Juergen Moldenhauer, Joachim Simon) is also gratefully acknowledged. My IWR junior colleagues have also been instrumental in bringing my thesis to completion. They taught me many things and helped me solve problems and correct mistakes, while at the same time being true friends without whom I would have found the experience of working in a foreign country so much more difficult. Ravi , Volker, Raul, Lavinia, Jens, Iliyana, Steffen, Stefan, Berthold, Georgiana, Andreas: thank you ever so much. Needless to say, help of nontechnical/nonscientific kind was needed at various points. For that I thank the people above, but also some very special friends who were there when I needed encouragement, someone to talk to or simply someone to share some laughs with. Margot, Dana, Maria, Sidonia, Andreea and Bogdan may not realise it, but this Dissertation also owes much to them. I would like also to thank those who were with me even when living in different countries : my family in Romania , Italy and the UK . Thanks to my mother Nina and sister Anamaria for their confidence, understanding and encouragement. A good part of my thesis was written while travelling between Heidelberg and Leeds to meet somebody that means a lot for me. The love, support, sense of humour and the optimism of Marcelo gave me energy to keep on going ahead and made my life enjoyable and worthwhile. At the end I would like to attribute this thesis in the memory of my father, who unfortunately can not share with me this important moment of my life.

Crina Heghes

Heidelberg, September 2006

Contents

1 Introduction

The discovery of fire heralded the beginning of a new age. The ability of employing fire was considered by many historians as the first human success and a step towards more advanced technology. While computers and electronics have revolutionized the way we live and access information, we still generate our electricity, heat our homes and power our vehicles using the same power source: fire. Knowledge of combustion phenomena is of great scientific interest due to its presence in a wide range of industrial processes and equipment. It is known that about 80% of the worldwide energy support is provided by combustion of liquids (such as gasoline and hydrocarbon fuels), solids (such as coal and wood) and gases (such as natural gas composed of methane and small amounts of other hydrocarbons such as ethane, propane and butane). The other 20% are accounted from other energy sources such as nuclear or renewable energy.

In the last two decades, the importance of the reduction of pollutant emissions has increased considerably due to both environmental consciousness and to governmental policies, being one of the most important aspects to assure the competitiveness of combustion-related industries. Pollutant emissions can be reduced by improving the efficiency of combustion processes, thereby increasing fuel economy.

Modern combustion systems are designed with the following goals: high combustion efficiency, high reliability, and minimum emission of the air pollutants. Numerical prediction is a feasible and economic way to establish the criteria for designing the combustors under these detriments. Application of numerical simulation in industry has grown rapidly during the last decades. It complements the theoretical investigations where nonlinearity, high number of degrees of freedom, or lack of symmetry are of importance, and complement experiment where devices are expensive, data is inaccessible, or the phenomen very complex. For the study of combustion, numerical simulations improve our understanding of flame structure and dynamics. They are widely used in the design and optimization of practical combustion systems because, compared to experimental testing and prototyping, the development costs of numerical simulation are very low. Today, no real progress in design or optimization can be made without numerical simulations.

1.1 Importance of combustion in various applications

Various applications of combustion in our lives show that this research field remains timely and useful.

Combustion plays an important role in the following areas [1]:

1. Power generation (e.g., coal particles are burned in the furnaces of power stations to produce steam for driving turbines in order to generate electricity), transportation (internal combustion engines in automobiles).

2. Production of engineering materials in the process industry (e.g., production of iron, steel, glass, refined fuels, etc., through thermal heating processes).

3. Household and industrial heating (e.g., heating of homes, factories, offices, hospitals, schools and other types of buildings).

4. Safety protection from unwanted combustion (e.g., prevention of forest and building fires, reduction of industrial explosions).

5. Ignition of various combustible materials for safety enhancement under emergency situations (e.g., inflation of airbags during collision of automobiles).

6. Pollutant emission control of combustion products (e.g., control of the temperature and chemical compositions of combustion products, reduction of soot and coke formation).

7. Active control of combustion processes (e.g., control of combustion instabilities in various propulsion systems).

1.2 Effects of combustion on the environment

In spite of the considerable benefits of combustion to our quality of life, combustion has also its dark face. Forests are destroyed every year, large amounts of pollutants are formed that lead to global warming and affect the planet's health. Another harmful effect of combustion on the environment is acid rain. It is produced mainly by the emissions of sulfur oxides and nitrogen oxides from the burning of fossil fuels in transport vehicles, as well as in energy and manufacturing industries. Acid rain causes lakes and rivers to become acidic (which damages fish and stops their reproduction), damages trees (acids react with many of their nutrients, thus starving them), and thereby human health (the ingestion of food or water with a great level of toxic metals produced by the consequences of acid deposition can produce diseases and damage our organism).

Smog is another factor of air pollution and also has negative consequences on human health.

It is belived by many scientists that global warming is a consequence of the increment of greenhouse gases in atmosphere, due to the development of industry. Stabilizing atmospheric concentrations of greenhouse gases will demand a major effort.

1.3 Outline of this work

The use of combustion in so many fields implies the necessity to ensure that the processes related to it are performed in the most efficient way. The increase in energy demand associated with the important issue of environmental pollution require major efforts to minimize the waste of energy and reduce environmental pollution. The work developed in this thesis contributes to these objectives.

Combustion of hydrocarbons such as alkanes is perhaps industrially the most important combustion system due to its use in many apparatuses such as car engines, gas turbine engines, heaters, incinerators, and hydrocracking furnaces that use methane and natural gases as fuels. The ability to perform detailed simulations of such processes would have significant impact on many industries as well as on our environment. To achieve this goal one must be able to develop fundamental kinetic models, which in principle must take into account all elementary chemical reactions occurring in the system, along with their kinetic parameters and the thermodynamic and transport properties of all chemical species involved. The completeness of the kinetic models should not require any assumption regarding reaction pathways.

Although the combustion of hydrocarbon fuels is conceptually simple in its overall plan, the details of how conversion of a hydrocarbon to carbon dioxide and water with concomitant release of energy occurs are enormously complex. The combustion of even a relatively simple hydrocarbon may involve thousands of elementary steps. Detailed knowledge of the energetics of each of these steps would permit fuels to be used with maximum efficiency and minimum pollution. Once the mechanism is generated, one needs to supply thermodynamic and transport properties for each species and kinetic parameters of each reaction.

Kinetic models lie at the heart of chemistry. They allow chemists to make valid predictions for systems of practical interest based on measurements made in highly simplified laboratory conditions. Models for important industrial processes are so valuable that companies often invest considerable funds in their development.

In this work, a detailed kinetic mechanism has been developed. It simulates the oxidation of up-to-C_4 hydrocarbon fuels under high-temperature conditions, and is based on the rate data compilation by Baulch et al. (2005) [2]. The mechanism presented consists of 412 elementary reactions and 61 species (see Appendix A). It is documented by Hegheş et al. (2005) [3] and Warnatz and Hegheş (2006) [4]. The approximate temperature range is from 900 K to 2500 K. For each development step of the mechanism and for each fuel considered, premixed laminar flame velocities have been calculated as well as ignition delay times, and compared to experiments for the largest possible conditions range (initial temperature, pressure, equivalence ratio) in order to test the validity of the developed mechanism. The flame modelling was used for two purposes:

1. To test the validity of the experimental methods;

2. To calculate flame velocities for comparison with experimental results.

Measurement and calculation of the dependence of ignition delay times on temperature and reactant composition provide powerful tools for modelling and understanding the combustion mechanism of a given fuel.

1.4 Structure of the thesis

As combustion is a technologically important process, its detailed description is desirable. Chapters 2-5 of this thesis include a theoretical background of disciplines involved in combustion studies.

Chemical kinetics and thermodynamics describe the fundamentals of reactive systems and are essential for combustion studies. In Chapter 2, we describe chemical processes in terms of rate laws together with rate coefficients and reaction orders, the determination of the rate law being one of the first steps in studying the kinetics of a chemical reaction. The study of temperature and pressure dependence reactions is necessary because chemical reactions depend on temperature and/or pressure. In 1889, Arrhenius analyzed rate coefficients and elaborated the well-known Arrhenius Law, which describes the relationship between the rate of a reaction and its temperature. The pressure dependence of the rate coefficient is described according to the modified Lindemann-Hinshelwood formalism proposed by Troe.

In Chapter 3 the focus is on reaction mechanisms. An important consideration in combustion processes is the formation of chain reactions. Chain-branching reactions are very important in the reaction mechanisms because they lead to the formation of radicals. A chain reaction mechanism consists of several steps (initiation, propagation, branching and termination) that are described in this chapter. Chain reactions are especially important for the chemistry of the atmosphere and combustion in flames.

Combustion mechanisms may consists of thousands of reactions. Many of these reactions can be neglected if changes in their rate coefficients have no influence on the output of the system. In modelling of the hydrocarbon kinetics, analyses of reaction mechanisms (reaction flow and sensitivity analyses) help us to understand the importance of the reactions and to identify the rate-limiting reactions in the system.

To obtain the validation of a reaction mechanism, ignition delay times and flame velocities simulations have to be compared with experimental data. In Chapter 4, we discuss the ignition processes, ignition limits and ignition delay time together with corresponding experimental techniques, showing the symbiotic connection between simulations and experiments. Continuous-flow devices and shock tubes are considered, as are experimental techniques used for measurements of ignition delay times. Measurement of the dependence of the ignition delay time on temperature, pressure and reactant composition provides a powerful tool for modelling and understanding the combustion mechanism of a given fuel.

Flames result from a complicated interaction of flow, heat conduction, diffusion and chemical reaction. Premixed flames occur when the fuel and oxidizer are homogeneously

mixed prior to ignition. Calculations of freely propagating one-dimensional flames have been extensively performed in the study of chemical kinetics. In Chapter 5, flame velocity and the mathematical equations that govern the modelling of premixed laminar one-dimensional flat flames (general conservation law, continuity equation, species conservation equation, enthalpy equation) are introduced. The heat released by the chemical reactions raises the temperature of the medium, and the heat is transferred to the surroundings by conduction, convection and radiation. Therefore, the study of heat transfer is also important.

The second part of the thesis presents the details of the computer modelling. It starts with Chapter 6, which contains simulation results for ignition delay times and flame velocities of different fuels. The simulation results are compared to experimental data. The mechanism tested in this work contains the oxidation reactions of hydrocarbons up to C_4 species. In Chapter 6, we also briefly describe the codes used to perform the simulations (MIXFLA for flame velocities and HOMREA for ignition delay times).

Chapter 7 concludes the thesis. The similarities and differences between the ignition delay times and flame velocities we have studied are considered, and general conclusions obtained by contrasting the results from our work with experimental data over a wide range of conditions (temperature, pressure and equivalence ratio) are presented.

We also include an appendix containing the details of the proposed reaction mechanism (reactions, rate coefficients, etc.).

2 Reaction Kinetics

Chemical kinetics is the branch of chemistry that studies the rates of chemical reactions. The term kinetics comes from the Greek *kinesis*, meaning movement. To understand how reactions take place at the molecular or microscopic level, a connection between chemistry and mathematics must be formed. Therefore, chemistry experiments (studies of chemical reactions as they proceed in time) must be interpreted in terms of a mathematical model (differential equations for the rates at which reactants are consumed and products are formed). The following considerations must also be taken into account:

- Molecules or atoms of reactants must collide with each other in chemical reactions.
- The collision must be of sufficient energy to break the bonds and initiate the reaction.
- In some cases, the orientation of the molecules during the collision must also be considered.

Although thermodynamics can predict the equilibrium composition of a reactive mixture, it cannot give the rate at which the reaction proceeds and its influence on the changes in composition, pressure and temperature. Both chemical kinetics and thermodynamics are needed to predict the reaction rates of reactive systems.

2.1 Rate law and reaction order

Rate law

One of the first steps in studying the kinetics of a chemical reaction is to determine the rate law of the reaction. Gas-phase reactions have a large impact on ignition and flame stabilization, on the heat release rate, and on pollutant emissions. The gas-phase chemistry is particularly important for the emission of carbon monoxide, unburnt hydrocarbons, aromatic compounds, soot and nitrogen oxides. Reactions that take place in the gas phase are known as homogeneous reactions.

Chemical processes are composed by a number of reversible (or irreversible) reactions that include N chemical species. Each one of these reactions can be represented in the general form

$$\sum_{i=1}^{N} \nu_i' A_i \rightarrow \sum_{i=1}^{N} \nu_i'' A_i \,, \tag{2.1}$$

where ν_i' and ν_i'' are the stoichiometric coefficients of the chemical species i and A_i are the species symbols, and N is the number of chemical species.

For a given reaction, the rate law is an equation which describes how fast a reaction proceeds and how the reaction rate depends on the concentration of the chemical species involved. The rate law describes the time dependence of a chemical reaction. The rate of a reaction whose stoichiometry is known can be measured in terms of the rate of appearance of any product or the rate of disappearance of any reactant. Appearance is normally indicated as a positive rate, with a positive sign, and disappearance as a negative rate, with a negative sign. Since a rate of a reaction often depends upon the concentration or pressure of a reactant, but not a product, rates of reactions are usually written in terms of rates of consumption of reactants. The rate law for Reaction (2.1) can be written as

$$\frac{\mathrm{d}c_i}{\mathrm{d}t} = \nu_i k_\mathrm{f} \prod_{i=1}^{N} c_i^{n_{i,1}} \,, \tag{2.2}$$

where $\nu_i = \nu_i'' - \nu_i'$, c_i is the concentration of species i, k_f is the rate coefficient, and $n_{i,1}$ is the reaction order with respect to species i.

For the reverse of Reaction (2.1),

$$\sum_{i=1}^{N} \nu_i'' A_i \rightarrow \sum_{i=1}^{N} \nu_i' A_i \,, \tag{2.3}$$

the rate law can be written as

$$\frac{\mathrm{d}c_i}{\mathrm{d}t} = -\nu_i k_\mathrm{r} \prod_{i=1}^{N} c_i^{n_{i,2}} \,, \tag{2.4}$$

where $n_{i,2}$ is the reaction order of the i-th product species. The equilibrium has been reached when the forward and backward reactions have the same microscopic rate,

$$\nu_i k_\mathrm{f} \prod_{i=1}^{N} c_i^{n_{i,1}} = \nu_i k_\mathrm{r} \prod_{i=1}^{N} c_i^{n_{i,2}} \,, \tag{2.5}$$

which means that no net reaction can be observed on a macroscopic level. The equilibrium constant of the reaction is

$$K_\mathrm{eq} = \frac{k_\mathrm{f}}{k_\mathrm{r}} = \prod_{i=1}^{N} c_i^{\nu_i} \,. \tag{2.6}$$

The equilibrium constant, K_eq, represents the ratio of the rate coefficients of the forward and reverse reactions. For an ideal gas, the equilibrium constant is calculated according to

$$K_\mathrm{eq} = \frac{k_\mathrm{f}}{k_\mathrm{r}} = \left(\frac{p^0}{RT}\right)^{\sum_{i=1}^{N} \nu_i} \exp\left[\frac{\Delta_R \bar{S}^0}{R} - \frac{\Delta_R \bar{H}^0}{RT}\right] \,, \tag{2.7}$$

where p^0 is the standard pressure ($p^0 = 1\,\text{bar}$), $\Delta_R\bar{S}^0$ is the molar entropy of the reaction,

$$\Delta_R\bar{S}^0 = \sum_{i=1}^{N} \nu_i \bar{S}_i^0 \,, \tag{2.8}$$

and $\Delta_R\bar{H}^0$ the standard molar enthalpy of the reaction,

$$\Delta_R\bar{H}^0 = \sum_{i=1}^{N} \nu_i \bar{H}_i^0 \,. \tag{2.9}$$

$\bar{S}_i^0$ and $\bar{H}_i^0$ are, respectively, the standard molar entropies and enthalpies of the species involved in the reaction.

Reaction orders

In a chemical process, two main types of reactions are distinguished: elementary reactions and overall reactions. Elementary reactions are those that take place as a result of a collision process and occur on a molecular level in a single step, without involving any intermediates. An example of elementary reaction is

$$\mathrm{OH} + \mathrm{H_2} \rightarrow \mathrm{H_2O} + \mathrm{H}. \tag{2.10}$$

These reactions depend on the intermolecular potential forces existing during the collision encounter, the quantum states of the molecules, and the transfer of energy. The reaction orders of elementary reactions are always integer and valid for all experimental conditions. For an elementary reaction, the reaction order coincides with the molecularity of the reaction. There are three kinds of elementary reactions: unimolecular, bimolecular and trimolecular reactions. In unimolecular reactions, a given reactive molecule dissociates to form products,

$$\mathrm{A} \rightarrow \text{Products}. \tag{2.11}$$

The reaction rate is first-order. That means that the rate of reaction doubles when the concentration of the reactive species doubles too.

Bimolecular reactions proceed by the collision of two molecules of the same or different chemical species, according to the reaction equations

$$\mathrm{A} + \mathrm{B} \rightarrow \text{Products} \tag{2.12}$$

or

$$\mathrm{A} + \mathrm{A} \rightarrow \text{Products}. \tag{2.13}$$

These are the most frequent type of reactions and their reaction rates are second-order (when the species concentrations are doubled, reaction rates quadruple).

Trimolecular reactions involve three reactant molecules, for example,

$$\mathrm{A} + \mathrm{B} + \mathrm{C} \rightarrow \text{Products} \tag{2.14}$$

or

$$\mathrm{A} + \mathrm{A} + \mathrm{B} \rightarrow \text{Products} \tag{2.15}$$

or

$$\mathrm{A} + \mathrm{A} + \mathrm{A} \rightarrow \text{Products.} \tag{2.16}$$

Generally, trimolecular reactions are recombination reactions and they obey a third-order rate law. Third-order reactions are very important. Radical recombination reactions, for example the reaction between OH and H to produce water, take place only if a third body, M, participates in the collision and hence these are third-order reactions. The reason a third body is needed is that recombination reactions are exothermic and the third body must carry away some of the energy.

On the other hand, overall reactions are those that are the consequence of several elementary reactions. An example of overall (global) reaction is

$$\mathrm{CH_4} + 2\mathrm{O_2} \rightarrow \mathrm{CO_2} + 2\mathrm{H_2O}. \tag{2.17}$$

Overall reactions have complex rate laws where in general the reaction order is not integer and depends on time and reaction conditions.

2.2 Experimental determination of rate laws

As we mentioned before, one of the first steps in studying the kinetics of a chemical reaction is to determine the rate law for the reaction. A rate law can be determined experimentally by measuring the concentration of species at particular times during the reaction and making characteristic kinetics plots. The slope of the kinetic plot can be used to determine the rate coefficient for the reaction. Another method for determining the rate law is the method of initial rates. The initial rate of a reaction is the rate at $t = 0$. The method involves measuring the rate of reaction at very short times before any significant changes in concentration occur. Suppose one is studying a reaction with the following stoichiometry:

$$\mathrm{A} + 2\mathrm{B} \rightarrow 3\mathrm{C}. \tag{2.18}$$

While the form of the differential rate law might be very complicated, many reactions have a rate law of the following form:

$$v = k[\mathrm{A}]^a[\mathrm{B}]^b \tag{2.19}$$

The initial concentrations of A and B are known; therefore, if the initial reaction rate is measured, the only unknowns in the rate law are the rate coefficient, k, and the exponents

a and b. One typically measures the initial rate for several different sets of concentrations and then compares the initial rates. One major disadvantage to using the method of initial rates is the need to perform multiple experiments. Another disadvantage is that it works only for relatively slow reactions. If the reaction proceeds too fast, the measured rate will have a large uncertainty.

A better method is the isolation method. In this method the concentration of one reactant is made much smaller than the concentrations of the other reactants. Under this condition, all reactant concentrations except one are essentially constant, and the simple zero-, first-, and second-order kinetic plots can usually be used to interpret the concentration-time data.

Another method is the fit to integrated form. It is known that from plotting the concentrations as function of time it is difficult to see the difference between a first-order and a second-order decay for a set of real experimental data. According to this method, the best way to look at the experimental data is to plot it in such a way that a straight line would be expected.

2.3 Rate coefficients

2.3.1 Temperature dependence of rate coefficients

It is known that the rate of chemical reactions depends on the temperature. At higher temperatures, the probability that two molecules will collide per unit time is higher. This higher collision rate results from a higher average kinetic energy. The activation energy is the amount of energy required to ensure that a reaction happens. In 1889, Arrhenius analyzed the characteristics of rate coefficients and elaborated the well-known Arrhenius Law.

The relationship between the rate of the reaction and its temperature is determined by the Arrhenius equation

$$k = A \exp\left(-\frac{E_\mathrm{a}}{RT}\right), \tag{2.20}$$

where k is the rate coefficient for the reaction, A is called the pre-exponential factor or frequency factor and is a constant specific to each reaction that depends on the chance the molecules will collide in the correct orientation (depends on the molecularity of the reaction and accounts for the number of collisions between molecules in a reaction system), E_a is the activation energy, R is the gas constant (R has the value of $8.314 \times 10^{-3}\,\mathrm{kJ/\,mole\,K}$), and T is the temperature (in K). A and E_a come from experiment or statistical mechanics calculations. It is known that not all molecular collisions will result in reaction, but only those with kinetic energy higher than the energy needed to break the reactant's chemical bonds. This energy barrier is described by the activation energy (see Fig. 2.1). Therefore, the proportion of collisions occurring between molecules that

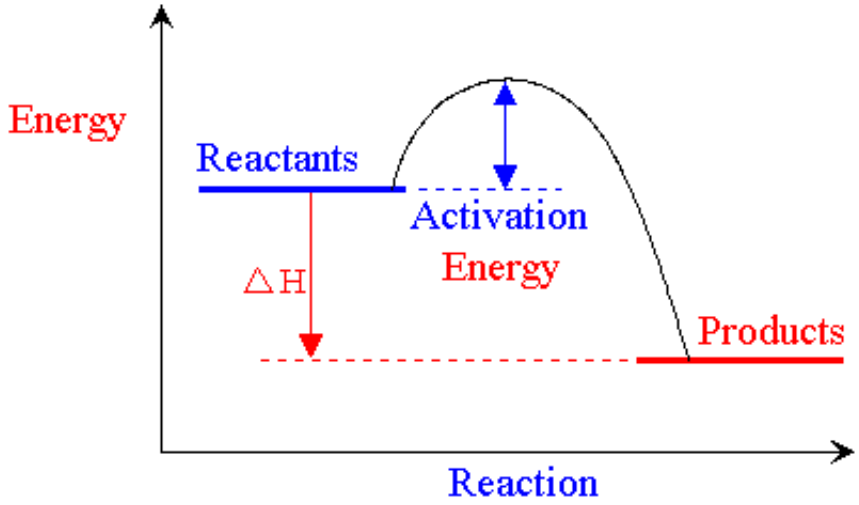

Figure 2.1: The energy profile (schematic) of a chemical reaction. The reaction coordinate represents the changes in bond lengths and bond angles that occur as the chemical reaction proceeds from reactants to products [5].

have kinetic energy higher than activation energy is given by $\exp(-E_a/RT)$; this results from the kinetic theory of gases. An analysis of the enthalpy of the system will give a decent account of the energetics of the reaction mixture. By calculating the amounts of energy required to break all the bonds of the reactant species and products, it is possible to calculate the energy difference between the reactants and the products. This is referred to as ΔH, where Δ means difference (energy used in bond breaking reactions minus energy released in bond making products), and H stands for enthalpy, a measure of energy which is equal to the heat transferred at constant pressure. ΔH is negative for exothermic reactions, and refers to the fact that the energy has been released in the form of heat.

The Arrhenius equation is used to determine the activation energies of chemical reactions. It can also be written as

$$\ln k = \ln A - \frac{E_a}{R}\left(\frac{1}{T}\right). \tag{2.21}$$

However, limitations of the accuracy of experimental data, and the fact that small differences among rate coefficients could cause considerable changes of rate coefficients, motivated the common acceptance of a simplified Arrhenius equation. Thus, a plot of $\ln k$ versus $1/T$ is called an Arrhenius plot, and it should be a straight line. But the Arrhenius plot for some reactions is not linear. The nonlinear behavior can be justified theoretically. The reaction rate is predicted to have the form

$$k = AT^m \exp\left(-\frac{E_a}{RT}\right), \tag{2.22}$$

where A, E^{a} and m are temperature-independent constants. If m is known, E_{a} can be determined from the slope of the plot of $\ln(k/T^m)$ against $1/T$.

Eqs. (2.20) and (2.22) are empirical expressions based on fits of experimental data. Rate coefficients are usually calculated for a finite temperature range.

An important point to notice is that the reaction rate coefficient increases very fast with temperature. This is the fundamental reason why combustion reactions occur at high temperatures and not at room temperature.

2.3.2 Pressure dependence of rate coefficients

The pressure dependence of the rate coefficient of unimolecular reactions can be understood using the Lindemann model [6]. This model explains how unimolecular reactions occur and provides a simplified representation of the physical processes that are involved in unimolecular reactions. According to Lindemann, the energy source for a unimolecular reaction is collision with other molecules, M. The excited molecule can deactivate through another collision, or decompose into the products. The Lindemann model for unimolecular reactions of the form

$$\mathrm{A} \underset{k_{-1}}{\overset{k_1}{\rightleftharpoons}} \mathrm{B} \tag{2.23}$$

can be written as

$$\mathrm{A} + \mathrm{M} \underset{k_{-1}}{\overset{k_1}{\rightleftharpoons}} \mathrm{A}^* + \mathrm{M} \tag{2.24}$$

$$\mathrm{A}^* \overset{k_2}{\rightarrow} \mathrm{B} \tag{2.25}$$

where A^* is is the energized reactant molecule and M is the collision molecule. The rate of product formation is given by

$$\frac{\mathrm{d}[\mathrm{B}]}{\mathrm{d}t} = k_2[\mathrm{A}^*]\,. \tag{2.26}$$

Because of the activation and deactivation of the reactant molecule A^*, the concentration of A^* is very small and the steady-state approximation can be assumed:

$$\frac{\mathrm{d}[\mathrm{A}^*]}{\mathrm{d}t} = 0 = k_1[\mathrm{A}][\mathrm{M}] - k_{-1}[\mathrm{A}^*][\mathrm{M}] - k_2[\mathrm{A}^*]\,. \tag{2.27}$$

The concentration of species A^* is

$$[\mathrm{A}^*] = \frac{k_1[\mathrm{M}][\mathrm{A}]}{k_2 + k_{-1}[\mathrm{M}]}\,, \tag{2.28}$$

and the rate law for the overall reaction is

$$\frac{\mathrm{d}[\mathrm{B}]}{\mathrm{d}t} = -\frac{\mathrm{d}[\mathrm{A}]}{\mathrm{d}t} = \frac{k_1 k_2[\mathrm{M}][\mathrm{A}]}{k_2 + k_{-1}[\mathrm{M}]}\,. \tag{2.29}$$

At very high pressures, the concentration of the collision partner M is high. If the rate of collisional deactivation is much larger than the rate of the unimolecular decomposition, $k_{-1}[\mathrm{A}^*][\mathrm{M}] \gg k_2[\mathrm{A}^*]$ or $k_{-1}[\mathrm{M}] \gg k_2$, then

$$\frac{\mathrm{d}[\mathrm{B}]}{\mathrm{d}t} = \frac{k_1 k_2}{k_{-1}}[\mathrm{A}] = k_\infty[\mathrm{A}]. \tag{2.30}$$

In this case, the reaction rate is first order in A, where the k_∞ represents the high-pressure rate coefficient. The reaction rate does not depend on the concentrations of the collision partners, because at high pressures collisions occur very often and, thus, the rate-limiting step is the decomposition of the activated molecule A^*.

At low pressures, the concentration of the collision partner M is very low. If the rate of collisional deactivation is much smaller than the rate of the reaction, $k_1[\mathrm{M}] \ll k_2$, then

$$\frac{\mathrm{d}[\mathrm{B}]}{\mathrm{d}t} = k_1[\mathrm{A}][\mathrm{M}] = k_0[\mathrm{A}][\mathrm{M}]\,, \tag{2.31}$$

where k_0 is the low-pressure rate coefficient. In this case, the rate law is first order in [A] and [M]. The overall reaction order is 2. The reaction rate is proportional to the concentration of species A and collision partner M, because the activation is slow at low pressures.

The physical meaning of this change of reaction order is that at low pressures, the bimolecular formation of $[\mathrm{A}^*]$ is the rate-limiting reaction. For the overall reaction, the equation of the global rate is

$$\frac{\mathrm{d}[\mathrm{B}]}{\mathrm{d}t} = k[\mathrm{A}][\mathrm{M}]\,, \tag{2.32}$$

where

$$k = \frac{k_1 k_2[\mathrm{A}]}{k_2 + k_{-1}[\mathrm{A}]} \tag{2.33}$$

or

$$\frac{1}{k} = \frac{k_{-1}}{k_1 k_2} + \frac{1}{k_1[\mathrm{A}]}\,. \tag{2.34}$$

The theory can be tested by plotting $1/k$ against $1/[\mathrm{A}]$; the result must be a straight line.

The Lindemann model illustrates the behavior of the reaction rate with concentration but does not explain in detail how the energy transfer processes take place. More accurate results for the pressure dependence of unimolecular reactions can be obtained from the theory of unimolecular reactions (see [7–9]). The theory of unimolecular reactions yields fall-off curves which describe the pressure dependence of k for different temperatures. As an example, a typical set of fall-off curves for the unimolecular reaction $\mathrm{C_2H_6} \rightarrow \mathrm{CH_3} + \mathrm{CH_3}$ obtained by Warnatz [10, 11] is shown in Fig. 2.2, which describes the pressure dependence of k for different temperatures. Usually the logarithm of the rate coefficient is plotted versus the logarithm of the pressure. For $p \rightarrow \infty$,

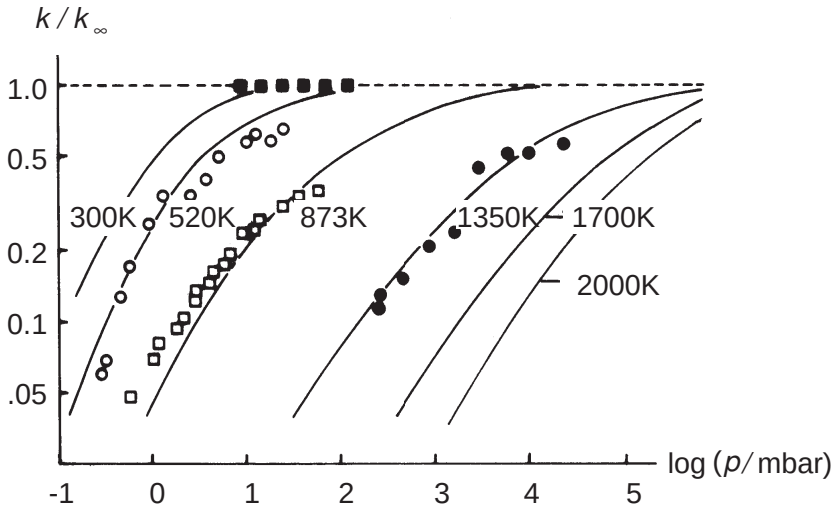

Figure 2.2: Fall-off curves for the unimolecular reaction $C_2H_6 \rightarrow CH_3 + CH_3$ ([12]).

$k = k_1 k_2[\mathrm{M}]/(k_{-1}[\mathrm{M}] + k_2)$ tends to the limit k_∞. At low pressures the rate coefficient k is proportional to $[\mathrm{M}] = p/RT$ (Eq. 2.31), and a linear dependence results. In the same way, if the effective activation energy of k_∞ is low, the rate coefficient k will decrease with temperature [13]. The fall-off curves depend very much on temperature. Thus, the rate coefficients of unimolecular reactions show different temperature dependencies at different values of the pressure.

Treatment of pressure-dependent reactions

As we mentioned before, for some dissociation/recombination and bimolecular reactions, it has been observed that under certain conditions reaction rates depend strongly on pressure as well on temperature. These reactions are called dissociation/recombination fall-off reactions and chemically activated bimolecular reactions. In the first ones, the rate of the reaction increases with pressure, while for the second type it decreases when the pressure increases. For a given combination and the reverse dissociation reaction,

$$\mathrm{A} + \mathrm{B} + \mathrm{M} \rightleftharpoons \mathrm{AB} + \mathrm{M}, \tag{2.35}$$

the rate law is described by

$$\frac{\mathrm{d}[\mathrm{AB}]}{\mathrm{d}t} = k[\mathrm{A}][\mathrm{B}]\,, \tag{2.36}$$

in which the second-order rate constant depends on [M]. The pressure dependence of the rates of these reactions is described by two limiting situations, the low-pressure and high-pressure limits. At low pressures (k_0), a third-body concentration is needed to provide enough energy to the collision to make possible the reaction. At high pressure

(k_∞), this contribution is not necessary. Between these two circumstances, there is an intermediate case, the fall-off region represented by a fall-off expression of k/k_∞ as a function of

$$\frac{k_0[\mathrm{M}]}{k_\infty} = \frac{[\mathrm{M}]}{[\mathrm{M}]_c}\,, \tag{2.37}$$

where $[\mathrm{M}]_c$ is the center of the fall-off curve and indicates the third body concentration for which the extrapolated k_0 would be equal to k/k_∞. The dependence of k on [M] is complicated and has to be analyzed by unimolecular rate theory. For moderately complex molecules at not too high temperatures the following expression is given [14]:

$$k = \frac{k_0 k_\infty[\mathrm{M}]}{k_0[\mathrm{M}] + k_\infty} F = k_0[\mathrm{M}] \left(\frac{1}{1 + [\mathrm{M}]/[\mathrm{M}]_c}\right) F = k_\infty \left(\frac{[\mathrm{M}]/[\mathrm{M}]_c}{1 + [\mathrm{M}]/[\mathrm{M}]_c}\right) F, \tag{2.38}$$

where F is called the broadening factor. At not too high temperatures, the broadening factor can be written as

$$\log F = \frac{\log F_c}{1 + \left[\dfrac{\log\left([\mathrm{M}]/[\mathrm{M}]_c\right)}{N}\right]^2} \tag{2.39}$$

where $N = 0.75 - 1.27 \log F_c$. The fall-off curve is characterized by k_0, k_∞, F_c and $[\mathrm{M}]_c$ ($[\mathrm{M}]_c = k_0/k_\infty$).

Troe (see [15], [16], [17]) estimated the temperature dependence of F_c by the following equation:

$$F_c = (1-a)\exp\left(-T/T^{***}\right) + a\exp\left(-T/T^{*}\right) + \exp\left(-T^{**}/T\right). \tag{2.40}$$

The two first terms are important for atmospheric conditions, but the last term becomes relevant only at high temperatures.

2.4 Thermodynamic data

The thermochemical properties of chemical species are tabulated as function of temperature. These tables include values of thermodynamic properties based on experimental data, complemented by theoretical calculations. Thermodynamic tables, such as Stull and Prophet 1971 (JANAF Tables) [18], Kee et al. 1987 [19], Burcat 1984 [20] etc. are found in the literature. In this work, most of the thermodynamic data are taken from a single publication, that prepared for the Sandia CHEMKIN Program [19]. On data sheets the standard enthalpy and entropy changes at 298 K and the equilibrium constant as function of the temperature are given for each reaction channel [2]. The equilibrium constant is expressed in the form

$$K_c(T) = AT^n \exp(B/T)\,,$$

where A, B and n are constants.

Heat capacities expressed as NASA polynomials were used to calculate $\Delta H^0, \Delta S^0$ and K_c in a temperature range between 300 K and 5000 K. The NASA polynomials have the form

$$\frac{C_p}{R} = a_1 + a_2 T + a_3 T^2 + a_4 T^3 + a_5 T^4 \,,$$

$$\frac{H}{RT} = a_1 + a_2 \frac{T}{2} + a_3 \frac{T^2}{3} + a_4 \frac{T^3}{4} + a_5 \frac{T^4}{5} + \frac{a_6}{T} \,,$$

$$\frac{S}{RT} = a_1 \ln T + a_2 T + a_3 \frac{T^2}{2} + a_4 \frac{T^3}{3} + a_5 \frac{T^4}{4} + a_7 \,,$$

where $a_1, a_2, \ldots, a_7$ are the numerical coefficients supplied in NASA thermodynamic files. H in the above equation is defined as

$$H(T) = H_\mathrm{f}(298\,\mathrm{K}) + [H(T) - H(298\,\mathrm{K})] \,, \tag{2.41}$$

so that, in general, $H(T)$ is not equal to $H_\mathrm{f}(T)$, and one needs to have the data for the reference elements to calculate $H_\mathrm{f}(T)$.

The format of the data base containing these information matches the SANDIA data base and, once generated, did not have to be changed. Examples are shown in the following:

```
CH4               121286C   1H   4          G  0300.00   5000.00  1000.00      1
 0.01683478E+02 0.10237236E-01-0.03875128E-04 0.06785585E-08-0.04503423E-12    2
-0.10080787E+05 0.09623395E+02 0.07787415E+01 0.01747668E+00-0.02783409E-03    3
 0.03049708E-06-0.12239307E-10-0.09825229E+05 0.13722195E+02                   4
CO                121286C   1O   1          G  0300.00   5000.00  1000.00      1
 0.03025078E+02 0.14426885E-02-0.05630827E-05 0.10185813E-09-0.06910951E-13    2
-0.14268350E+05 0.06108217E+02 0.03262451E+02 0.15119409E-02-0.03881755E-04    3
 0.05581944E-07-0.02474951E-10-0.14310539E+05 0.04848897E+02                   4
CO2               121286C   1O   2          G  0300.00   5000.00  1000.00      1
 0.04453623E+02 0.03140168E-01-0.12784105E-05 0.02393996E-08-0.16690333E-13    2
-0.04896696E+06-0.09553959E+01 0.02275724E+02 0.09922072E-01-0.10409113E-04    3
 0.06866686E-07-0.02117280E-10-0.04837314E+06 0.10188488E+02                   4
```

3 Reaction mechanisms

A reaction mechanism is a complete set of elementary reactions together with their rate coefficients. Reaction mechanisms describe how a reaction takes place at the molecular level, which bonds are broken or formed and in which order, and what the relative rates of the steps are. Therefore, understanding of the properties of reactants and products is required. Each step of the mechanism involves rearrangement or combinations of molecular species. The interaction of these steps produces the overall balanced stoichiometric chemical equation of the global reaction. When more than one mechanism is consistent with the data, new experiments are needed to test their validity and choose between mechanisms.

3.1 Radical-chain reaction

An important consideration in combustion processes is the formation of radical-chain reactions. The basic premise of chain reaction mechanisms is that free radicals play a leading role in the destruction of reactant molecules. Chain branching reactions, if they occur, take a very important role in the mechanism as they lead to the formation of increasing concentrations of radicals. Reaction time and temperature have a bearing on radical concentration, and the type of reaction initiating the consumption of the reactant. Radical-chain reactions can be defined as those reactions in which an intermediate product produced in one step generates a reactive intermediate species in a subsequent step, then that intermediate generate another reactive intermediate, and so on [21].

A chain reaction mechanism consists of several steps: initiation, propagation, branching (not always present), and termination. This can be illustrated, for certain ranges of temperature and pressure, by some of the reactions in the following hydrogen oxidation mechanism. The initiation step is responsible for the initial decomposition of the reactants and involves the formation of the radicals. The initiation step is slow and usually involves thermal or photochemical dissociation of a relatively stable reactant, e.g. in the hydrogen/oxygen system (see Eq. 3.1).

$$H_2 + O_2 \rightarrow 2OH\bullet\,. \tag{3.1}$$

In chain initiation steps, the reactive species (characterized by the dot) are formed from stable species. In chain propagation steps, the reactive intermediate species react with stable species forming another reactive species (see Eq. 3.2). These are normally rapid

steps, and the radicals are known as chain carriers:

$$H_2 + OH\bullet \rightarrow H\bullet + H_2O\,. \tag{3.2}$$

In chain-branching steps, the reactive species reacts with a stable species forming two reactive species (see Eqs. 3.3 and 3.4):

$$H\bullet + O_2 \rightarrow OH\bullet + O\bullet\,, \tag{3.3}$$

$$O\bullet + H_2 \rightarrow OH\bullet + H\bullet\,. \tag{3.4}$$

Reactions (3.2–3.4) lead to an increase in the concentration of H and OH radicals. This increase in number of chain carriers (the reactive species H, OH, O) may lead to an explosion. For example, the generation of a flame in combustion is due to branching reactions predominating over termination, with a large generation of radicals resulting in the fast decomposition of the fuel. At low pressures, it is found that the reaction is steady. The branching reactions are slow at low pressures and so, other reactions which destroy the H atoms (termination reactions) are competitive. The explosive growth of chain carriers is thus controlled. In chain termination steps, the reactive species react to stable species (e.g., see Eq. 3.5 at the vessel surface and Eq. 3.6 in the gas phase):

$$H\bullet \rightarrow 1/2H_2\,, \tag{3.5}$$

$$H\bullet + O_2 + M \rightarrow HO_2 + M\,. \tag{3.6}$$

where M is any gas (a third body needed to carry off the excess energy that the newly formed HO_2 molecule has; if this energy is not dissipated, the molecule will fall apart immediately). The termolecular reaction leading to destruction of H becomes important as the pressure is raised. At high pressures, Reaction (3.6) removes H atoms and reduces the rate of chain branching, thus inhibiting the explosion; the result is a steady reaction.

If one sums up the chain propagation and chain branching steps, one can see that in this mechanism radicals are formed from the reactants [13]. The rates of reactions (3.3) and (3.4) increase when the pressure is raised (because they depend on $[O_2]$ and $[H_2]$). An explosion can result at the point where the branching reactions overwhelm the termination reactions.

Propagation steps do not affect the overall radical concentration, since each step involves a radical, a reactant and product. The overall radical concentration is determined by a balance between the initiation reactions which form them, and the termination reactions which remove them. The average number of propagation steps, which occur between initiation and termination is called the chain length and is determined by the relative rates of the propagation and termination (or initiation) reactions [22].

These chain reactions have the remarkable property that only a small number of chain carriers are needed to produce very many product molecules. The chemistry of the atmosphere and combustion in flames are some examples which involve many such chain reactions.

3.2 Analysis of reaction mechanisms

It is known that complete reaction mechanisms for hydrocarbons may consists of thousands of elementary reactions. The rates of the elementary reactions in combustion processes differ greatly. For many of the elementary reactions, a change in the rate coefficients has nearly no influence on the output of the system. On the other hand, for a few of elementary reactions, changes in the rate coefficients have really large effects on the otcome of the system (rate-limiting reactions). Sensitivity analysis and reaction flow analysis are two methods which can be used to simplify the reaction mechanism and to identify the sensitive reaction of a considered mechanism.

3.2.1 Sensitivity analysis

Many researchers have modelled hydrocarbon kinetics and performed sensitivity analysis to understand the relative importance of reactions in the system, to reduce the number of reactions in a given problem and to identify the rate limiting reaction steps in the system.

For a reaction mechanism consisting of R reactions and S species, the rate law can be written as a system of first order ordinary differential equations:

$$\frac{\mathrm{d}c_i}{\mathrm{d}t} = F_i\left(c_1, ..., c_S; k_1, ..., k_R\right), \qquad c_i\left(t = t_0\right) = c_i^0, \qquad i = 1, 2, ..., S. \tag{3.7}$$

The species concentrations, c_i, are the dependent variables, while time t is the independent variable, k_R are the parameters of the system and c_i^0 are the initial concentrations.

The solution of Eq. (3.7) depends on the initial conditions and parameters. The sensitivity is defined as the dependence of the solution c_i on the parameters k_R. The absolute sensitivity is defined as

$$E_{i,r} = \frac{\partial c_i}{\partial k_r}. \tag{3.8}$$

The relative sensitivity is defined as

$$E_{i,r}^{\mathrm{rel}} = \frac{k_r}{c_i}\frac{\partial c_i}{\partial k_r}. \tag{3.9}$$

The results of the computation of sensitivity coefficients give the partial derivative of the concentration [B] with respect to the rate coefficients:

$$E_{\mathrm{B},k_1}(t) = \frac{\partial[\mathrm{B}]}{\partial k_1} = [\mathrm{A}]_0 \frac{k_2}{\left(k_1 - k_2\right)^2}\left\{\left(k_2 t - k_1 t - 1\right)\exp(-k_1 t) + \exp(-k_2 t)\right\},$$

$$E_{\mathrm{B},k_2}(t) = \frac{\partial[\mathrm{B}]}{\partial k_2} = [\mathrm{A}]_0 \frac{k_1}{\left(k_1 - k_2\right)^2}\left\{\exp(-k_1 t) + \left(k_1 t - k_2 t - 1\right)\exp(-k_2 t)\right\}.$$

The relative sensitivities are computed according to Eq. (3.9) [12] as

$$E^{\mathrm{rel}}_{\mathrm{B},k_1}(t) = \frac{k_1}{[\mathrm{B}]} E_{\mathrm{B},k_1}(t)\,, \tag{3.10a}$$

$$E^{\mathrm{rel}}_{\mathrm{B},k_2}(t) = \frac{k_2}{[\mathrm{B}]} E_{\mathrm{B},k_2}(t)\,. \tag{3.10b}$$

The relative sensitivity coefficients for a simple reaction sequence can be plotted against time. The concentration of the product [B] is dimensionless, $k_1 = \tau^{-1}$, $k_2 = 100\tau^{-1}$ and $[\mathrm{A}]_0 = 1$ (τ is the lifetime; see Fig. 3.1).

The sensitivity analysis (see Fig. 3.2) shows a high sensitivity in case of the $\mathrm{H} + \mathrm{O}_2 \rightarrow \mathrm{O} + \mathrm{OH}$ reaction (the rate-limiting reaction) and a low sensitivity for $\mathrm{O} + \mathrm{OH} \rightarrow \mathrm{H} + \mathrm{O}_2$ reaction, the fast reaction (not rate-limiting).

Sensitivity analysis is done numerically by generating a differential equation system for the sensitivity coefficients by formally differentiating (Eq. 3.7),

$$\frac{\partial}{\partial k_r}\left(\frac{\partial c_i}{\partial t}\right) = \frac{\partial}{\partial k_r} F_i\left(c_1, ..., c_s; k_1, ..., k_R\right) \tag{3.11}$$

$$\frac{\partial}{\partial t}\left(\frac{\partial c_i}{\partial k_r}\right) = \left(\frac{\partial F_i}{\partial k_r}\right)_{c_l, k_{l\neq r}} + \sum_{i=1}^{S}\left\{\left(\frac{\partial F_i}{\partial c_n}\right)_{c_{l\neq n}, k_l}\left(\frac{\partial c_n}{\partial k_r}\right)_{k_{l\neq j}}\right\} \tag{3.12}$$

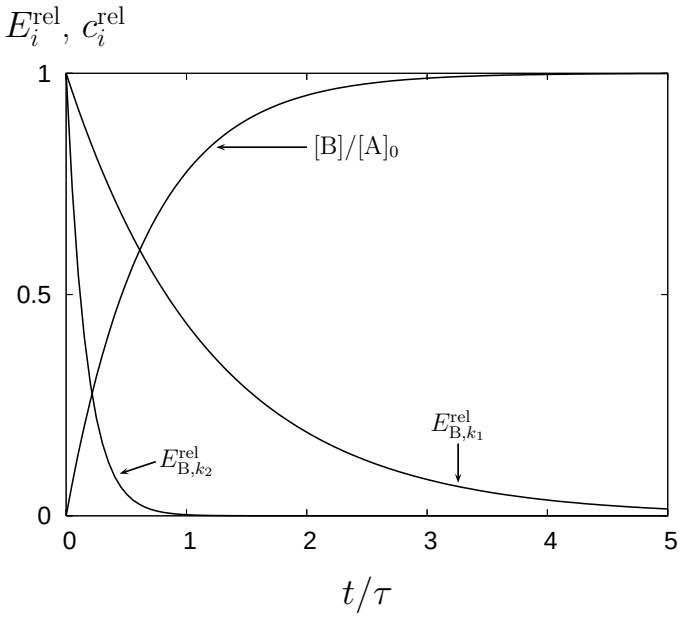

Figure 3.1: Behavior of the relative sensitivity coefficients for a reaction of the $\mathrm{A} \xrightarrow{k_1} \mathrm{I} \xrightarrow{k_2} \mathrm{B}$ type [12].

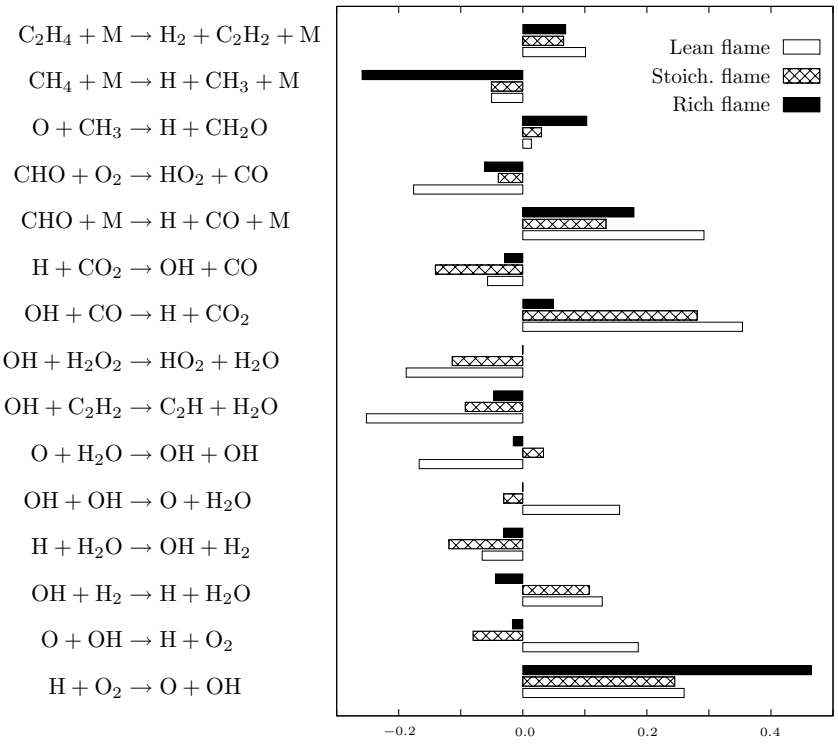

Figure 3.2: Sensitivity analysis for premixed stoichiometric propane flame in air at 1 bar and 298 K unburnt gas temperature.

$$\frac{\partial}{\partial t}E_{i,r} = \left(\frac{\partial F_i}{\partial k_r}\right)_{c_l, k_{l\neq r}} + \sum_{i=1}^{S}\left\{\left(\frac{\partial F_i}{\partial c_n}\right)_{c_{l\neq n}, k_l} E_{n,r}\right\} . \tag{3.13}$$

In these equations, c_l after the partial derivatives means that all c_l are held constant during the differentiation, and $c_{l\neq n}$ after the partial derivatives means that all c_l are held constant, except c_n. This system of linear differential equations can be numerically solved, software packages being available (see [23–25]).

The rate coefficients of elementary reactions with high sensitivities have to be well known, because they have a great influence on the results of the mathematical modelling. If reactions have low sensitivities, only approximate values for the rate coefficients have to be known. Thus, sensitivity analysis reveals a few of the many elementary reaction rates, which require accurate determination, usually through experimental measurement [13].

3.2.2 Reaction flow analysis

Reaction flow analysis is performed in order to identify the important chemical pathways over a wide range of conditions and it shows the percentage of the contribution of different reactions r ($r = 1, \ldots, R$) to the formation or consumption of the chemical species s

Reaction Number	Chemical Species					
	1	2	3	$\cdots$	$S-1$	S
1	31.0%	2.2%	0%	$\cdots$	0%	0%
2	0.1%	0%	0%	$\cdots$	0%	0%
3	2.9%	5.0%	0%	$\cdots$	80.0%	5.0%
4	0%	0%	2.0%	$\cdots$	20.0%	92.0%
$\vdots$	$\vdots$	$\vdots$	$\vdots$	$\cdots$	$\vdots$	$\vdots$
$R-1$	66.0%	90.4%	98.0%	$\cdots$	0%	3.0%
R	0%	2.4%	0%	$\cdots$	0%	0%

Table 3.1: Schematic illustration of the output of reaction flow analysis.

$(s = 1, \ldots, S)$ as shown on Table 3.1.

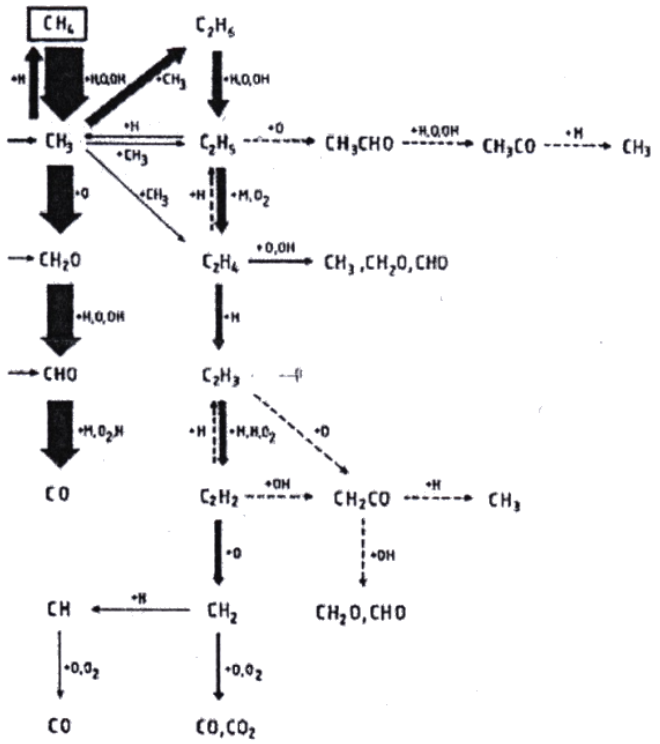

Figure 3.3: Integral reaction flow analysis in a premixed stoichiometric CH_4/air flame at $p = 1\,\text{bar}$ and $T_u = 298\,\text{K}$ [12].

It can be seen that 31.0% of the formation of Species 1 can be attributed to Reaction 1, 0.1% to Reaction 2, 2.9% to Reaction 3, and 66% to Reaction $R-1$. The percentages in the columns have to add to 100%. After obtaining the percentage output of all the species for each reaction, integral and local reaction flow analysis can be performed. Integral reaction flow analysis takes into account the overall formation or consumption of species. Local reaction flow analysis considers the formation or consumption of species locally at specific times in time-dependent problems (e.g., ignition processes) or at specific locations in steady processes (e.g., flat flame). An example of a reaction flow diagram is shown on Fig. 3.3, [12].

4 Ignition processes

The time-dependent process of starting with reactants and evolving in time towards a steadily burning flame is called ignition [13]. Example of ignition processes include induced ignition (such as occurs in gasoline engines induced by a spark), autoignition (such as occurs in Diesel engines), and photo-ignition (caused by photolytic generation of radicals).

4.1 Ignition limits

Experimentally, it was observed that a pressure vessel containing hydrogen and oxygen under certain conditions of temperature and pressure can explode. The explosion is observed after an ignition-delay time (or induction time). The existence of explosion limits in a closed vessel can be understood from qualitative considerations of competition between chain-terminating and chain-branching reactions on surfaces and in the gas phase. Typical experimentally determined explosion limits for hydrocarbons are illustrated on the schematic p-T explosion diagram in Fig. 4.1. At low pressures, ignition does not take place, but a slow reaction continues. The lower explosion limit is determined by a balance between the removal of chain carriers (radicals) by gas-phase reactions. In this low-pressure range, the number of collisions and the rate of production of chain carriers are both low. As the pressure is raised above a certain value (first ignition limit), the rate of production of chain carriers by gas-phase reactions increases, and a spontaneous ignition is observed. Then, the reaction is slow and, again, one does not observe the ignition.

The second explosion limit is governed by the competition of chain branching and chain termination in the gas phase. The existence of the second explosion limit can be explained also if the three-body reactions are added to the scheme (recombination reactions). Thus, there is a particular pressure level above which the rate of removal of free radicals exceeds the rate of formation of free radicals by chain-branching reactions. This explains the existence of the second explosion limit.

At some pressure level above the second explosion limit, there is a rapid increase in the number of radicals and the third explosion (thermal explosion) limit can be observed. This third explosion limit is governed by the competition of heat production by chemical reactions and heat losses to the vessel wall (see Warnatz et al. 2006 [13]). Regions can be found where ignition takes place after the emission of short light pulses (multistage ignition) or where combustion takes place at low temperatures (cool flames).

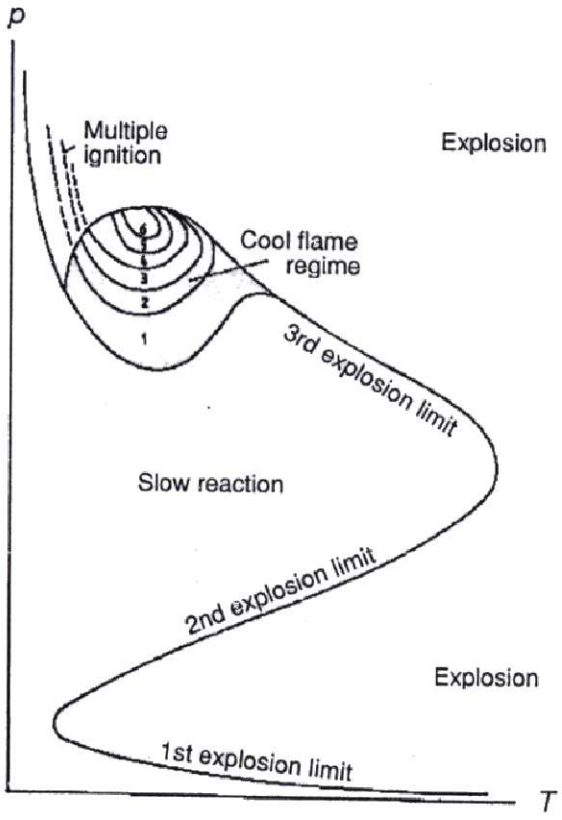

Figure 4.1: Schematic illustration of ignition limits for hydrocarbons (see Warnatz 1981 [26]) [13].

4.2 Ignition-delay time

It is widely recognized that ignition of a fuel-air mixture comprises a series of overlapping physical and chemical processes which have characteristic times that combine to form an overall induction or ignition delay time. During ignition, there is a rapid depletion of the primary fuel, very high radical concentrations, and an exponential rise in temperature and pressure. The ignition delay time can be defined as the period between the creation of a combustible mixture, as by injection of fuel into an oxidizing environment, and the onset of the rapid reaction phase leading to the rise in temperature and pressure.

The ignition delay time is a measurable quantity. Measurement of the dependence of the ignition delay time on temperature, pressure and reactant composition provides a powerful tool for modelling and understanding the combustion mechanism of a given fuel. Over the years, a wide variety of experimental techniques has been used to measure ignition delay-times of fuels, including constant-volume bombs, continuous-flow test

apparatus, and shock tubes.

4.2.1 Continuous-flow devices

In a continuous flow device, fuel is injected into a flowing air stream at high temperature, and the combustible mixture ignites at some distance downstream of the fuel injection location, depending upon the velocity of the flow. The procedure to acquire ignition delay data consists of first establishing a prescribed condition within the test duct regarding pressure, composition and flow rates of reactants. Then, the inlet air (or/and fuel) temperature is increased (or decreased) until autoignition of the fuel-air mixture occurs within or at the exit of the duct. The occurrence of autoignition is determined by observance of a visible flame and a rapid increase in temperature at the flame front location. Ignition delay times are calculated from the known length of the duct, defined as the distance between the injector and flame front location, and the mean free stream flow velocity.

Continuous-flow devices for ignition studies permit ample time for measuring and regulating the variables of interest (e.g., temperature, pressure, stoichiometry). They have a limitation in the maximum level of air temperature which they provide (up to 1000 K), limitation given by their use of electrical resistance-type air heaters. Consequently, as will be discussed subsequently, the shock tube techniques have a larger range of operating conditions.

4.2.2 Shock tube technique

Many measurements of the ignition delay time are carried out in shock tubes. Kineticists all over the world use the shock tube as a high-temperature-wave reactor for obtaining rate-coefficient data under diffusion-free conditions because it provides a nearly one-dimensional flow with practically instantaneous heating of reactants.

The gas-phase homogeneous kinetic experiments carried out in the shock wave reactor are characterized by

- high dilution of the reactants by an inert gas (usually argon),
- high sensitivity of the diagnostic techniques employed to monitor species.

In its simplest form, the shock tube consists of a uniform cross-section tube divided into a driver and a driven section separated by a diaphragm [27]. The driven section contains the test gas at low pressure; this is the gas whose physical or chemical processes at high temperature are to be studied. The pressure of the low-molecular-weight gas (hydrogen or helium) in the driver section is increased until the diaphragm burst propagating a shock wave down the tube (driven section) and instantaneously heating the gas. Simultaneously, another shock wave travels in the opposite direction trough the driver section; it is reflected at the end boundary wall of the tube, thus additionally

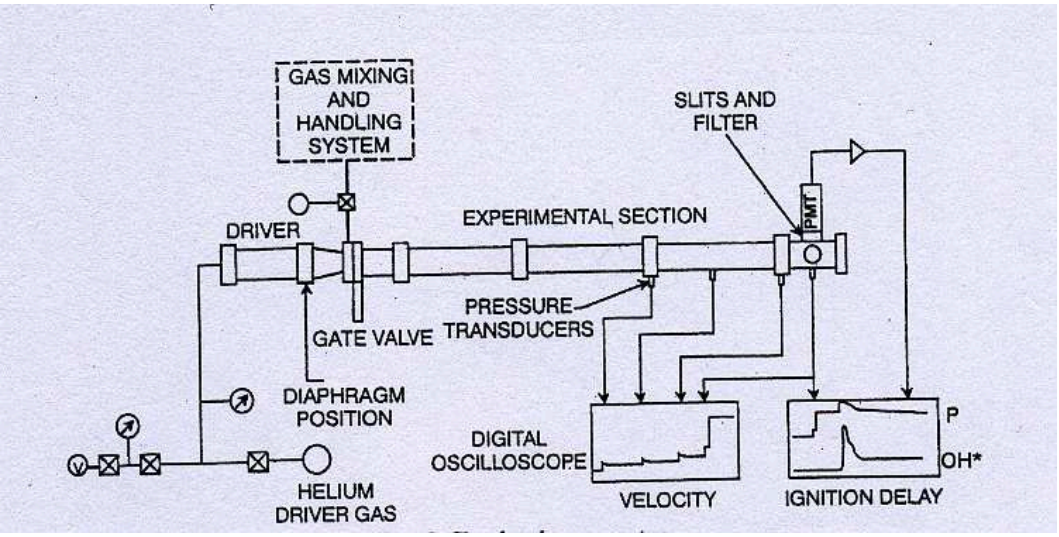

Figure 4.2: Shock tube apparatus.

increasing the temperature and pressure. A schematic illustration of the shock tube it is presented in Fig. 4.2.

Both incident and reflected waves can be used to create test conditions suitable for autoignition studies [28]. The reflected shock technique has been widely used to elucidate the mechanisms and kinetics of methane oxidation reactions. The reflected shock technique has three advantages over the incident shock one:

1. It produces higher temperature.
2. It eliminates spurious ignition caused by diaphragm bursting.
3. It creates an essentially quiescent gas behind the reflected wave.

The incident shock technique suffers from a physical limitation. Shocks strong enough to ignite the fuel mixture can be accelerated by the strong density gradients behind the wave. This phenomenon increases the shock strength along the length of the tube and can lead to detonation.

In thermal ignition processes the temperature increases at once. In explosions of hydrogen or hydrocarbon-air mixtures it is observed that the temperature increases and the explosion takes place after a period of time (ignition-delay time), see Fig. 4.3. According to Warnatz, the delay is characteristic for radical-chain explosions [13].

During the ignition-delay period, the radical-pool population is increasing at an exponential rate. Yet, the amount of fuel consumed, and hence the amount of energy eliberated, is too small to be detected. Thus, important chemical reactions (chain branching, formation of radicals) take place during the induction time, whereas the temperature remains nearly constant, [13].

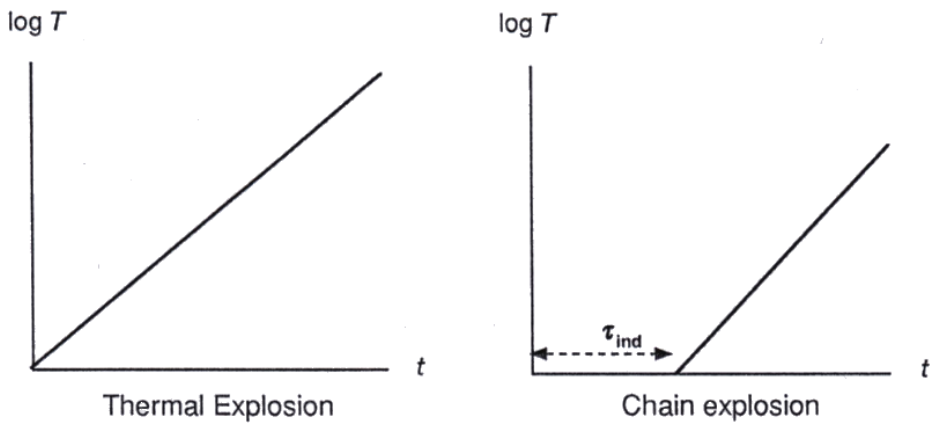

Figure 4.3: Simplified time behavior of thermal (left) and chain-branching explosion (right) in an adiabatic system [13].

Finally, the radical pool becomes large enough to consume a significant fraction of the fuel, and rapid ignition will take place.

The accuracy of the shock tube data depends on the exact measurement of the shock velocity. This is usually determined by measuring the time taken for the shock wave to travel between four or more points separated by a known distance along the length of the tube and taking the average value. The arrival of the shock front is detected by pressure transducers and the time intervals are recorded by an electric timer.

A more sensitive technique for measuring the ignition delay time consists of monitoring of the emission of electronically excited hydroxyl radicals formed during the induction period. Ignition delay times are determined by measuring the time between the arrival of the reflected shock wave and the initial rapid rise of OH emission. Ideal ignition experiments should be independent of the test configuration and free of surface effects.

5 Laminar flames

5.1 General characteristics

While the basis of combustion relies on exothermic chemical reactions, the physical processes involved in combustion are mainly energy and mass transport, heat diffusion, chemical species diffusion, convection and radiation. The combustion reaction appears when the fuel and the oxidizer (in most cases air) are mixed and burned.

On the basis of their main features, flames are classified in two categories:

1. In *premixed flames*, the fuel and oxidizer mix before combustion takes place, see Fig. 5.1.

2. In *nonpremixed flames*, the fuel and oxidizer burn as they mix.

Premixed and nonpremixed flames are subdivided in *laminar* and *turbulent* flames, depending on the laminar or turbulent character of the fluid flow. Examples of nonpremixed laminar flames are candles and wood fire. Nonpremixed turbulent combustion takes place in aircraft turbine engines, Diesel engines and H_2/O_2 rocket motors. Spark-ignited gasoline engines are typical applications of premixed turbulent combustion. This thesis focuses on laminar premixed one-dimensional flat flames.

Premixed flames occur when the fuel and oxidizer are homogeneously mixed prior to ignition. A typical example of premixed laminar flame is the Bunsen burner [12], where the air enters the fuel stream and the mixture burns in the wake of the riser tube walls forming a nicely stable flame.

Premixed laminar flames are characterized by an equivalence ratio, ϕ. The equivalence ratio is defined as the ratio of the actual fuel-oxidant ratio to the ratio for a stoichiometric process. Physically, a stoichiometric reaction can be considered as a unique reaction in which the oxidizer is present in just the right amount required to completely burn the quantity of fuel in the system. If the fuel and oxidizer consume each other completely forming only carbon dioxide and water, then $\phi = 1$, and the flame is called stoichiometric. If there is an excess of oxidizer, the system is called fuel-lean ($\phi < 1$); if there is an excess of fuel, the system is called fuel-rich ($\phi > 1$). If combustion is rich, then fuel fragments may collide to form larger hydrocarbons. This process leads to soot, which are agglomerated solid particles. In a hot flame, soot radiates intensely, giving rich flames their characteristic yellow color. Premixed flames have many advantages in terms of control of temperatures and products and pollution concentration. However, they introduce also some dangers, of which autoignition is an example.

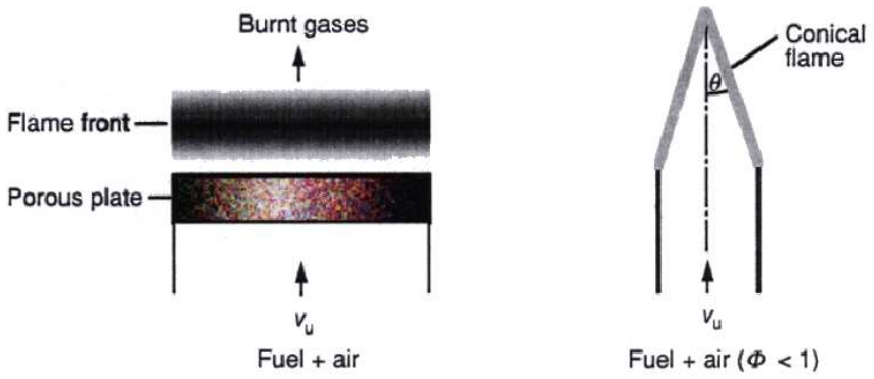

Figure 5.1: Premixed laminar flame (left) and Bunsen Flame (right), [13]

5.2 Flame structures

In this research, an insight into the high-temperature reaction mechanism governing flame propagation is provided by calculations for CH_4, C_2H_6, C_3H_8, and C_4H_{10} flames based on the reaction mechanism shown in Table 1. These calculations show a very simple result, which can be extended to higher alkanes (see Fig. 5.2). After initial attack on the alkane by H, O, and OH, thermal decomposition proves to be the only relevant high temperature reaction of the higher alkyl radicals. Other reactions are completely unimportant for propyl and the higher alkyl radicals. Thus, fast alkyl radical pyrolysis reduces the problem of alkane oxidation to that of the oxidation of methyl and ethyl radicals, which is relatively well understood [29].

An example of a premixed flame is given by the combustion of propane-oxygen mixture. Fig. 5.3 shows the structure of a propane-oxygen flame, which is diluted with argon in order to reduce the temperature, at $p = 100\,\text{mbar}$ [30]. The concentration profiles have been determined by mass spectroscopy (except for OH, which is measured by UV-light absorption), the temperature is measured by Na-D-line reversal (see Warnatz et al. 2006 [13] for more details).

5.3 Flame velocity

Calculations of freely propagating one-dimensional flames have been extensively performed in the study of chemical kinetics. The pioneering works of Warnatz [31–33], Westbrook and Dryer [34–36], Miller et al. [37–39], Dixon-Lewis [40, 41], and Coffee [42–44] have established the viability of using the structure and propagation speed of the one-dimensional, planar, adiabatic premixed flame for the study of flame kinetics. Furthermore, due to its importance to many combustion applications, the laminar flame speed is one of the parameters that are essential to combustion designs. The flame velocity

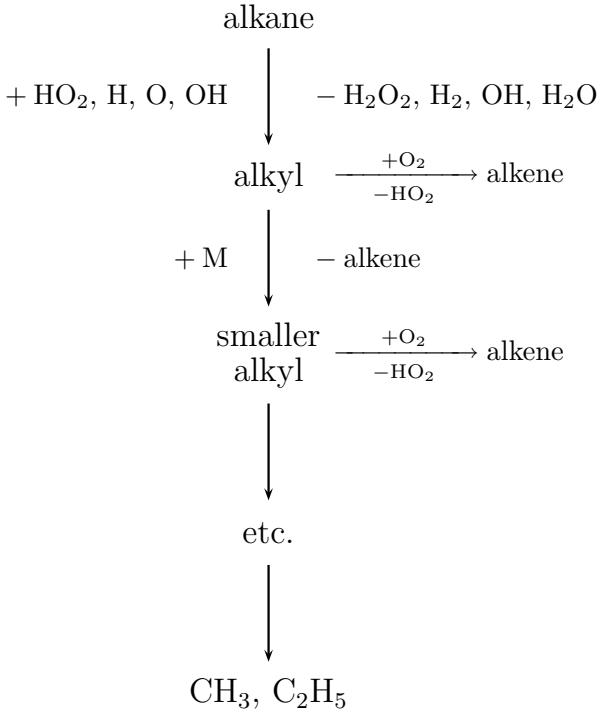

Figure 5.2: Mechanism of alkane oxidation via initial H-atom abstraction, subsequent alkyl radical decomposition, and oxidation of CH_3 and C_2H_5.(*cf.* Warnatz 1981 [29].)

is a vital characteristic of combustion of a fuel. The speed at which a laminar flame propagates through a premixture of fuel and air in theory is dominated by combustion chemistry (in particular the activation energy of reaction). In practice this is not entirely true since surfaces have a profound effect acting as heat sinks but also soaking up radicals and terminating the reaction.

The laminar flame speed is an experimentally determined property characterizing the propagation velocity of the flame normal to the flame front into the reactants under laminar flow conditions.

The laminar flame speed depends strongly on the composition, temperature, and pressure of the unburnt mixture. If the flame velocity of a flat flame, v_L, is less then the velocity of the unburnt gases, v_u, the flames blows off. Therefore, the inequality $v_\mathrm{L} > v_\mathrm{u}$ is necessary for a flat flame. In case of a premixed Bunsen flame attached to the exit of a round pipe, the flame front is approximately flat. It follows (see 5.1) that

$$v_\mathrm{L} = v_\mathrm{u} \sin\theta \,. \tag{5.1}$$

Thus, a measurement of θ and of the inlet gas velocity v_u will lead to a measure of v_L [13].

There are three methods for the measurement of laminar flame speed:

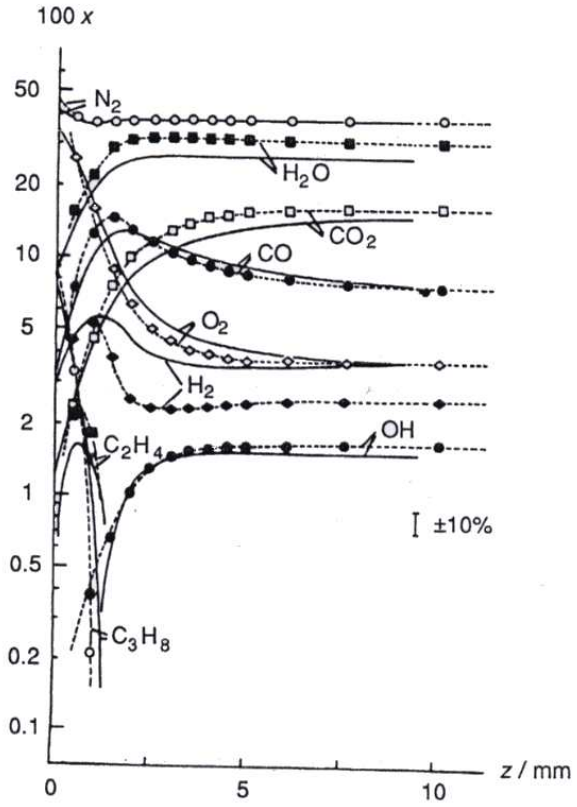

Figure 5.3: Structure of a laminar premixed C_3H_8-O_2 flame diluted with Ar at $p = 100\,\mathrm{mbar}$([13]).

1. Propagation in a tube.
2. Measurement of the growth of a spherical flame kernel in a bomb.
3. Measurement of the cone angle of a Bunsen flame.

Method 1 has a disadvantage: Unless the tube is large, surface effects will affect the result. Calculations of burning velocity are difficult because of internal effects. The burning velocity increases with pressure and reactants temperature.

5.4 Mathematical modelling of premixed laminar flat flames

High-temperature oxidation or combustion of hydrocarbons is very complicated as it is governed by energy and mass transfer as well as chemical kinetics and thermodynamics.

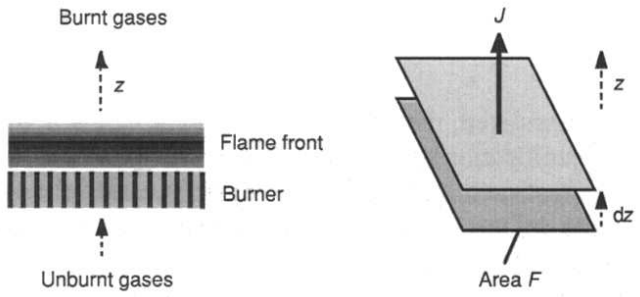

Figure 5.4: Laminar premixed flat flame on a flat burner [13].

Flames result from a complicated interaction of flow, heat conduction, diffusion and chemical reaction; the use of simple flow conditions and simple flame geometries is advisable for their study. A schematic illustration of a laminar premixed flame is shown in Fig. 5.4. This figure shows the burner through which premixed fuel and air flow. The gases emerge from the disk and flow into flame. If one assumes that the burner diameter is large enough, effects at the edge of the burner can be neglected as an approximation. The flat flame front can be observed within the edges (see [13]). The properties in this flame (e.g., temperature and gas composition) depend on the distance from the burner.

In the formulation of the conservation equations for a laminar one-dimensional flat flame, the following assumptions are made [45–47]:

1. The ideal gas law is valid ($p = cRT$).
2. External forces are negligible.
3. The mean free path of the molecules is small compared to the flame thickness, therefore the system can be considered to be continuous.
4. The flame burns at constant pressure.
5. The kinetic energy of the gas flow can be neglected.
6. The reciprocal thermo-diffusion (Dufour) effect can be neglected.
7. Heat flux caused by radiation of gases and particles can be neglected.
8. The system is in local thermal equilibrium.
9. The flame is stationary, i.e., there are no temporal changes.

It is also assumed that the pressure is constant and no momentum equation has to be solved.

5.4.1 General conservation law

The general conservation equation used to derive the conservation equation of mass for the individual species and for the total mass, enthalpy and specific energy of the mixture is

$$\frac{\partial D}{\partial t} + \frac{\partial F}{\partial z} = Q, \tag{5.2}$$

where z is a distance normal to the front flame, t is the time, D is the density of the conserved variable, F is the flux density of the conserved variable and Q is the source (or sink) of the conserved variable. Eq. (5.2) is a statement of the fact that accumulation can be accomplished by influx (or outflux) and by a source (or sink) [12].

5.4.2 The continuity equation

The continuity equation is also called the mass equation and states that, in chemical reactions, mass can neither be created or destroyed. Thus, the source term in the mass equation is zero. In the conservation equation of total mass, the density D in Eq. (5.2) is given by the total mass density, ρ, (in $\mathrm{kg/\,m^3}$). The flux, F, is given as the product of density and flow velocity, (in $\mathrm{kg\,m^{-2}\,s^{-1}}$).

The continuity equation for a one-dimensional system is:

$$\frac{\partial \rho}{\partial t} + \frac{\partial (\rho v)}{\partial z} = 0\,. \tag{5.3}$$

5.4.3 The species conservation equation

The source term of the species conservation equation describes the formation or consumption of species i in chemical reactions. The term is written as

$$Q = M_i \frac{\partial c_i}{\partial t} = r_i\,,$$

where M_i is the molar mass of species i in $\mathrm{kg/\,mole}$, $\partial c_i/\partial t$ is the chemical rate of production of species i in chemical reactions, in $\mathrm{mole\,m^{-3}\,s^{-1}}$ and, r_i is the chemical rate of production, in $\mathrm{kg\,m^{-3}\,s^{-1}}$.

The density, D, is given by the partial density, ρ_i, of species i. The partial density is defined as the mass of species i per unit volume:

$$\rho_i = \frac{m_i}{V} = \left(\frac{m_i}{m}\right)\left(\frac{m}{V}\right) = w_i \rho\,.$$

The flux, F, is given by

$$F = \rho_i v_i = w_i \rho_i v_i\,,$$

where v_i is the flow velocity of species i. The flux units are $\mathrm{kg\,m^{-2}\,s^{-1}}$. Inserting these terms in Eq. (5.2), the following equation is obtained:

$$\frac{\partial(\rho w_i)}{\partial t} + \frac{\partial(\rho w_i v_i)}{\partial z} = r_i. \tag{5.4}$$

The flow velocity of the species i can be written as

$$v_i = v + V_i\,, \tag{5.5}$$

where v is the flow velocity (or mean mass velocity) and V_i is the molecular diffusion velocity associated with molecular transport (due to concentration gradients of the species i). After some manipulations of the equations, the result is

$$w_i\frac{\partial \rho}{\partial t} + \rho\frac{\partial w_i}{\partial t} + \rho v\frac{\partial w_i}{\partial z} + w_i\frac{\partial(\rho v)}{\partial z} + \frac{\partial j_i}{\partial z} = r_i\,, \tag{5.6}$$

where j_i is called the diffusion flux of species i:

$$j_i = \rho w_i V_i = \rho_i V_i\,. \tag{5.7}$$

From Eq. (5.3) and (5.7), the species mass conservation equation is obtained:

$$\rho\frac{\partial w_i}{\partial t} + \rho v\frac{\partial w_i}{\partial z} + \frac{\partial j_i}{\partial z} = r_i\,. \tag{5.8}$$

5.4.4 The enthalpy equation

If we recall Eq. (5.2), the terms are given by

$$D = \sum_i \rho_i h_i = \sum_i \rho w_i h_i$$
$$F = \sum_i \rho_i v_i h_i + j_q = \sum_i \rho v_i w_i h_i + j_q$$

and $Q = 0$ (energy conservation).

In these equations, h_i is the specific enthalpy of species i (in $\mathrm{J/\,kg}$) and j_q is the heat flux caused by energy transport (due to temperature gradients). The term $\sum_i \rho_i v_i h_i$ describes the change of enthalpy due to the flow of chemical species. The flow of the species, v_i, is written as the sum of the mass velocity and the diffusion velocity, V_i:

$$v_i = v + V_i\,.$$

Substituting the terms in Eq. (5.2), the energy equation formulated in terms of enthalpy is obtained:

$$\sum_i \frac{\partial}{\partial z}\left(\rho v w_i h_i\right) + \sum_i \frac{\partial}{\partial z}\left(\rho V_i w_i h_i\right) + \frac{\partial j_q}{\partial z} + \sum_i \frac{\partial}{\partial t}\left(\rho w_i h_i\right) = 0\,. \tag{5.9}$$

These conservation equations form a system of differential equations, which are solved by numerical methods.

5.5 Heat and mass transport

Empirical observations show that heat conduction is characterized by heat transport due to temperature gradients. Fourier's law is an empirical law based on observation and states that the heat flux density, j_q, is proportional to the temperature gradient. For the heat flux density, j_q, the law can be written in the form

$$j_q = -\lambda \frac{\partial T}{\partial z}\,, \tag{5.10}$$

where j_q is given in units of $\mathrm{J}/\,\mathrm{m}^2\,\mathrm{s}$, and λ is the heat conductivity of the mixture in units of $\mathrm{J}/\,\mathrm{K}\,\mathrm{m}\,\mathrm{s}$.

Diffusion in gases is characterized by mass transport due to concentration gradients. Mass flux, j_i, can be written in an extended form of Fick's law,

$$j_i = \frac{c^2}{\rho} M_i \sum_j M_j D_{ij} \frac{\partial x_j}{\partial z} - \frac{D_i^{\mathrm{T}}}{T} \frac{\partial T}{\partial z}\,, \tag{5.11}$$

where j_i is given in units of $\mathrm{kg}/\,\mathrm{m}^2\,\mathrm{s}$, c is the molar concentration in $\mathrm{mole}/\,\mathrm{m}^3$, D_{ij} are the multicomponent diffusion coefficients, in units of $\mathrm{m}^2/\,\mathrm{s}$, x_j are the mole fractions, and D_i^{T} is the thermal diffusion coefficient of species i, in units of $\mathrm{kg}/\,\mathrm{m}\,\mathrm{s}$. Thermal diffusion is also called the Soret effect and is characterized by species transport due to the temperature gradient. Eq. (5.11) can be written in a simplified form,

$$j_i = -D_i^{\mathrm{M}} \rho \frac{w_i}{x_i} \frac{\partial x_i}{\partial z} - \frac{D_i^{\mathrm{T}}}{T} \frac{\partial T}{\partial z}\,, \tag{5.12}$$

where D_i^{M} is the diffusion coefficient for species i into the mixture of the other species.

6 Computer modelling

One of the many challenges in combustion science is to develop the understanding of the pathways of formation of exhaust gases. Combustion phenomena are characterized by chemical and physical processes. Knowledge of chemical kinetics is essential to understand these processes in detail. This knowledge can be applied to formulate strategies to reduce the formation of pollutants. Development of detailed kinetic mechanisms is critical because they can be dynamically reduced and subsequently used in engineering applications such as Diesel engine simulations [48].

Over the last decade, numerical modelling has gained in importance, development and modelling of detailed chemical reaction schemes being vital in understanding the nature of combustion. Due to increased computer performance, numerical computations can be applied at an acceptable cost. On the other hand, the experiments are still expensive and very time-consuming. However, since numerical models need to be validated with experimental data, they can never fully replace the experimental studies. As a result of consistent pursuit of mechanism development over several decades, detailed mechanisms with hundreds of elementary reactions and species are now available for the combustion of alkanes. The detailed reaction mechanisms describe how a reaction takes place at the molecular level, which bonds are broken or formed and in which order, and what the relative rates of the steps are. Therefore, the understanding of properties of reactants and products is necessary. The requirements for a valid mechanism are: Its result must equal the overall balanced equation, its predictions of intermediates must not be contrary to the experimental observations and its predicted rate law must agree with the experimental data. When more then one mechanism is consistent with the data, new experiments are needed to test their validity and choose between mechanisms.

The chemical reaction scheme presented in this work was developed on the basis of a previously available one [49] and includes the oxidation reactions of high-temperature combustion of H_2, CO, CH_4, C_2H_6, C_3H_8 and C_4H_{10}. The mechanism consists of 412 elementary reactions (without counting the duplicate reactions) or 782 forward and backward reactions of 61 species and is based on a rate-data compilation by Baulch et al.(2005) [2]. It is documented by Heghes et al. (2005) [3] and Warnatz and Heghes (2006) [4]. The approximate temperature range is from 900 K to 2500 K. Rate coefficients are given in the three-parameter form

$$k = A(T/\mathrm{K})^b \exp(-E_\mathrm{a}/RT), \tag{6.1}$$

where A is the preexponential factor in units of $\mathrm{cm^3\,molecule^{-1}\,s^{-1}}$, b is the dimensionless temperature exponent and E_a is the activation energy in $\mathrm{kJ/\,mol}$ ($R = 8.314 \times$

10^{-3} kJ/ mol. K). For pressure-dependent reactions, values of the rate coefficients are calculated according to the modified Lindemann-Hinshelwood formalism proposed by Troe [16, 50]. In some cases, only the low-pressure limit rate coefficient k_0 is available, and collision efficiencies have been reported relative to H_2 [51]:

H_2	O_2	N_2	H_2O	CO	CO_2	CH_4	Ar	He
1.0	0.4	0.4	6.5	0.75	1.5	3.0	0.35	0.35

The rate coefficients of the reactions exhibiting high sensitivity are thought to strongly influence the modelling of the combustion processes. To reduce significantly the discrepancy between simulations and experiments, the rate coefficients may have been slightly changed, but always within the estimated uncertainty.

Thermochemical properties of the species are tabulated as a function of temperature. These tables includes values of thermodynamic properties based on the experimental data, also complemented by theoretical calculations. In this work, most of thermodynamic data is taken from a single publication, the one describing the Sandia Chemkin code [19] which is based mainly on the JANAF tables [18]. Thermochemical data not listed there were taken from Benson 1976 [52].

For each development step of the mechanism and for each fuel considered, premixed laminar flames have been calculated, as well as ignition-delay times, and compared with experiments for the largest possible condition range (initial temperature, pressure, equivalence ratio). Calculations of flame velocities and ignition-delay times are performed to test the validity of the developed mechanism. The steps used for validating the mechanism are shown in a general structure in Fig. 6.1. Measurements of ignition-delay times

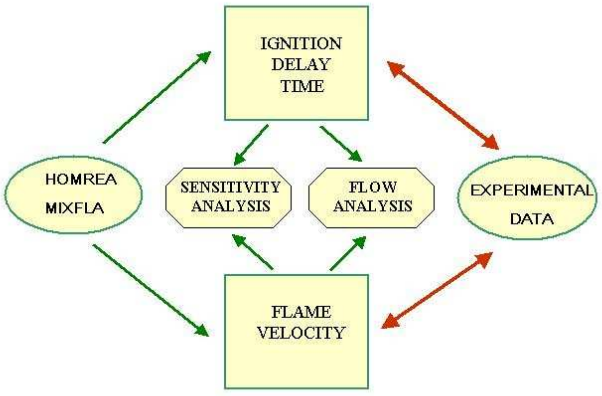

Figure 6.1: General structure of the modelling process.

are made behind reflected shock waves by observing the time delay in the onset of emission from excited hydroxyl radicals. Measurements of flame velocities are studied in the laboratory mainly in burner-stabilized flames.

Sensitivity analyses have been performed in order to identify the rate-limiting reactions and to understand the behavior of the chemical system under different conditions. The rates of elementary reactions in combustion processes differ greatly. Some reactions are so fast (and therefore not rate-limiting) that the accuracy of the rate coefficients only has a minor influence on the results of the mathematical modelling. For sensitive reactions, on the other side, rate coefficients values must be well known.

Furthermore, reaction flow analyses have been conducted to elucidate the important chemical pathways over a wide range of conditions. Integral flow analysis gives the percentage contributions of different reactions to the formation (or consumption) of chemical species.

In the majority of reactions, the recommended Arrhenius parameters by Baulch et al. 2005 [2] were used. Nevertheless, to obtain a better agreement between simulations and experiments, for a small number of reactions the recommended values had to be varied within the limits of experimental error of these reactions, depending on the positive or negative sensitivity of the reaction. In the case of ignition, the positive sensitivity has the meaning of OH radicals formation. For example, if we want to increase the calculated ignition-delay time in order to obtain a better agreement with experimental data, we need to decrease the values of the rate coefficients for the reactions showing a positive sensitivity, and vice-versa. Regarding the flame velocity, positive sensitivity indicates the formation of H atoms. If we want to increase the calculated flame velocity in order to obtain a better agreement with the experiments, we have to increase the values of the rate coefficients for the reactions showing a positive sensitivity and vice-versa. The rate coefficients for the following reactions have been slightly modified within the error limits:

$$\mathrm{HCCO + O \rightarrow CO + CO + H} \tag{6.2}$$
$$\mathrm{C_2H + O_2 \rightarrow HCCO + O} \tag{6.3}$$
$$\mathrm{C_2H + O_2 \rightarrow CO_2 + CH} \tag{6.4}$$
$$\mathrm{C_2H_2 + O \rightarrow {}^3CH_2 + CO} \tag{6.5}$$
$$\mathrm{C_2H_2 + H \rightarrow C_2H + H_2} \tag{6.6}$$
$$\mathrm{C_2H_2 + OH \rightarrow H_2O + C_2H} \tag{6.7}$$
$$\mathrm{C_2H_3 + O_2 \rightarrow CH_2O + CHO} \tag{6.8}$$
$$\mathrm{C_2H_3 + M(1) \rightarrow C_2H_2 + H + M(1)} \tag{6.9}$$
$$\mathrm{C_2H_4 + M(1) \rightarrow C_2H_2 + H_2 + M(1)} \tag{6.10}$$
$$\mathrm{C_2H_4 + OH \rightarrow C_2H_3 + H_2O} \tag{6.11}$$
$$\mathrm{C_2H_5 + O_2 \rightarrow C_2H_4 + HO_2} \tag{6.12}$$

$$C_2H_5 + M(1) \rightarrow C_2H_4 + H + M(1) \quad (6.13)$$

$$C_2H_5OH + OH \rightarrow CH_3CHOH + H_2O \quad (6.14)$$

$$C_2H_5OH + OH \rightarrow CH_2CH_2OH + H_2O \quad (6.15)$$

The values of their parameters can be seen in Table A.1 of Appendix A.

The value of the rate coefficient of Reaction (6.2) is recommended by Baulch et al. 2005 [2] and is based on the studies of Vinckier et al. [53] and Frank et al. [54]:

$$k = 1.6 \times 10^{-10}\,\mathrm{cm^3\,molecule^{-1}\,s^{-1}}\,, \quad (6.16)$$

over the range 280 K-2500 K, where $A = 9.636 \times 10^{13}\,\mathrm{cm^3\,mol^{-1}\,s^{-1}}$, $n = 0$ and $E_a = 0.0\,\mathrm{kJ\,mol^{-1}}$. The reliability is given by $\Delta \log k = \pm 0.2$ over the range 280 K-2500 K. The value of the rate coefficient considered in our mechanism ($A = 1.53 \times 10^{14}\,\mathrm{cm^3\,mol^{-1}\,s^{-1}}$, $n = 0$ and $E_a = 0.0\,\mathrm{kJ\,mol^{-1}}$) was obtained by modifying the recommended value of the rate coefficient within the error limit (increasing it within the maximum error limit).

Unfortunately, for Reactions (6.3) and (6.4) only few data are available at high temperatures. The preferred value of the rate coefficient given by Baulch et al. 2005 [2] is obtained from a fit to the data of Lander et al. [55], Opansky et al. [56], Van Look and Peeters [57], Thiesmann and Taatjes [58], Chastaing et al. [59] and Vakhtin et al. [60] which are in excellent agreement over the range 150 K-700 K,

$$k = 2.7 \times 10^{-10} T^{-0.35}\,\mathrm{cm^3\,molecule^{-1}\,s^{-1}}\,, \quad (6.17)$$

over the range 200-1500 K. The reliability is given by $\Delta \log k = \pm 0.2$ at 200 K, rising to ± 0.3 at 1500 K. No branching ratio is known. In order to get a better agreement between simulations and experimental data, we attributed a higher importance for the Reaction (6.3) ($k_{(6.3)} : k_{(6.4)} = 9 : 1$). The new value of the rate coefficients are obtained by increasing the value of the recommended rate coefficient within the maximum error limit. For Reaction (6.3), $A = 3.25 \times 10^{14}\,\mathrm{cm^3\,mol^{-1}\,s^{-1}}$, $n = -0.35$ and $E_a = 0.0\,\mathrm{kJ\,mol^{-1}}$. For Reaction (6.4), $A = 2.92 \times 10^{15}\,\mathrm{cm^3\,mol^{-1}\,s^{-1}}$, $n = -0.35$ and $E_a = 0.0\,\mathrm{kJ\,mol^{-1}}$. However more studies are required before any recommendations can be made.

For Reaction (6.5), the rate coefficient is well defined over a wide range of temperatures. The expression of k recommended by Baulch et al. 2005 [2] is:

$$k = 0.39 \times 10^{-15} T^{1.40} \exp(-1110/T)\,\mathrm{cm^3\,molecule^{-1}\,s^{-1}}\,, \quad (6.18)$$

over the range 200 K-2500 K. The reliability is given by $\Delta \log k = \pm 0.2$ over the range 200 K-2000 K, rising to ± 0.3 at 2500 K. The Arrhenius diagram drawn by Baulch et al. 2005 [2] shows a number of studies ([61–72]) which are in a good agreement with their preferred expression. The branching ratio of the Reaction (6.5) is $k_1/k = 0.2$. The new value of the rate coefficient ($A = 1.48 \times 10^8\,\mathrm{cm^3\,mol^{-1}\,s^{-1}}$, $n = 1.4$ and $E_a = 9.23\,\mathrm{kJ\,mol^{-1}}$) was obtained by modifying the recommended value of the rate coefficient within the error limit (decreasing it within the error limit).

The recommended expression of Baulch et al. 2005 [2] of k for Reaction (6.6) is:

$$k = 1.67 \times 10^{-14} T^{1.64} \exp(-15250/T)\,\mathrm{cm^3\,molecule^{-1}\,s^{-1}}\,, \tag{6.19}$$

over the range 300 K-3000 K. The reliability is given by $\Delta \log k = \pm 0.2$ at 300 K, rising to ± 0.7 at 3000 K. The rate coefficient taken in our mechanism ($A = 2.01 \times 10^9\,\mathrm{cm^3\,mol^{-1}\,s^{-1}}$, $n = 1.64$ and $E_\mathrm{a} = 126.79\,\mathrm{kJ\,mol^{-1}}$) is obtained by decreasing the recommended value within the maximum error limit.

The mechanism of the Reaction (6.7) was discussed in detail by Miller and Melius [73], based on ab initio calculations. At high temperatures, the reaction proceeds to HOC_2H+ H, CH_2CO+H, CH_3+CO and C_2H+H_2O. Miller and Melius [73] provide rate parameters for each of the channels, their overall rate being in a good agreement with the expression recommended by Baulch et al. 2005 [2]. The channel leading to CH_3 + CO is of low efficiency over the whole range. The channel discussed here (C_2H+H_2O) is considered to be predominant (82% at 2000 K). The recommended expression of Baulch et al. 2005 [2] for k is:

$$k = 1.3 \times 10^{-10} \exp(-6800/T)\,\mathrm{cm^3\,molecule^{-1}\,s^{-1}}\,, \tag{6.20}$$

over the range 1000 K-2000 K. The reliability is given by $\Delta \log k = \pm 0.5$ at 1000 K, rising to $\pm 1.$ at 2000 K. The new value of the rate coefficient taken in our mechanism ($A = 6.42 \times 10^{14}\,\mathrm{cm^3\,mol^{-1}\,s^{-1}}$, $n = 0$ and $E_\mathrm{a} = 56.54\,\mathrm{kJ\,mol^{-1}}$) is obtained increasing the recommended rate within the maximum error limit.

The rate coefficient of the Reaction (6.8) has the following expression:

$$k = 6.4 \times 10^{-12} \exp(120/T)\,\mathrm{cm^3\,molecule^{-1}\,s^{-1}} \tag{6.21}$$

over the range 290 K-900 K. The reliability is given by $\Delta \log k = \pm 0.1$ at 290 K, rising to ± 0.3 at 900 K. The experimental studies of Marinov and Malte [74] and Hidaka et al. [75] and the theoretical studies of Bozzelli and Dean [76](using RRK theory) and Mebel et al. [77](using ab initio methods and RRKM calculations) are compatible with the preferred expression of Baulch et al. 2005 [2]. The new rate coefficient taken in our mechanism ($A = 7.71 \times 10^{12}\,\mathrm{cm^3\,mol^{-1}\,s^{-1}}$, $n = 0$ and $E_\mathrm{a} = -1.0\,\mathrm{kJ\,mol^{-1}}$) is obtained by increasing its value within the maximum error limit.

For Reaction (6.9), Baulch et al. 2005 [2] take the recent values of Knyazev and Slagle [78] which are consistent with the data of Payne and Stief [79], Keil et al. [80], Ellul et al. [81], and Gordon et al. [82,83] for the reverse recombination reaction. The F_c valued are from Reference [78]. The rate coefficient expressions recommended by Baulch et al. 2005 [2] are:

$$k_0 = 4.3 \times 10^3 T^{-3.4} \exp(-18020/T), \mathrm{M} = \mathrm{N_2},\ \mathrm{cm^3\,molecule^{-1}\,s^{-1}} \tag{6.22}$$

$$k_\infty = 3.9 \times 10^8 T^{1.62} \exp(-18650/T),\ \mathrm{s^{-1}} \tag{6.23}$$

$$F_c = 0.35, \mathrm{M} = \mathrm{N_2}. \tag{6.24}$$

The reliabilities are given by $\Delta \log k_0 = \pm 0.3$ for M = N_2 over the range 200 K-2000 K and $\Delta \log k_\infty = \pm 0.3$ over the range 200 K-2000 K. The new rate coefficients value taken in our mechanism (see Appendix) are modified for both, k_0 and k_∞ within the maximum error limit (for k_0, $A = 3.24 \times 10^{27}\,\mathrm{cm^3\,mol^{-1}\,s^{-1}}$, $n = -3.4$ and $E_a = 149.82\,\mathrm{kJ\,mol^{-1}}$; for k_∞, $A = 7.8 \times 10^8\,\mathrm{cm^3\,mol^{-1}\,s^{-1}}$, $n = 1.62$ and $E_a = 155.06\,\mathrm{kJ\,mol^{-1}}$).

For Reaction (6.10), the rate data recommended by Baulch et al. 2005 [2] are based on an average of data reported by Roth and Just [84], Just et al. [85], Tanzawa and Gardiner [86] and Zelson et al. [87]. The recommended expression is:

$$k_0 = 3.4 \times 10^{-7} T \exp(-39390/T)\,\mathrm{cm^3\,molecule^{-1}\,s^{-1}}, \mathrm{M = Ar} \qquad (6.25)$$

over the range 1500 K-3200 K, with reliability given by $\Delta \log k_0 = \pm 0.3$ for M = Ar over the range 1500 K-3200 K. There is no information from experiments about the high pressure rate coefficient. The rate coefficient taken in our mechanism ($A = 2.92 \times 10^{17}\,\mathrm{cm^3\,mol^{-1}\,s^{-1}}$, $n = 1$ and $E_a = 327.49\,\mathrm{kJ\,mol^{-1}}$) is obtained by decreasing its recommended value within the maximum error limit, in order to obtain a better agreement with experimental data.

For Reaction (6.11), the rate coefficient measurements have been carried out by monitoring the OH removal, which has usually been assumed to occur by hydrogen abstraction (see (6.11)). Recent ab-initio calculations by Hippler and Viskolcz [88] have caste doubt on the importance of this direct abstraction channel [2]. On the other side, Hidaka et al. [75] find that the results in their shock-tube study of C_2H_4 oxidation at 1100 K-2100 K are best explained in terms of $C_2H_3 + H_2O$ formation. However, further experimental studies are required to test these possibilities. We now take the formation of $C_2H_3 + H_2O$ being the most important channel, with the previous recommended value of Baulch et al. [89],

$$k = 3.4 \times 10^{-11} \exp(-2990/T)\,\mathrm{cm^3\,molecule^{-1}\,s^{-1}}\,, \qquad (6.26)$$

over the range 650 K-1500 K, with the reliability $\Delta \log k_0 = \pm 0.5$ over the range 650 K-1500 K. The rate coefficient taken in our mechanism ($A = 6.48 \times 10^{12}\,\mathrm{cm^3\,mol^{-1}\,s^{-1}}$, $n = 0$ and $E_a = 24.90\,\mathrm{kJ\,mol^{-1}}$) is obtained by decreasing the recommended rate coefficient value within the maximum error limit, in order to obtain a better agreement with experimental data.

The rate coefficient recommended by Baulch et al. 2005 [2] for Reaction (6.12) is:

$$k = 1.0 \times 10^{-13}\,\mathrm{cm^3\,molecule^{-1}\,s^{-1}}\,, \qquad (6.27)$$

over the range 700 K-1500 K, with reliability $\Delta \log k = \pm 0.2$ at 700 K, rising to ± 0.4 at 1500 K. The preferred value is based on the data of Slagle et al. [90] and Wagner et al. [91]. The values obtained from the theoretical model of Miller and Klippenstein [92] are in excellent agreement with the recommended value of Baulch et al. 2005 [2]. The value of the rate coefficient taken in our mechanism was modified (by decreasing its recommended value) within the maximum error limit ($A = 2.41 \times 10^{10}\,\mathrm{cm^3\,mol^{-1}\,s^{-1}}$, $n = 0$ and $E_a = 0.0\,\mathrm{kJ\,mol^{-1}}$).

For Reaction (6.13), the rate coefficients expressions recommended by Baulch et al. 2005 [2] are:

$$k_0 = 1.7 \times 10^{-6} \exp(-16800/T), \mathrm{M} = \mathrm{C_2H_6},\ \mathrm{cm^3\,molecule^{-1}\,s^{-1}} \tag{6.28}$$

$$k_\infty = 8.2 \times 10^{13} \exp(-20070/T),\ \mathrm{s^{-1}} \tag{6.29}$$

$$F_c = 0.25 \exp(-T/97) + 0.75 \exp(-T/1379), \mathrm{M} = \mathrm{C_2H_6}. \tag{6.30}$$

The reliabilities are given by $\Delta \log k_0 = \pm 0.3$ for $\mathrm{M} = \mathrm{C_2H_6}$ over the range 700 K-900 K, $\Delta \log k_\infty = \pm 0.3$ over the range 700 K-1100 K, $\Delta F_c = \pm 0.1$ for $\mathrm{M} = \mathrm{C_2H_6}$ over the range 700 K-1100 K. This evaluation is unchanged from the previous evaluation of Baulch et al. [89] and is based on a theoretical analysis (using unimolecular rate theory [15, 50]) of the rate data of Loucks and Laidler [93], Pacey and Wimalasena [94–96], Simon et al. [97], and Feng et al. [98]. The values of the rate coefficients taken in our mechanism, for both k_0 and k_∞ were modified (by decreasing their recommended value by Baulch et al. 2005 [2]) within the maximum error limit (for k_0, $A = 3.65 \times 10^{18}\,\mathrm{cm^3\,mol^{-1}\,s^{-1}}$, $n = 0$ and $E_\mathrm{a} = 139.68\,\mathrm{kJ\,mol^{-1}}$; for k_∞, $A = 4.1 \times 10^{13}\,\mathrm{cm^3\,mol^{-1}\,s^{-1}}$, $n = 0$ and $E_\mathrm{a} = 166.80\,\mathrm{kJ\,mol^{-1}}$).

For reaction $\mathrm{C_2H_5OH+OH}$ there are three possible channels, $\mathrm{CH_3CHOH+H_2O}$ (6.14), $\mathrm{CH_2CH_2OH + H_2O}$ (6.15), and $\mathrm{CH_3CH_2O + H_2O}$. The expression of k recommended by Baulch et al. 2005 [2] is given by

$$k = 3.0 \times 10^{-17} T^{1.78} \exp(425/T)\,\mathrm{cm^3\,molecule^{-1}\,s^{-1}}\,, \tag{6.31}$$

where $k = k_1 + k_2 + k_3$ over the range 290-1250 K, with reliability $\Delta \log k = \pm 0.1$ at 290 K, rising to ± 0.2 at 1250 K. The branching ratio for the first channel, Reaction (6.14), is based on the study of Meier et al. [99,100], who obtained $k_1/k = (0.75 \pm 0.15)$ at 298 K. The branching ratio for the second channel, Reaction (6.15), recommended by Baulch et al. 2005 [2] is based on Hess and Tuly study [101], $k_2/k = 0.15$ at 600 K. The values of the rate coefficients taken in our mechanism in case of Reactions (6.14)($A = 2.14 \times 10^7\,\mathrm{cm^3\,mol^{-1}\,s^{-1}}$, $n = 1.78$ and $E_\mathrm{a} = -3.53\,\mathrm{kJ\,mol^{-1}}$) and (6.15)($A = 1.13 \times 10^6\,\mathrm{cm^3\,mol^{-1}\,s^{-1}}$, $n = 1.78$ and $E_\mathrm{a} = -3.53\,\mathrm{kJ\,mol^{-1}}$) were modified (by increasing the value of the recommended rate coefficients by Baulch et al. 2005 [2]) within the error limits.

6.1 Simulations of ignition-delay times

The validation of the reaction mechanism is provided by comparison of computed ignition-delay times with corresponding experimental results from shock-tube studies. Homogenous simulations were performed using the software package HOMREA [102], written as a FORTRAN code (FORTRAN 77). The code allows for calculation of ignition-delay times, time-varying concentrations of species, temperature and pressure, sensitivity coefficients, and chemical flows. In the governing equations, the following assumptions are made:

1. The ideal gas approximation is valid.

2. The heat flux caused by radiation of gases is negligible.

The expressions for the concentration variables are [103]:

$$p \text{ and } T \text{ constant:} \qquad \dot{c}_i = \omega_i + c_i \left\{ \frac{\dot{p}}{p} - \frac{RT \sum \dot{\omega}_i}{p} - \frac{\dot{T}}{T} \right\}, \qquad i = 1, 2, \ldots, n, \quad (6.32a)$$

$$p \text{ and } V \text{ constant:} \qquad \dot{c}_i = \omega_i - c_i \frac{\dot{V}}{V}, \qquad i = 1, 2, \ldots, n, \quad (6.32b)$$

where c is the concentration (mole/m^3), n is the number of species from the mixture considered, p is the pressure (bar), R is the gas constant, T is the temperature (K), V is the relative volume (m^3), ω_i is the chemical source term (mole/s $\cdot$ m^3). The temperature can be calculated from enthalpy conservation assuming adiabaticity.

To perform ignition-delay time simulations, input and thermodynamic data, as well as the mechanism, are needed. The input data control the execution of the program. An example of input data is:

```
COMMENT:Mechanism of the CH4 Reactions
----**********************************************************************
OPTIONS.....................(Format 7(A4,2X,I3,1X), end with -END -)
VPRO     /         /TIGNIT  3/         /         /         /         /
TABLES  2/PLOTS   2/OUTP    2/         /         /         /         /
LSEN    2/         /         /         /         /         /         /
END      /         /         /         /         /         /         /
----**********************************************************************
SPECIES.....................(Format  7(2A4,1X,A1), end with -END -)
H       ,H2      ,CH      ,O2      ,OH      *H2O     ,CHO
3CH2    ,HO2     *H2O2    ,O       ,CO      ,CO2     ,CH3
CH3O    ,CH3O2   ,CH4     ,CH3OH   ,CH3O2H  ,CH2OH   ,CH2O
C2H2    ,C2H4    ,C2H6    ,1CH2    ,C2H     ,HCCO    ,C2H3
C4H2    ,CH2CO   ,CH2CHO  ,CH3CO   ,C3H6    ,C3H4    ,CH3CHO
C2H5    ,C2H5O   ,CH3CHOH ,CH2CH2OH,C2H5OH  ,AR
END
----**********************************************************************
CONDITIONS.....(FORMAT     A8,1X,E10.2,14X,E10.2, end with -END-)
----****
CH4     :  3.33E-02
O2      :  6.66E-02
AR      : 90.00E-02
----****
T       : 16.88E+02               0.00E+00   KELVIN
P       :  3.94E-01               0.00E+00   BAR
V       :  1.00E+00        TIME =  0.00E+00   DIMENSIONLESS (RELATIVE)
----****                                     *
----****                                      OUTPUT CONTROL
NT      =  2.00E+03                           NUMBER OF TIMESTEPS
TSTA    =  0.00E-00                            TIME OF FIRST OUTPUT
TEND    =  1.00E-02
----****                                     *
```

```
----****                                    INTEGRATION CONTROL
STEP    =  1.00E-16                          INITIAL STEPSIZE
RTOL    =  1.00E-03                          RELATIVE TOLERANCE
ATOL    =  1.00E-09                          ABSOLUTE TOLERANCE
RTOS    =  1.00E-02                          REL. TOL. FOR SENSITIVITY
ATOS    =  1.00E-07                          ABS. TOL. FOR SENSITIVITY
END
----*****************************************************************
COLLISION EFFICIENCIES....
M(1)    =H2      +H2O     +O2      +AR      +CO      +CO2     +CH4
          1.0      6.5      0.4      0.35     0.75     1.5      3.0
M(2)    =H2      +H2O     +O2      +AR      +CO      +CO2     +CH4
          1.0      2.55     0.4      0.15     0.75     1.5      3.0
M(3)    =H2      +H2O     +O2      +AR      +CO      +CO2     +CH4
          1.0      6.5      0.4      0.29     0.75     1.5      3.0
M(4)    =H2      +H2O     +O2      +AR      +CO      +CO2     +CH4
          1.0      6.5      0.4      0.35     0.75     1.5      0.66
END
```

In the input file, the species are defined and also the conditions of the reactions. The first line represents the heading. In the next line appears in the format A4 the word -OPTI(ONS)-. In the following lines, in the format options, finally closed by the string -END-. The meaning of the options from this example are:

- VPRO = Volume (or density) profile specified.
- TIGN(IT) = Induction time calculated from profile of species.
- TABL(ES) = Printing of tables at the end of the computation ((1) for species marked with '$*$' in species list, (2) for all species).
- PLOT(S) = Printing of small plots at the end of the computation ((1) for species marked with '$*$' in species list, (2) for all species).
- OUTP(UT) = Printing the results during integration
- LSEN(SI) = (1) Calculation of local sensitivities for species marked with '$*$' in species list and with respect to reactions marked with '$*$' in the reaction list; (2) for all species; (3) with additional information on integration.

Species names are followed by the initial mole fraction (or volume part; normalization to unit is automatic), 'T' is the temperature in K followed by a time in s, 'P' is the pressure in bar followed by a time in s, 'V' is a relative volume followed by a time in s. The time interval with defined temperatures must be larger than the integration time interval; if not, the last defined temperature is used for the times following.

The following lines define NT - the number of time steps, TSTA - the start time in s, TEND - the end time in s, STEP - an estimate of the initial time step in s, ATOL and RTOL - the absolute and relative tolerances for the simulation of mole fractions and temperatures and ATOL and RTOL - for the simulation of sensitivities.

The other data set needed is the mechanism file. This contains the reaction scheme, for example

```
MECHANISM  H2 O2
****************************************
****     01.   H2-O2 React. (no HO2, H2O2)
****************************************
----CODATA 2003,k=(2.065E+14/-0.097/62.853),
----(800-3500K, dlogk=+-0.1 at 800K rising to +-0.2 at 3500K)
O2      +H       =OH      +O                  2.065E+14 -0.097    62.853
----CODATA 2003,k=(3.818E+12/0/33.256+1.025E+15/0/80.23),
----(298-3300 K, dlogk=+-0.2 over the range 298-3300K)
H2      +O       =OH      +H                  3.818E+12  0.000    33.256
**** BEGIN DUPLICATE REACTION
H2      +O       =OH      +H                  1.025E+15  0.000    80.230
**** END DUPLICATE REACTION
----CODATA 2003,k=(2.168E+08/1.52/14.466),
----(250-2500 K, dlogk=+-0.1 at 250K rising to +-0.3 at 2500K)
H2      +OH      =H2O     +H                  2.168E+08  1.520    14.466
----CODATA 2003,k=(3.348E+04/2.42/-8.064),
----(250-2400 K, dlogk=+-0.15 over the range 250-2400K)
OH      +OH      =H2O     +O                  3.348E+04  2.420    -8.064
****************************************
****     02.   Recombination Reactions
****************************************
----CODATA 2003, k=(10.157E+16/-0.6/0)
----(k WRITTEN HERE FOR H2, MEASURED FOR AR, 200-5000 K, dlogk=+-0.5)
H       +H       +M(1)    =H2      +M(1)      1.015E+17 -0.600     0.000
----86 TSA/HAM,  k=(5.400E+13/0.000/-7.48)
----(k WRITTEN HERE FOR H2, MEASURED FOR AR, 200-4000 K, dlogk=+-1.3)
O       +O       +M(1)    =O2      +M(1)      5.400E+13  0.000    -7.4
----CODATA 2003, k=(5.56E+22/-2.0/0.0)
----(k WRITTEN HERE FOR H2, MEASURED FOR AR, 300-3000 K, dlogk=+-0.3)
H       +OH      +M(2)    =H2O     +M(2)      5.560E+22 -2.000     0.000
****************************************
****     03.   HO2 Formation/Consumption
****************************************
---- CODATA 2003, k_inf=(1.29E+12/0.56/0 + 1.74E+17/0/0), (298-1500K, dlog k=+-0.5)
----              k_0(Ar)=(2.36E+19/-1.2/0), (298-2000K, dlog k=+-0.2)
----              Fc=(0.5)
H       +O2      +M(3)    =HO2     +M(3)      1.297E+12  0.560     0.0
                                    LOW       2.367E+19 -1.200     0.0
                                    TROE   0.5       0.0     0.0     0.0
**** BEGIN DUPLICATE TROE REACTION
H       +O2      +M(3)    =HO2     +M(3)      1.746E+17  0.000     0.0
                                    LOW       2.367E+19 -1.200     0.0
                                    TROE   0.5       0.0     0.0     0.0
**** END DUPLICATE TROE REACTION
----CODATA 2003, k=(4.457E+14/0/5.819),(250-1000 K, dlogk=+-0.15)
HO2     +H       =OH      +OH                 4.457E+14  0.0       5.819
----CODATA 2003, k=(10.540E+13/0/8.56),(250-1000 K, dlogk=+-0.3)
HO2     +H       =H2      +O2                 1.054E+14  0.0       8.563
----CODATA 2003, k=(1.445E+12/0/0),(298 K, dlogk=+-0.5 over the range 250-1000 K)
HO2     +H       =H2O     +O                  1.445E+12  0.0       0.000
----CODATA 2003, k=(1.626E+13/0/-1.862),(220-1000 K, dlogk=+-0.1 rising to +-0.5)
HO2     +O       =OH      +O2                 1.626E+13  0.0      -1.862
----CODATA 2003, k=(9.275E+15/0/73.246),(1300-2000 K, dlogk=+-0.5)
HO2     +OH      =H2O     +O2                 9.275E+15  0.0      73.246
*********************************************************************
END
000  COMPLEX REACTIONS
END
COLLISION EFFICIENCIES....
M(1)    =H2      +H2O     +O2      +AR
         1.0      6.5      0.4      0.35
M(2)    =H2      +H2O     +O2      +AR
         1.0      2.55     0.4      0.15
M(3)    =H2      +H2O     +O2      +AR
         1.0      6.5      0.4      0.29
END
```

Lines starting with '−−−−' or '****' are interpreted as comments. The mechanism has to start with the keyword -MECH-. The rest of the line is used as a heading. The following lines are the elementary steps of the mechanism, where the three numbers represent the pre-exponential factor (cm, mole, s), temperature exponent and activation energy (kJ/mole). Pressure dependent reactions need two additional lines containing the keywords 'LOW' and 'TROE' containing seven parameters describing the fall-off. The input of the mechanism is finished by the keyword 'END'.

The THERMO file containing the thermodynamic data has been described in Section 2.4. It contains polynomial fit parameters of heat capacities, standard enthalpies and standard entropies. Once generated, these data do not require modification.

6.2 Simulations of flame velocities

The flame calculations presented in this work are performed using the MIXFLA code. The program is used for the simulation of velocity and structure of a stationary laminar premixed flat 1-dimensional flame [45–47]. In case of laminar premixed flames, the fuel and oxidizer are already completely mixed before they enter the reaction zone. In this work, the simulations in MIXFLA are always performed as a free flame. The MIXFLA package consists of three parts:

1. MIXINP for data input, preprocessing and storage in a linkfile, STORAG.
2. MIXRUN (reading STORAG) for the integration of the conservation equations and output of the results.
3. MIXMEC for the analysis of the reaction mechanism.

To run the program we need an input file for MIXINP specifying the species symbols, initial and boundary values, flame conditions, collision efficiencies, experimental temperatures (optionally), sensitivity analysis option (if necessary). For example,

```
OPTIONS:                                                                  00000200
BEGIN    ,NONEW    ,         ,OLDT     ,ENLARGE  ,         ,         ,  00000300
         ,         ,         ,         ,         ,         ,         ,  00000300
END                                                                       00000400
SPECIES:                                                                  00000500
H        ,O        ,OH       ,HO2      ,H2O2     ,CHO      ,C2H5O    ,  00000600
CH       ,C        ,H2O      ,CH2O     ,CH3CHOH  ,C2H4     ,C2H5     ,
3CH2     ,CH3      ,CH3O     ,CH3O2    ,CH2CH2OH ,CH3OH    ,CH3O2H   ,
CH2OH    ,C2H2     ,C2H5OH   ,C2H6     ,1CH2     ,C2H      ,HCCO     ,
C2H3     ,C4H2     ,CH2CO    ,CH2CHO   ,CH3CO    ,C3H6     ,C3H4     ,
CH3CHO   ,H2       ,CO2      ,CO       ,O2       ,CH4      ,N2       ,  00000600
END                                                                       00001200
UNBURNT GAS COMPOSITION:
CH4      / 09.57E-02/..............INITIAL X, T(K), P(BAR)                00001500
O2       / 18.98E-02/..............INITIAL X, T(K), P(BAR)                00001400
N2       / 71.43E-02/..............INITIAL X, T(K), P(BAR)
P        / 1.000E+00/..............INITIAL X, T(K), P(BAR)                00001700
T        / 2.980E+02/..............INITIAL X, T(K), P(BAR)                00001800
END                                                                       00001900
```

```
BURNT   GAS COMPOSITION:
OH       / 2.260E-02/..............FINAL   X, T(K), P(BAR), ESTIM.
CO       / 4.393E-02/..............FINAL   X, T(K), P(BAR), ESTIM.     00002500
CO2      / 4.742E-02/..............FINAL   X, T(K), P(BAR), ESTIM.     00002000
H2O      / 1.487E-01/..............FINAL   X, T(K), P(BAR), ESTIM.     00002500
O2       / 2.199E-02/..............FINAL   X, T(K), P(BAR), ESTIM.     00002800
N2       / 6.816E-01/..............FINAL   X, T(K), P(BAR), ESTIM.
T        / 2.872E+03/..............FINAL   X, T(K), P(BAR), ESTIM.     00002900
END                                                                    00003000
CONDITIONS:                                                            00003100
NT  ...../ 9000.0   /..............NUMBER OF TIME STEPS (-)            00003200
DT  ...../  0.600   /..............RELATIVE TIME STEP   (-)            00003300
NL  ...../   61.0   /..............GRID POINT NUMBER    (-)            00003400
TH  ...../    .1    /..............FLAME THICKNESS      (CM)           00003500
DI  ...../    0.0   /..............BURNER DIAMETER      (CM)     (STAB)00003600
VU  ...../    0.0   /..............UNBURNT GAS VELOCITY (CM/S)   (STAB)00003700
CO  ...../    1.0   /..............GRID CONTROL PARAMETER             00003700
END                                                                    00004000
COLLISION EFFICIENCIES
M(1)    =H2      +H2O     +O2      +N2      +CO      +CO2     +CH4
         1.0      6.5      0.4      0.4      0.75     1.5      3.0
M(2)    =H2      +H2O     +O2      +N2      +CO      +CO2     +CH4
         1.0      2.55     0.4      0.4      0.75     1.5      3.0
M(3)    =H2      +H2O     +O2      +N2      +CO      +CO2     +CH4
         1.0      6.5      0.4      0.67     0.75     1.5      3.0
M(4)    =H2      +H2O     +O2      +N2      +CO      +CO2     +CH4
         1.0      6.5      0.4      0.4      0.75     1.5      0.66
END
EXPERIMENTAL TEMPERATURES [K]:                                         00004800
END                                                                    00008400
SENSITIVITY ANALYSIS:                                                  00004700
END                                                                    00004950
```

The meaning of the options from this example are:

- BEGI(N) -begin with arbitrary S-shaped profiles.
- NONE(WTON) -Newton iteration suppressed.
- OLDT(RANS) -old transport model is used.
- ENLA(RGE) -enlarge grid points 31 → 61 (only active for BEGIN).

Inert species must be located at the end of the list.

In the following lines we have the input of initial and final conditions (unburnt and burnt gas composition): mole fractions (or volume parts), the initial temperature in K, the initial pressure in bar and the final temperature of the burnt gas, in K. This input is finished by the character string -END-.

Then comes the input of flame conditions. The maximum number of time steps is 10000. The relative time step should be 1 but it can be reduced in case of instability. The flame thickness should be estimated carefully. All flames need the variables (NT, DT, NL, TH), free flames additionally need CO. The grid control parameter CO should be 1. It can be chosen larger, if a larger coordinate range is desired, and smaller for a smaller range.

The input of collision efficiencies contains the 3rd body's symbol, the species symbols and the corresponding collision efficiencies (7 species at maximum). The input of collision efficiencies is stopped by the character string -END-.

Another input file we need is the one containing the reaction mechanism. The format of this file is the one described in the section devoted to ignition-delay times simulations.

Complex reactions cannot be used in this version of the program. Reverse reactions are added automatically, using the information in the THERMO file.

Further input for MIXINP consists of 2 additional data sets with species data, MOLDAT and THERMO97.IWR. These data have to be in the same directory as the files MIXINP, MIXRUN and MIXMEC.

MIXRUN prompts for an empty data set used for the storage of the results needed for a potential restart.

More information about the MIXFLA package can be found in literature [29, 45].

6.3 Results and discussion

To describe the combustion of hydrocarbons with a detailed reaction mechanism, the elementary reaction rate studies should be in accord with experimental results of flame and ignition chemistry. The chemistry of hydrocarbon oxidation at high temperatures is defined by:

- reactions of fuel decomposition;
- reactions of radicals with initial molecules;
- chain-branching reactions;
- recombination reactions.

The ignition-delay time is a characteristic quantity of the fuel and depends on initial temperature, pressure and mixture composition. Applied to the shock-tube technique, the ignition-delay time is defined as the time interval between heating the gas and the detection of the reaction. The delay is characterized by a radical-poor situation [4]. In this case the chemistry is determined by the competition of chain-branching and chain-terminating processes, while radical-radical reactions are unimportant. For flames, radical-radical reactions are important because of the large radical concentrations in a fully developed flame front. The hydrocarbon fuel is attacked by H, O, and OH radicals. The alkyl radicals formed are decomposed to smaller alkyl radicals and alkene. Only for the smallest alkyl radicals (CH_3 and C_2H_5) does the relatively slow thermal decomposition compete with recombination and with oxidation by O or O_2. This part of the mechanism is rate-controlling in alkane and alkene flames and is responsible for the similarity of all alkane and alkene flame properties [31, 51]. As we said before, ignition-delay time and flame velocities for hydrocarbons up to C_4 were simulated over a wide

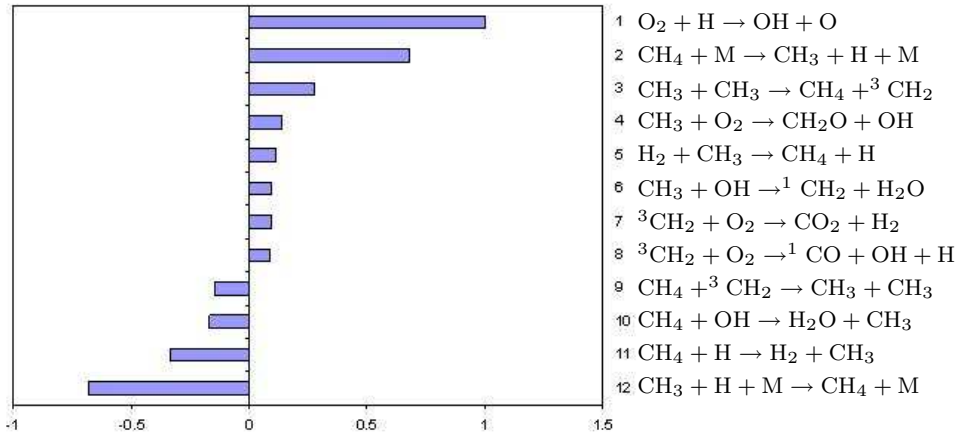

Figure 6.2: Sensitivity analysis for the OH concentration during ignition-delay time for a methane-air mixture at stoichiometric conditions, $T_u = 298\,K$, $p = 1\,bar$.

range of conditions. The results are presented in the following. As a general observation regarding the mechanism developed in this work, the H_2-O_2, CO and CH_4 (together with C_2-hydrocarbons) reactions form the most sensitive part of high-temperature combustion mechanisms.

Combustion chemistry models always include a complete H_2 oxidation mechanism. H_2-O_2 mechanisms have been used in the modelling of chemical kinetics, multidimensional chemical reaction flows, sensitivity analyses, detonation and ignition. Many versions of this mechanism can be found in literature, differing from one another in the expressions used for the rate coefficients and by including various reactions of secondary importance for the combustion chemistry. High-temperature H_2 oxidation mechanisms have been described by many workers ([41, 104–107] and many others). One common feature of these mechanisms is that all of them include the main initiation, propagation, termination and chain branching steps. The hydrogen oxidation mechanism presented in this work includes 20 elementary reactions and 9 species. The most important elementary steps of hydrogen oxidation prove to be the ones that provide chain-branching and propagation:

$$O_2 + H \rightarrow OH + O, \tag{6.33}$$

$$H_2 + O \rightarrow OH + H, \tag{6.34}$$

$$H_2 + OH \rightarrow H_2O + H, \tag{6.35}$$

$$OH + OH \rightarrow H_2O + O. \tag{6.36}$$

Reaction (6.33) is the most sensitive reaction of the mechanism. This can be seen performing, for example, a sensitivity analysis with respect to the ignition-delay time (see Fig. 6.2).

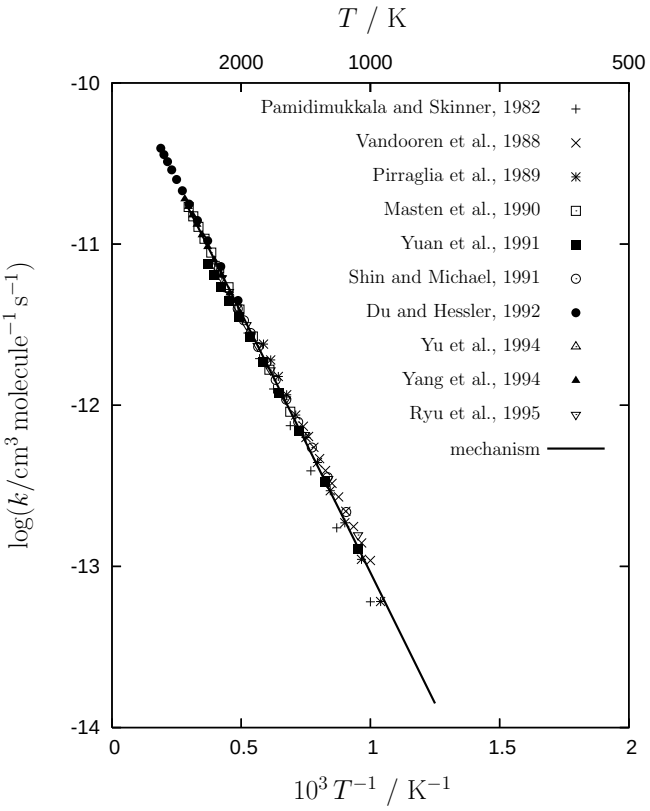

Figure 6.3: Arrhenius plot of the reaction rate coefficient of $H + O_2 \rightarrow O + OH$

Processes that reduce the H atoms and reactions that compete with Reaction (6.33) will tend to inhibit the combustion. The removal of H atoms means that they are unavailable for reaction with O_2 through $O_2 + H \rightarrow OH + O$, thereby reducing the rate of chain-branching and slowing the overall rate of combustion. It can be observed that the calculated ignition-delay times in hydrocarbon-fuel mixtures are sensitive to the choice of the rate coefficients involving the R–H fuel. This reaction is the basic chain-branching process in high-temperature combustion of hydrocarbon fuels, consuming one H atom and producing two radical species, O and OH. Therefore, ignition and flame velocity are very sensitive to the value of this rate coefficient: Oxidation processes are accelerated (or slowed down) by an increase (or decrease) of the formation rate of hydrogen atoms [4]. There have been numerous studies of this reaction, many authors have investigated it in details using a variety of techniques, [14, 51, 108, 109]. Due to its large activation energy, caused by an endothermicity of $\Delta H^0_{298} = 70.2\,\mathrm{kJ/mole}$, it is one of the rate-controlling elementary reactions. A collection of the data for this reaction given by Codata [2] is shown on the Arrhenius diagram on Fig. 6.3. There is no non-Arrhenius behavior in the temperature dependence of the rate coefficient, as shown by measurements performed

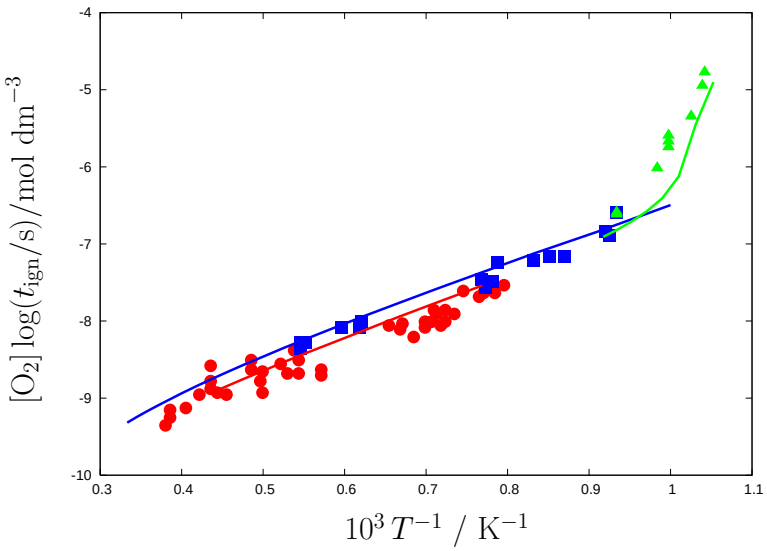

Figure 6.4: Ignition-delay time for H_2-O_2-Ar mixtures. Red: 4% H_2, 2% O_2 and 94% Ar, $p = 1$ bar; Blue: 1% H_2, 2% O_2 and 97% Ar, $p = 1$ bar; Green: 8% H_2, 2% O_2 and 90% Ar, $p = 5$ bar. Points: experimental results, lines: simulations.

at temperatures up to 3500 K and pressures between 0.013 bar and 4 bar [110–119].

In the mechanism presented in this work, the preferred reaction rate coefficient evaluated by Codata [2] has been taken. Using this value ($k = 3.43\times10^{-10}T^{-0.097}\exp(17560/T$, $cm^3\,molecule^{-1}\,s^{-1}$), we obtained a very good agreement between the simulations and experimental data for ignition-delay times in H_2-O_2 mixtures.

The simulations of ignition-delay times were performed in different conditions (see Fig. 6.4). The red line represents the simulations for mixtures containing 4% H_2, 2% O_2 and 94% Ar, for temperatures between 1300 K and 2300 K, at a pressure of 1 bar. The blue line represents the simulations for mixtures containing 1% H_2, 2% O_2 and 97% Ar, for temperatures between 1000 K and 3000 K, at 1 bar. The green line represents the simulations for mixtures containing 8% H_2, 2% O_2 and 90% Ar, for temperatures between 950 K and 1090 K, at a pressure of 5 bar. The points are the experimental results [120].

The adiabatic burning velocity of a given fuel-oxidizer mixture is an important parameter for the flame behavior that governs the combustion processes. It can be defined as the burning velocity of a fuel-oxidizer mixture in a tube, assuming that the flow is flat and there is no heat exchange with the wall of the tube. Many studies have been done on measurements and simulations of this parameter, especially for hydrocarbons because of their widespread use in domestic as well as industrial burners. To determine the adiabatic burning velocity, the flame should be as flat as possible and one-dimensional (the ideal case). However, flat flames traditionally stabilize on a burner, which implies heat loss and therefore do not represent an adiabatic state. It is thus necessary to circumvent these problems in either case (a non-adiabatic but flat flame, or else an adiabatic but

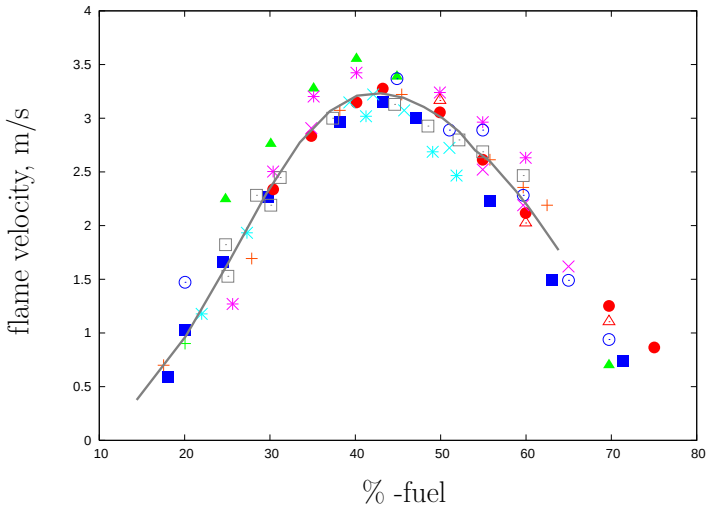

Figure 6.5: Flame velocities for H_2-air mixtures, $T_u = 298\,K$, $p = 1\,bar$.

stretched flame):

1. In case of a stretched flame, experiments are performed at various stretch rates. These stretch rates can be plotted and extrapolated to zero stretch.

2. In case of a burner stabilized flame, the flame can be tuned until it destabilizes, for example because the inlet velocity becomes higher than the adiabatic burning velocity. When the heat loss to the burner can be measured, the heat loss can be determined as a function of the inlet velocity, and the results extrapolated to zero heat loss. This corresponds to an adiabatic state, with consequently adiabatic burning velocity.

Also in case of flame, the $H + O_2 \rightleftharpoons OH + O$ reaction is the most sensitive in the whole mechanism. Therefore, flame propagation is highly sensitive to the value of its rate coefficient. Because of the

$$H + O_2 + M \rightarrow HO_2 + M \tag{6.37}$$

reaction, there is a pressure- and temperature-dependent competition with $H + O_2 \rightarrow O + OH$ that has consequences for the combustion process. Reaction (6.37) is a chain-terminating reaction, and the HO_2 radical is relatively unreactive. At high temperatures and low pressures the reaction $H + O_2 \rightarrow O + OH$ leads to O atoms as a further chain-branching agent. Formation of O and OH is followed by H-atom regeneration in H_2-O_2 flames by

$$O + H_2 \rightarrow OH + H \tag{6.38}$$

and

$$OH + H_2 \rightarrow H + H_2O. \tag{6.39}$$

Fig. 6.5 shows a comparison of simulated and measured flame velocities for the H_2-air system. The line represents our simulations and the points reproduce the experimental data [121, 122]. An excellent agreement between simulations and experimental points is obtained. Because of its relative simplicity, the H_2-O_2 system has been investigated in detail by many workers, and its kinetics is now well understood.

Reactions involving CO and CO_2 are also very important in hydrocarbon combustion, the

$$CO + OH \rightleftharpoons CO_2 + H \tag{6.40}$$

and

$$CO_2 + H \rightleftharpoons CO + OH \tag{6.41}$$

reactions having a central role in the oxidation process. CO is oxidized almost exclusively by OH to form CO_2 in the Reaction (6.40) [29, 122], while the reverse reaction (6.41) is necessary to establish the water-gas equilibrium [123]. The oxidation rate of CO has little effect on ignition-delays (because of the late occurance of these steps during the combustion process), but is very important for determining the rate of flame propagation. Variations of its rate coefficient strongly influence the flame propagation.

The reaction $CO + HO_2 \rightarrow CO_2 + OH$ is minor in flames, and the recombination reaction $CO + O + M \rightarrow CO_2 + M$ requires high pressures as well as high O atom concentration to be significant.

Considerable amounts of CO are also produced through reaction

$$CHO + M \rightleftharpoons CO + H + M. \tag{6.42}$$

However, more exact rate measurements seem to be desirable for this important reaction.

Results of the flame velocities simulations for H_2-CO-air mixtures are presented in Fig. 6.6. The red line represents the simulations for mixtures containing 50% CO and 50% H_2 at $p = 1\,\mathrm{bar}$ and $T_\mathrm{u} = 298\,\mathrm{K}$. The blue line represents the simulations for mixtures containing 95% CO and 5% H_2 at $p = 1\,\mathrm{bar}$ and $T_\mathrm{u} = 298\,\mathrm{K}$. The red and blue points are McLean's experimental data [124], and the pink points are Scholte's experimental data [125]. Simulations are in satisfactory agreement with the experiments, but give slightly high values for fuel-rich mixtures.

The next step in our hierarchy is the methane (CH_4) mechanism. Methane is a very important practical fuel and is produced during the combustion of most other hydrocarbons. The reaction mechanism of hydrocarbon oxidation at high temperatures has been discussed by many workers ([126–138]). Even though there are some uncertain chemical aspects, differences in the number of species and elementary reactions, and other details, general features of the CH_4 oxidation mechanism are believed to be established. The most important reactions in the mechanism, in case of the flame, can be identified also using sensitivity analysis. Sensitivity analyses with respect to flame velocity for lean, stoichiometric and rich methane-air flames are shown on Fig. 6.7. It can be seen that in this case $H + O_2 \rightarrow O + OH$ reaction again is the most sensitive in all conditions.

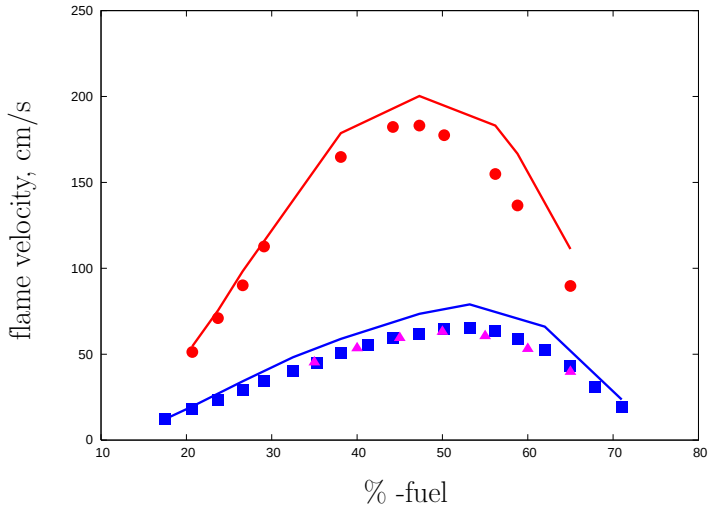

Figure 6.6: Flame velocities for H_2-CO-air mixtures, $T_u = 298\,K$, $p = 1\,bar$.

The results of the simulations of flame velocities for CH_4-air mixtures can be seen in Fig. 6.8. Due to strain effects, the adiabatic burning velocity of methane-air was for a long time reported to have its maximum at 42 cm/s, but more recent experiments have revealed that $36 - 37$ cm/s is a value that much better represents the burning velocity of a strain-free flame. In fact, when the old measurements are recalculated (extrapolated) using a more recent and insightful strain model, the results of the old measurements become lower and coincide with recent measurements [139].

The agreement between calculated and measured values is excellent; note that the measurements have been carried out using experimental techniques that produce non-stretched flames [140–143]. One of these techniques is the heat flux method, which is used for smaller alkanes at atmospheric pressure. This method is based on measuring the net heat loss from the flame to the burner and tuning the inlet velocity of the unburnt gas mixture to a value where no net heat loss to the burner is observed. This leads to an adiabatic state of the flame. The flame is effectively adiabatic when the heat loss equals the heat gain, resulting in a zero net heat flux and therefore a constant temperature across the burner plate.

Simulation results of our proposed mechanism (the mechanism is given in the Appendix) for methane ignition are shown on Fig. 6.9. Ignition-delay times for a CH_4-O_2-90% Ar mixture at a pressure of 0.39 bar were calculated. In Fig. 6.9, the blue line represents the simulations in rich conditions ($\phi = 2$), for a mixture containing 2.5% CH_4 and 5% O_2, at temperatures between 1833 K and 2101 K. The red line represents the simulations in stoichiometric conditions ($\phi = 1$), for a mixture containing 3.33% CH_4, 6.66% O_2, at temperatures between 1688 K and 2000 K. The green line represents the simulations in lean conditions ($\phi = 0.5$), for a mixture containing 2% CH_4 and 8% O_2, at

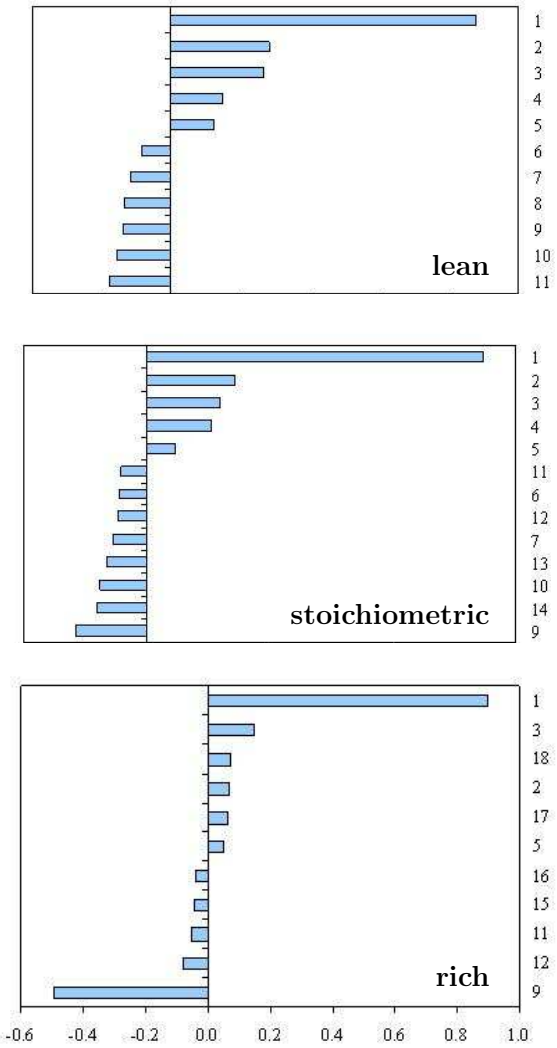

Reactions:

1. $H + O_2 \rightarrow O + OH$
2. $OH + CO \rightarrow H + CO_2$
3. $CHO + M_1 \rightarrow H + CO + M_1$
4. $OH + H_2 \rightarrow H + H_2O$
5. $OH + CH_3 \rightarrow H_2O +^1 CH_2$
6. $OH + CHO \rightarrow H_2O + CO$
7. $OH + H_2O_2 \rightarrow HO_2 + H_2O$
8. $CHO + O_2 \rightarrow HO_2 + CO$
9. $CH_4 + M_4 \rightarrow H + CH_3 + M_4$
10. $O + OH \rightarrow H + O_2$
11. $H + O_2 + M_3 \rightarrow HO_2 + M_3$
12. $H + CHO \rightarrow H_2 + CO$
13. $H + CO_2 \rightarrow OH + CO$
14. $H + H_2O \rightarrow OH + H_2$
15. $CH + H_2 + M_1 \rightarrow CH_3 + M_1$
16. $H + HCCO \rightarrow^3 CH_2 + CO$
17. $CH_3 + CH_3 + M_1 \rightarrow C_2H_6 + M_1$
18. $^3CH_2 + CH_3 \rightarrow H + C_2H_4$

Figure 6.7: Sensitivity analysis in a methane-air flame: lean (top), stoichiometric (middle) and rich (bottom) conditions, $T_u = 298\,K$, $p = 1\,bar$.

temperatures between 1698 K and 2325 K. The points are the experimental data [144]. A good agreement between simulations and experiments has been obtained.

The ignition-delay times are also sensitive to the rate coefficients of the reactions of H, O and OH with CH_4. It is known that for CH_4, which is the smallest hydrocarbon fuel, the general sequence of oxidation processes at high-temperature, as shown in [51], is:

$$CH_4 \rightarrow CH_3 \rightarrow CH_2O \rightarrow CO \rightarrow CO_2.$$

The link between these chains is shown by the fact that CO is part of CH_2O oxidation, which is also part of the CH_4 oxidation. In the oxidation process of CH_4 to CO_2 and

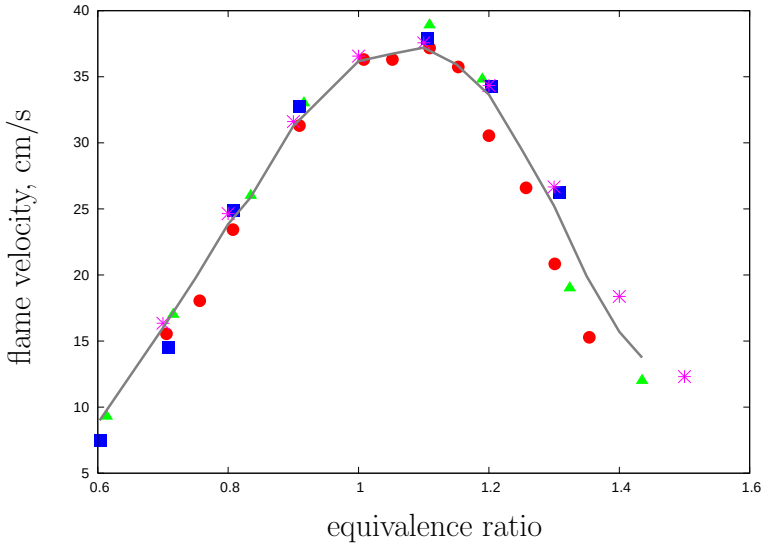

Figure 6.8: Flame velocities for CH_4-air mixtures, $T_u = 298\,K$, $p = 1\,bar$.

H_2O the fuel decomposition is slow, the radical concentration at the beginning of the reaction being small. The chain initiating step in methane ignition at high temperatures is the methane thermal decomposition

$$CH_4 + M \rightarrow CH_3 + H + M. \tag{6.43}$$

Another important step is the attack of the radicals (O, OH, H and H_2O) on the fuel:

$$CH_4 + O \rightarrow CH_3 + OH \tag{6.44}$$
$$CH_4 + H \rightarrow CH_3 + H_2 \tag{6.45}$$
$$CH_4 + OH \rightarrow CH_3 + H_2O \tag{6.46}$$
$$CH_4 + HO_2 \rightarrow CH_3 + H_2O_2. \tag{6.47}$$

These reactions convert CH_4 to CH_3, so that the CH_3 concentration is the highest among the radicals during ignition-delay. Together with the reactions

$$CH_3 + O_2 \rightarrow CH_2O + OH \tag{6.48}$$
$$CH_3 + O_2 \rightarrow CH_3O + O \tag{6.49}$$
$$CH_3 + O \rightarrow CH_2O + H \tag{6.50}$$

the they control fuel disappearance and CH_2O generation [51]. The reaction of CH_3 radicals with O_2 is one of the most important propagation reaction in the combustion chemistry of CH_4. This endothermic reaction ($\Delta H^0_{298} = 120\,kJ/mole$) is a branching step, followed by decomposition of the methoxy radicals into formaldehyde and OH.

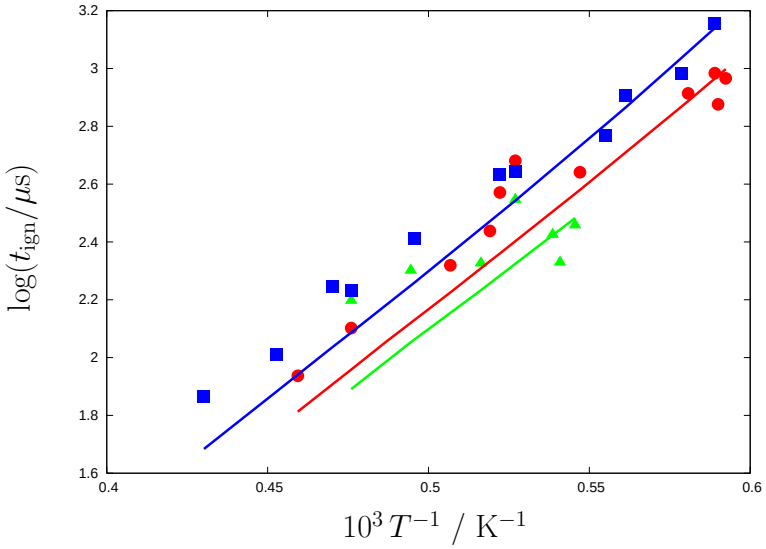

Figure 6.9: Ignition-delay time for CH_4-O_2-Ar mixtures, 0.39 bar. Green: $\phi = 0.5$, 2% CH_4, 8% O_2; Red: $\phi = 1$, 3.33% CH_4, 6.66% O_2; Blue: $\phi = 2.5$, 2.5% CH_4, 5% O_2. Points: experimental results, lines: simulations.

The formation of formaldehyde and methoxy radicals from CH_3 and O_2 reaction are important under the radical-poor situation (ignition), while the formation of formaldehyde from CH_3 and O reaction dominates in the radical-rich situation, that is, in flame fronts. This reaction is very fast ($\Delta H^0_{298} = -293\,\mathrm{kJ/mole}$) and one of the main sinks of CH_3 radicals in flame propagation. Therefore, flame propagation is sensitive to the rate coefficient of this step.
Reaction (6.49) is also an important chain-branching reaction, because methoxy radicals are unstable at flame temperatures and quickly decompose via

$$CH_3O + M \rightarrow CH_2O + H + M. \tag{6.51}$$

Along time, many authors have suggested that the $CH_3O + O$ formation channel is the dominant one [145–148]. The second channel of formaldehyde formation ($\Delta H^0_{298} = -223\,\mathrm{kJ/mole}$) was favored by many workers too [149–155]. In our mechanism, the recommended value by Golden has been taken for this reaction. The two high-temperature product channels were also proposed by Golden [156]:

$$CH_3 + O_2 \rightarrow CH_2O + OH,$$

having the rate expression $k_1 = 68.6T^{2.86}\exp(-4916/T)$ in $\mathrm{cm^3\,mole^{-1}\,s^{-1}}$, and

$$CH_3 + O_2 \rightarrow CH_3O + O,$$

having the rate expression $k_2 = 6.08 \times 10^7 T^{1.54}\exp(-14005/T)$ in $\mathrm{cm^3\,mole^{-1}\,s^{-1}}$.

The first channel, formation of formaldehyde, has been found to be the dominant one over the entire experimental temperature range. Usually CH_3 radicals do not significantly decompose to form other radicals as CH_2 or CH. Instead, their reaction and CH_2O reaction define the kinetics of CH_4 oxidation.

Thermal decomposition of CH_2OH leads to the formation of formaldehyde and H atoms, and therefore accelerates the oxidation process for both, flame and ignition-delay time:

$$CH_2OH + M \rightarrow CH_2O + H + M. \tag{6.52}$$

The similarities in combustion behavior of different hydrocarbons are mainly due to the fact that larger hydrocarbon molecules and radicals quickly decompose to smaller molecules and radicals.

Performing the reaction flow analysis, we can get a better understanding of the path of chemical reactions and information about the percentage of species consumed (or formed) in the reactions system. Different reaction paths are followed, depending on the stoichiometry even though the chemical mechanism is the same. This can be seen in Figs. 6.10-6.12 in an example of integral flow analysis for a methane-air flame at pressure of 1 bar and T_u of 298 K.

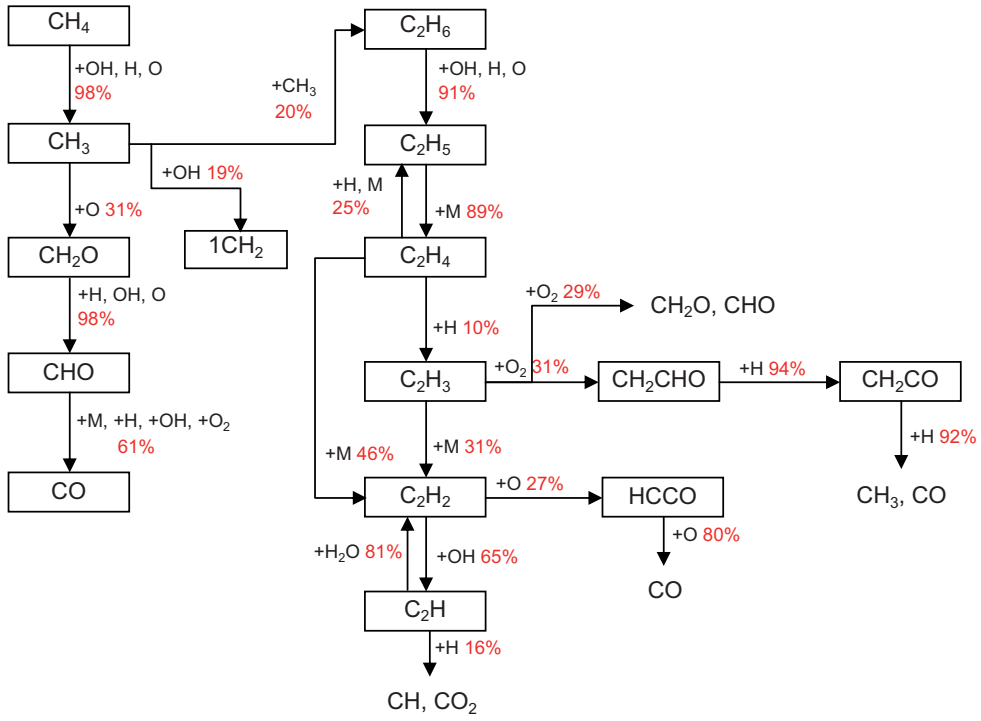

Figure 6.10: Integral flow analysis in a stoichiometric methane-air flame, $T_u = 298\,K$, $p = 1\,bar$.

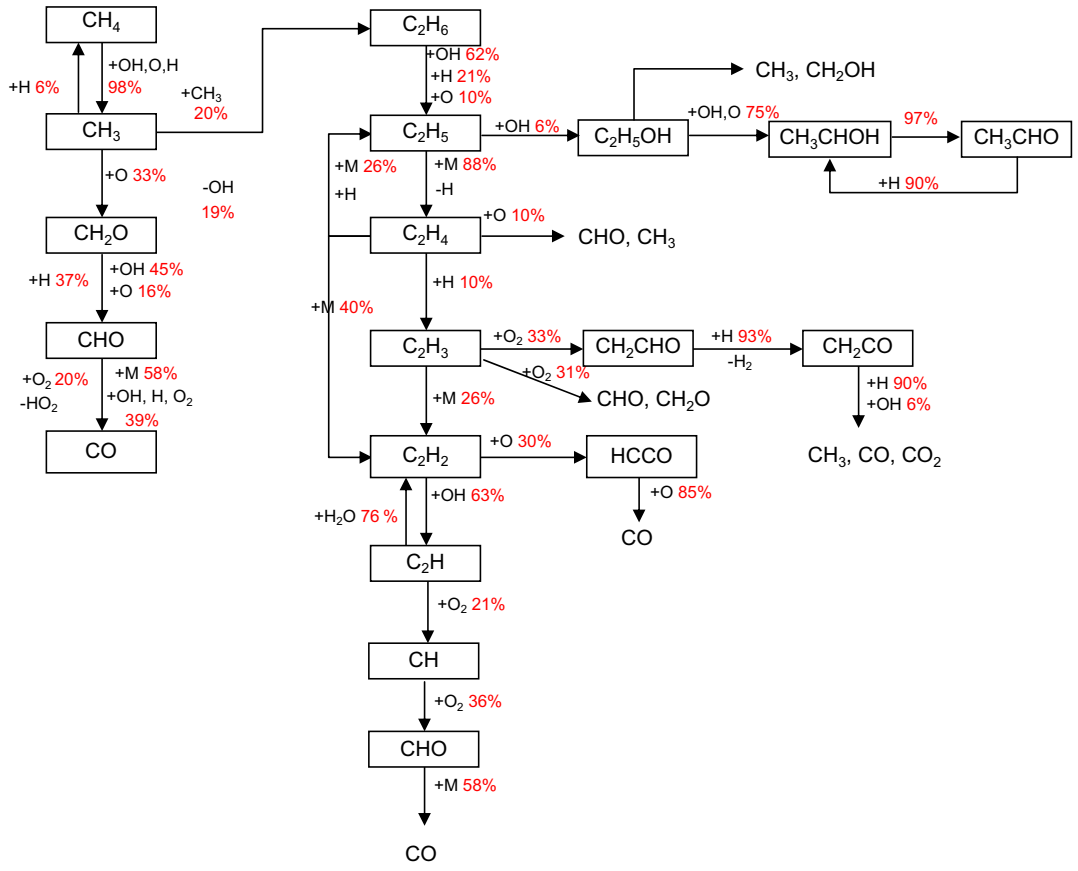

Figure 6.11: Integral flow analysis in a lean methane-air flame, $T_u = 298\,K$, $p = 1\,bar$.

Methane oxidation starts when the bond between carbon and hydrogen breaks to form radicals, for example Reaction (6.43) and

$$CH_4 + O_2 \rightarrow CH_3 + HO_2. \tag{6.53}$$

These two initiating reactions are of a minor influence for combustion, but important for the ignition. Reaction (6.43) is less important for the flame because of the large activation energy of the thermal decomposition of methane. But this thermal decomposition of methane strongly influences its ignition. As can be seen on the reaction flow analysis, O, H and OH radicals react with the methane molecule, and this leads at an increment of CH_3 radicals via Reactions (6.44, 6.45, 6.46). The sensitivity of flame propagation to their rate coefficient is small, but ignition-delay times are sensitive at their rate coefficients.

The CH_3 radicals react with the oxygen molecules producing methoxy radical and formaldehyde by Reactions (6.48) and (6.49). CH_3O reacts quickly to form formalde-

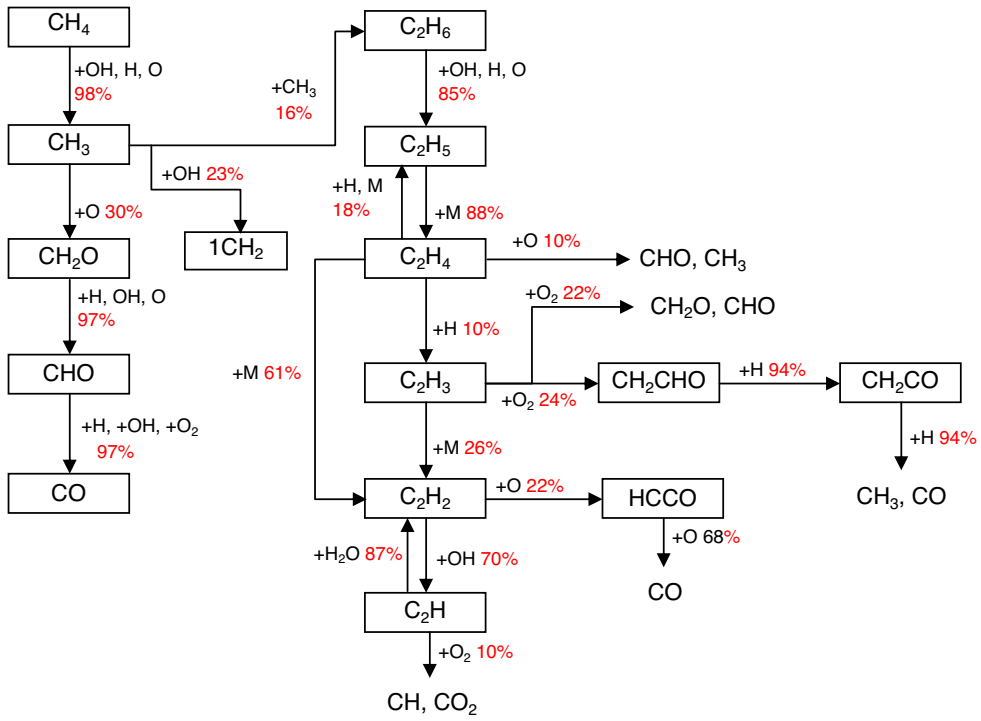

Figure 6.12: Integral flow analysis in a rich methane-air flame, $T_u = 298\,\mathrm{K}$, $p = 1\,\mathrm{bar}$.

hyde via Reaction (6.51). This thermal decomposition represents the main consumption channel for methoxy radicals, followed by reactions with H atoms and molecular oxygen. This reaction is so fast that it has a very small sensitivity. The formaldehyde formed reacts rapidly to generate HCO, formyl by reactions:

$$CH_2O + OH \rightarrow HCO + H_2O \tag{6.54}$$
$$CH_2O + H \rightarrow HCO + H_2 \tag{6.55}$$
$$CH_2O + O \rightarrow HCO + OH. \tag{6.56}$$

The formyl is converted to carbon monoxide, for example:

$$HCO + OH \rightarrow CO + H_2O \tag{6.57}$$
$$HCO + O_2 \rightarrow CO + HO_2. \tag{6.58}$$

Oxidation of methane finishes with the oxidation of CO to CO_2.

In the stoichiometric flame, methane is mainly oxidized directly, whereas methyl radicals formed in the rich flame recombine to form ethane (C_2H_6), which is then oxidized.

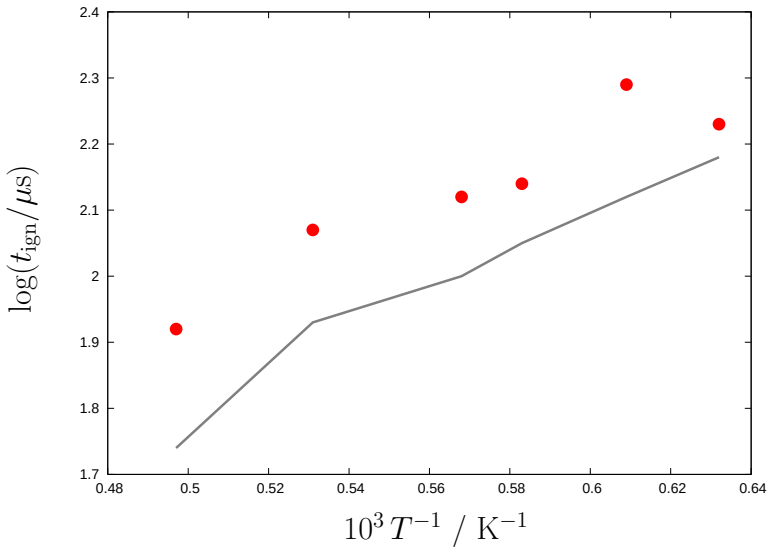

Figure 6.13: Ignition-delay times for C_2H_2-O_2-Ar mixtures (0.5% C_2H_2, 0.8% O_2, 98.7% Ar), $p = 0.64$ bar-0.78 bar.

This suggests that a satisfactory mechanism for CH_4 oxidation also demands an additional mechanism for C_2H_6 oxidation. Thus, the oxidation of C_2 species has also an important role in hydrocarbon combustion. As we mentioned before, another sensitive and very important reaction both for flame propagation and ignition, since it competes with the oxidation reaction of CH_3, is

$$CH_3 + CH_3 + M \rightleftharpoons C_2H_6 + M. \tag{6.59}$$

This recombination reaction becomes very important at high temperature, especially in fuel-rich mixtures where it is an important source of C_2 hydrocarbons, leading eventually to the formation of soot in rich CH_4 flames. It is the principal path by which the methyl radicals disappear.

Reactions of C_2H_6 lead to formation of ethyl radical (C_2H_5), ethylene (C_2H_4), and acetylene (C_2H_2).

Acetylene is a practical fuel and it is an important contributor to the formation and growth of soot. The C_2H_2 reactions are generally important for fuel-rich hydrocarbon combustion. Our simulations results of ignition-delay times on acetylene oxidation are shown on the logarithmic plot, Fig. 6.13. The line represents the ignition-delay time simulations for a mixture containing 0.5% C_2H_2, 0.8% O_2, 98.7% Ar, at pressures between 0.64 bar and 0.78 bar and temperatures between 1580 K–2010 K. The points are the experimental data [157]. The results are not in a good agreement with the experimental data, as it can be seen we obtained longer ignition-delay times at comparable conditions.

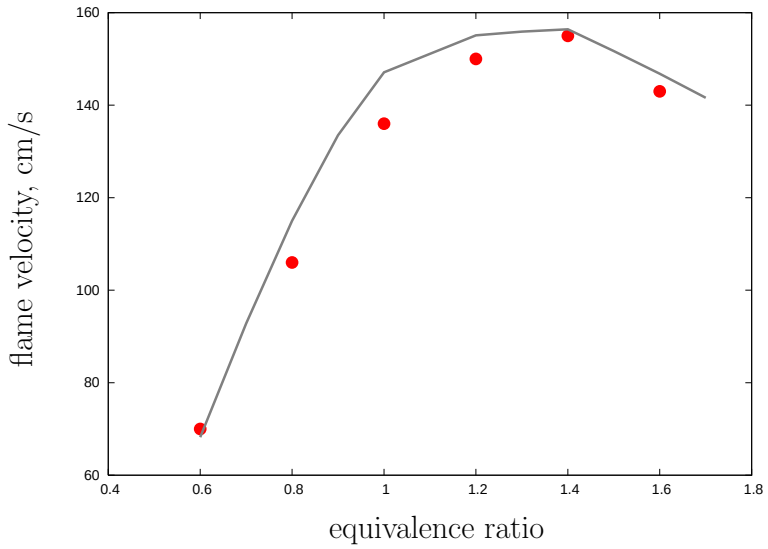

Figure 6.14: Flame velocities for C_2H_2-air mixtures, $T_u = 298\,K$, $p = 1\,bar$.

C_2H_2 and its oxidation reactions are part of the reaction mechanisms for most other hydrocarbon fuels. Under oxidation conditions, the reaction of C_2H_2 with O_2,

$$C_2H_2 + O_2 \rightleftharpoons HCCO + OH\,, \tag{6.60}$$

is very important for the ignition-delay time. The flame speed is not affected by this reaction because the fuel is already consumed by reactions with O and H atoms:

$$C_2H_2 + O \rightleftharpoons {}^3CH_2 + CO \tag{6.61}$$
$$C_2H_2 + O \rightleftharpoons HCCO + H \tag{6.62}$$
$$C_2H_2 + H \rightleftharpoons C_2H + H_2. \tag{6.63}$$

The flame speeds is very sensitive to the rate coefficient of the reaction

$$C_2H_2 + OH \rightleftharpoons C_2H + H_2O. \tag{6.64}$$

This step can partly explain the PAH formation via C_2H in rich hydrocarbon fuels, [158–161].
The calculated flame velocities for C_2H_2-air mixtures at $p = 1\,bar$ and $T_u = 298\,K$ are shown on Fig. 6.14. The line represents our simulations and the points represent the experimental data. The numerical results are in good agreement with the experimental data [162].

The mechanisms of C_2H_4 and C_2H_6 oxidation are also necessary to understand the CH_4 oxidation mechanism, because these species are formed in the course of CH_4 oxidation.

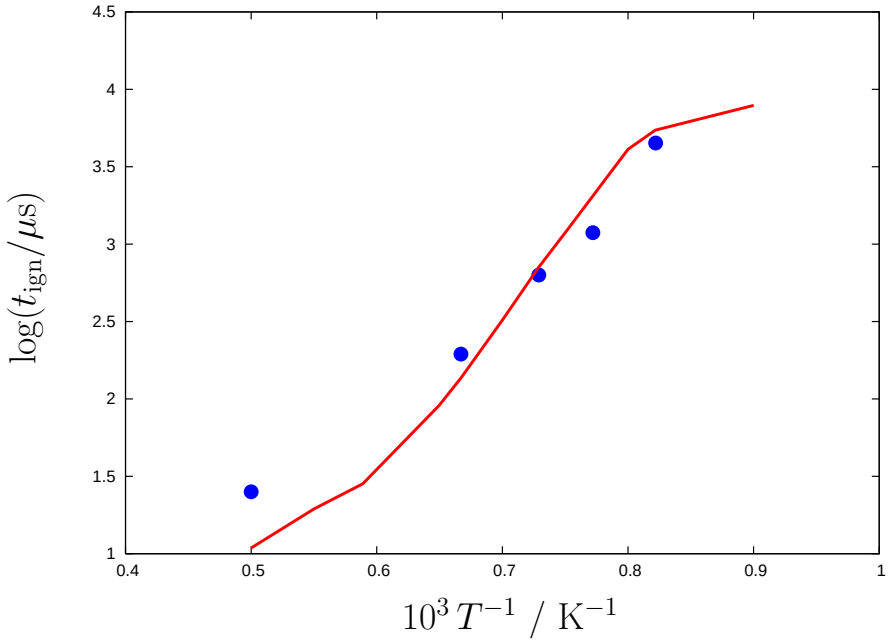

Figure 6.15: Ignition-delay time for C_2H_4-O_2-Ar mixtures (1% C_2H_4, 1.5% O_2, 97.5% Ar), $p = 3\,\mathrm{bar}$.

Ethylene is a primary fuel itself and an important intermediate produced during the combustion of CH_4, C_2H_6, and other higher hydrocarbons.

The reaction

$$C_2H_4 + OH \rightleftharpoons C_2H_3 + H_2O \tag{6.65}$$

is very sensitive for flame and ignition-delay time simulations. Together with

$$C_2H_4 + H \rightleftharpoons C_2H_3 + H_2, \tag{6.66}$$

it accounts for C_2H_4 consumption in flames and during ignition.

The results of ignition-delay times on ethylene oxidation are shown on the logarithmic plot in Fig. 6.15. The line represents the ignition-delay time simulations for a mixture containing 1% C_2H_4, 1.5% O_2, 97.5% Ar, at a pressure of 3 bar and temperatures between 1111 K-2000 K. The points are the experimental data [163]. Comparisons between the simulations and experimental data were found to be satisfactory.

It can be observed that at high-temperatures the ignition-delay times have the tendency to be shorter at comparable conditions.

The calculated flame velocities for C_2H_4-air mixtures at $p = 1\,\mathrm{bar}$ and $T_\mathrm{u} = 298\,\mathrm{K}$ are shown in Fig. 6.16. The calculated results are in good agreement with the experimental data [162, 164–169].

It is known that for larger hydrocarbons, the chain-initiation step is the one in which the C-C bond is broken to form hydrocarbon radicals, the C-C bond being weaker than

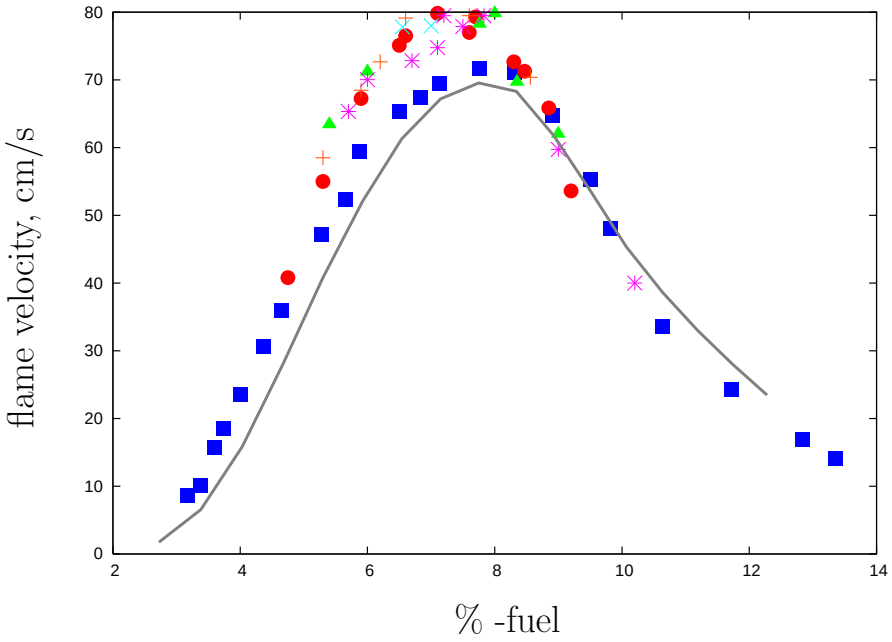

Figure 6.16: Flame velocities for C_2H_4-air mixtures, $T_u = 298\,K$, $p = 1\,bar$.

the C-H bonds. However, at high temperatures, some C-H bonds are also broken, as in

$$C_2H_6 + H \rightarrow C_2H_5 + H_2. \tag{6.67}$$

Usually, the radicals resulting from removal of one of the H atoms from the fuel fragment to olefines and smaller radicals. For example, in case of C_2H_5, the olefin is C_2H_4 and an H atom becomes the chain center, as in

$$C_2H_5 + M \rightarrow C_2H_4 + H + M. \tag{6.68}$$

The result is that the total radical concentration is higher, reactions are faster, and ignition occurs more quickly. Thus, the initial fuel is consumed early in the induction zone, a situation which differs from the methane case.

Reactions of C_2H_5 radicals are important because of the rate-determining character of the competition between thermal decomposition, oxidation and recombination of C_2H_5 [4]. The thermal decomposition reaction (6.68) of C_2H_5 is an important rate-determining step for both flame propagation and ignition-delay time; this is so because of the formation of hydrogen atoms. The reactions

$$C_2H_5 + H \rightarrow CH_3 + CH_3, \tag{6.69}$$

$$C_2H_5 + C_2H_5 \rightarrow C_2H_4 + C_2H_6 \tag{6.70}$$

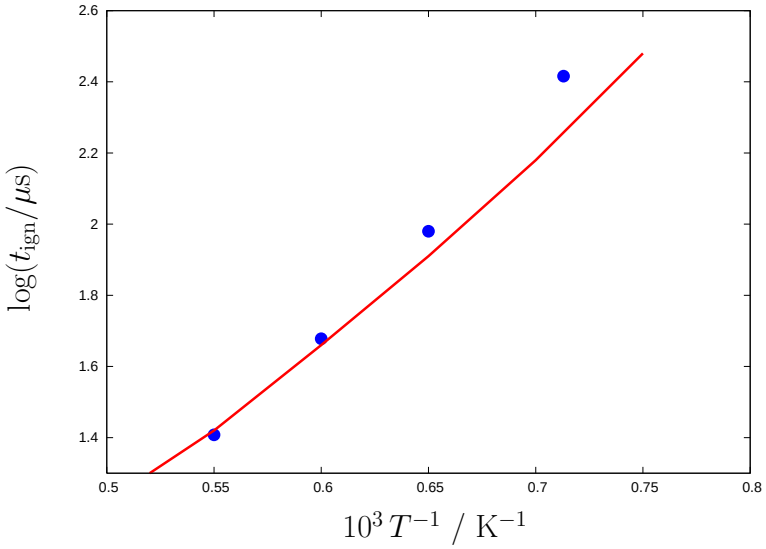

Figure 6.17: Ignition-delay time for C_2H_6-O_2-Ar mixtures (2.22% C_2H_6, 7.78% O_2,90% Ar), $p = 0.3$ bar.

have a chain-terminating character because of the low reactivity of the CH_3 radical compared to C_2H_5 [Reaction (6.69)] and because of the stability of the molecules formed when compared to C_2H_5 [Reaction (6.70)].

Fig. 6.17 shows calculated ignition-delay times for a mixture containing 2.22% C_2H_6, 7.78% O_2 and 90% Ar, at 0.3 bar and a temperature range of 1333 K-2000 K. The points are the experimental data [163]. A good agreement between simulations and experiments has been obtained.

For C_2H_6-air mixtures, the calculated flame velocities do not give a satisfactory agreement, see Fig. 6.18. A discrepancy can be observed for the rich-mixture. The points represent the experimental data [125, 162, 165, 166, 170].

The disagreement is caused by the uncertainty of the Reaction (6.59). Its reverse path is the dominant one and has a significant terminating effect in situation, where the ethyl radicals are presented in large concentrations, as in the C_2H_6 flames. In general, the characteristics of the oxidation of C_2H_6 and larger aliphatics are similar to CH_4 oxidation, but CH_4 presents some different characteristics from all other hydrocarbons. The dissociation energy of the C-H bond in CH_4 is 435 kJ/mole ([171–174]). It is much higher than the C-C bond dissociation in C_2H_6 (370 kJ/mole), and higher than the C-H bond dissociation energy in C_2H_6 (410 kJ/mole). For this reason it is more difficult to ignite CH_4 than other hydrocarbons.

An understanding of C_3 and C_4 hydrocarbons combustion mechanisms can be gained by consideration of the importance of formation of C_2H_5 radicals. As C_2H_5 is more reactive than CH_3, flames of fuels producing C_2H_5 propagate faster than those of fuels

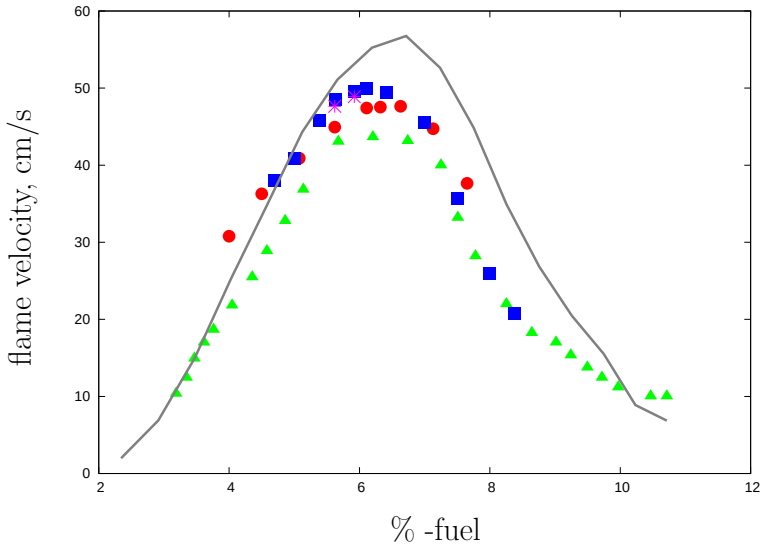

Figure 6.18: Flame velocities for C_2H_6-air mixtures, $T_u = 298\,K$, $p = 1\,bar$.

producing CH_3 (for example, methane-air and ethane-air flames). In ignition processes the rate of formation of CH_3 and C_2H_5 also plays an important role because C_2H_5 leads rapidly to chain-branching by thermal decomposition into C_2H_4 and H atoms [Reaction (6.68)]. The relative rates of formation of CH_3 and C_2H_5 are influenced by three processes [11]:

1. attack of H, O and OH on alkanes and formation of alkyl radical isomers;
2. thermal decomposition of the alkyl radical isomers to form smaller alkyl radicals, or H atoms, by alkene elimination;
3. reactions of propene and butene, which are formed by alkyl radical thermal decomposition.

In the case of propane, one observes the same three stages as in case of methane: the fuel decomposition, an intermediate stage with a steady concentration of radicals and intermediate products, and a final self-accelerated stage. The chain-initiation step is one in which the C-C bond is broken to form hydrocarbon radicals:

$$C_3H_8 + M \rightarrow CH_3 + C_2H_5 + M. \tag{6.71}$$

The results for the ignition-delay time and flame velocity simulations for C_3H_8 are shown in Figs. 6.19 and 6.20, respectively.

In Fig. 6.19, the blue line represents the simulations for a lean mixture containing 0.8% C_3H_8, 8% O_2 and 91.2% Ar, at pressures between 6.6 bar and 8.6 bar and a temperature range of 1292 K–1550 K. The red line represents the simulations for stoichiometric mixtures containing 1.6% C_3H_8, 8% O_2, 90.4% Ar, at pressures between 2.25 bar

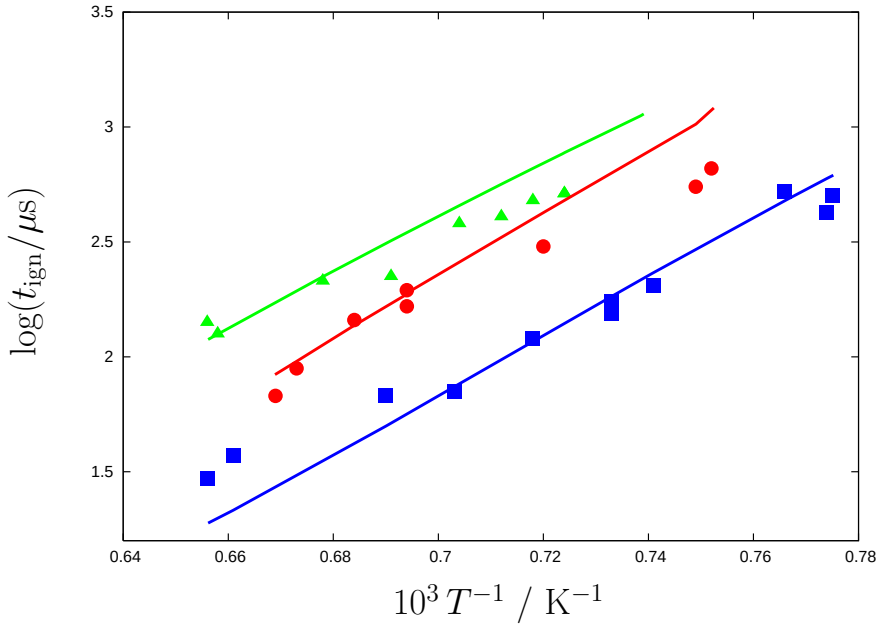

Figure 6.19: Ignition-delay time for C_3H_8-O_2-Ar mixtures. Blue: 0.8% C_3H_8, 8% O_2, 91.2% Ar, p = 6.6 bar-8.6 bar; Red: 1.6% C_3H_8, 8% O_2, 90.4% Ar, p = 2.25 bar-2.62 bar; Green: 1.6% C_3H_8, 4% O_2, 94.4% Ar, p = 7.24 bar-8.66 bar.

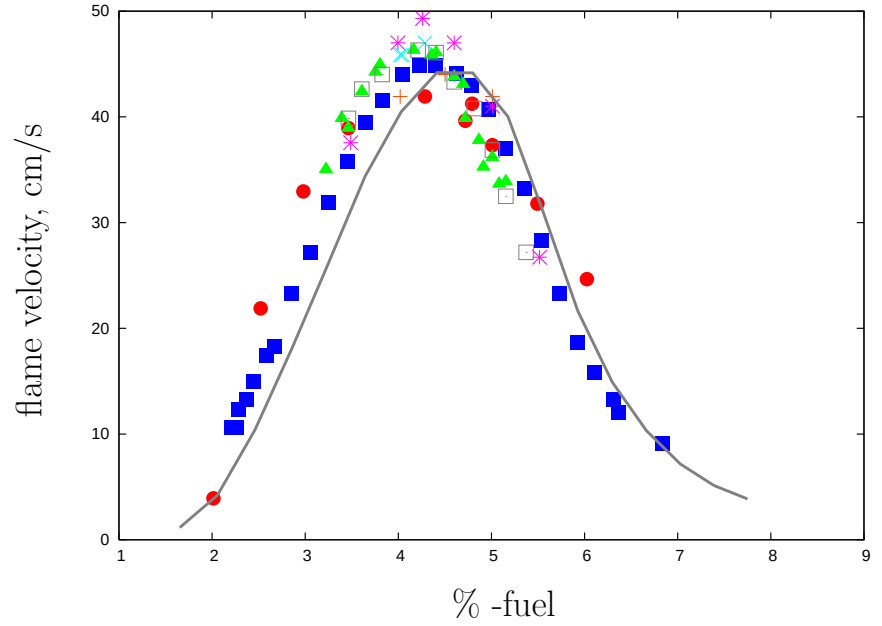

Figure 6.20: Flame velocities for C_3H_8-air mixtures, T_u = 298 K, p = 1 bar.

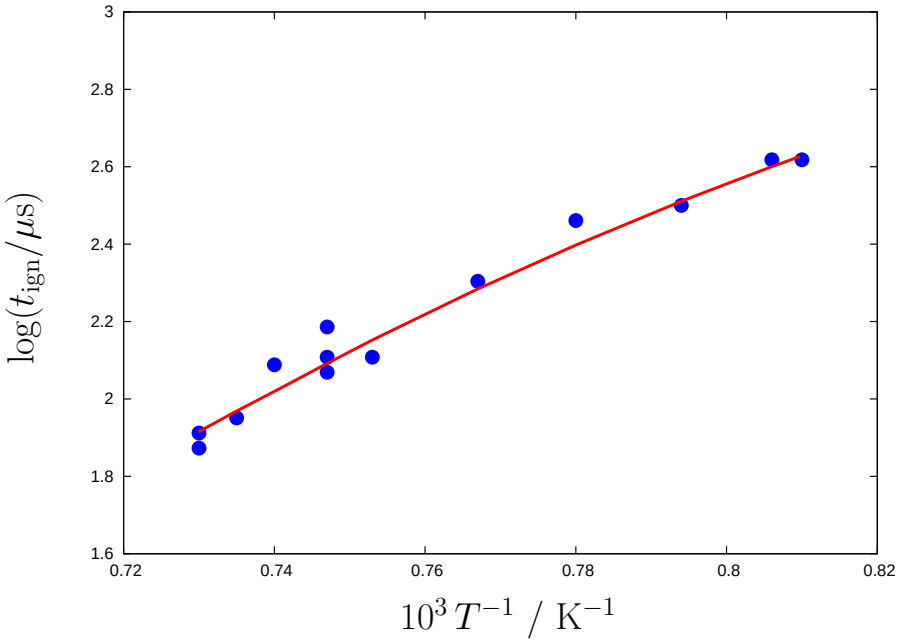

Figure 6.21: Ignition-delay time for C_4H_{10}-O_2-Ar mixtures (2.5% C_4H_{10}, 16.25% O_2, 81.25% Ar), $p = 9$ bar.

and 2.62 bar and a temperature range of 1300 K-1495 K. The green line represents the simulations for rich mixtures containing 1.6% C_3H_8, 4% O_2 and 94.4% Ar, at pressures between 7.24 bar and 8.66 bar and a temperature range of 1354 K-1550 K. The points are the experimental results [175].

A good agreement between simulations and experiments has been obtained, although it can be seen that slightly long ignition-delay times have been obtained in the rich mixtures case.

For C_3H_8-air mixtures, at $p = 1$ bar and $T_u = 298$ K, a good agreement is observed between flame velocity simulations and experiments [125,162,165–167,176], as illustrated on Fig. 6.20.

The results of the ignition-delay time and flame velocity simulations for C_4H_{10} are shown in Figs. 6.21 and 6.22, respectively.

Fig. 6.21 shows the simulations of ignition-delay times for a mixture containing 2.5% C_4H_{10}, 16.25% O_2 and 81.25% Ar, at 9 bar and temperature between 1235 K and 1370 K. The points are the experimental values [177]. There is a very good agreement between experimental data and simulations.

Comparison between calculated and experimental [125, 140, 166, 167, 176] flame velocities and for C_4H_{10}-air mixtures at $p = 1$ bar and $T_u = 298$ K also shows a very good agreement, see Fig. 6.22.

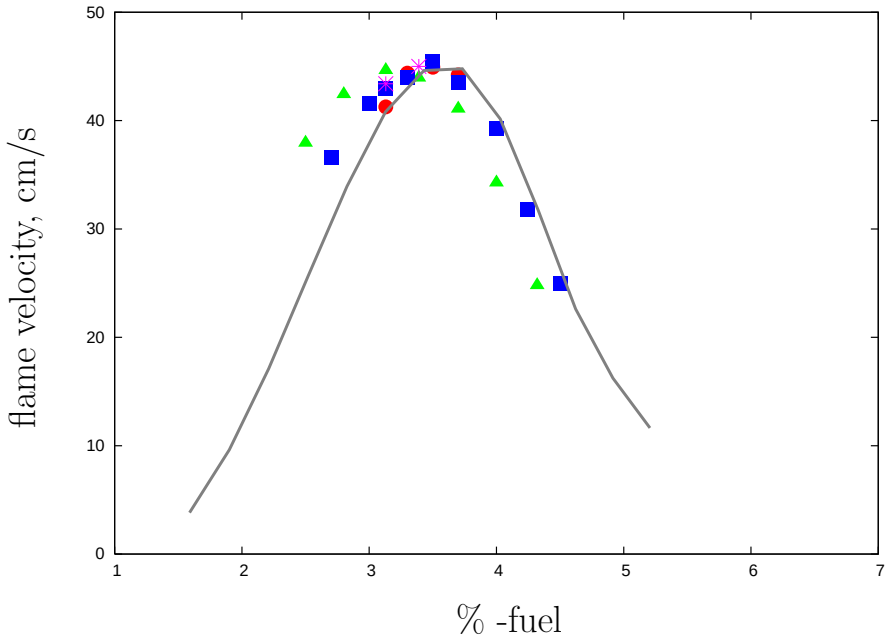

Figure 6.22: Flame velocities for C_4H_{10}-air mixtures, $T_u = 298\,K$, $p = 1\,bar$.

In this case of propane and butane, as in methane and ethane case, the fuel is consumed by the reactions of H, O and OH abstraction. The HO_2 radical is unimportant due to its low concentration. Due to the instability of the C_3 and C_4 alkyl radicals that are formed after attack of H, O and OH radicals on the fuel, with respect to thermal decomposition [Reaction (6.71)], the competing reactions with O or O_2 and recombination reactions are unimportant in flame propagation. For C_3 and C_4 hydrocarbon oxidation, the rate coefficients for attack on specific C–H single bonds are important, because the formation rates of different alkyl isomers (e.g., n-C_4H_9 and s-C_4H_9 for n-butane) are different.

Propene and butene are important intermediates in the decomposition of propyl and butyl radicals and must be consumed somehow in the reaction zones of flames of C_3- and higher hydrocarbons. There is no evidence that the propene and butene reactions play a rate controlling role in high-temperature combustion or ignition processes [51]. The reactions forming C_3H_4 and C_4H_2 are important in fuel-rich high temperature combustion, C_4H_2 being also very important in the oxidation of C_2H_2.

The C_3 and C_4 reactions have minor influence on the propagation of all C_1 and C_2 fuels, and this explain the small effect they have on the calculated flame speeds. Their influence on the C_3H_8 flames is also weak, demonstrating that the flame speed of higher hydrocarbons depend more strongly on the kinetics involving the lower carbon species.

7 Conclusion

In the present work, a reaction mechanism containing values of the rate coefficients recommended by the most recent critical review of Baulch et al. 2005 [2] is proposed. Only the mechansims of H_2 and CO oxidation can be considered well understood in the sense that elementary reaction rate studies are fully in accord with experimental results of flame and ignition chemistry. To describe the combustion of hydrocarbons with a detailed reaction mechanism, one has to adjust some of the elementary reaction rate parameters within the experimental error limits. These data are then of great utility for the study of combustion phenomena in practical situations.

The similarities in the combustion behaviour of different hydrocarbons are mainly due to the fact that larger hydrocarbon molecules and radicals quickly decompose to smaller molecules and radicals. Therefore, reaction flow analyses have been conducted to elucidate the important chemical pathways over a wide range of conditions.

Flame velocities and ignition-delay times have similarities and essential differences. One of the main differences is that in self-propagating flames, diffusive transport of radicals before the main reaction zone makes the chain initiation irrelevant. As a result of the high temperature in flame fronts, all reactions are faster, and because of the higher radical concentrations, radical-radical reactions are more important than during ignition.

Another difference between flames and ignition is the presence of pre-heat zones in flames but not in ignition. For stable fuels like methane (CH_4), little or no pyrolysis occurs in this zone, but for other hydrocarbons considerable fuel degradation occurs; the fuel fragments surviving this zone comprise mainly smaller hydrocarbons, alkenes, and hydrogen. A major consequence of this is that, in the reaction zone, the composition of flames burning larger hydrocarbons varies little with fuel. For this reason, flame temperatures and burning velocities vary little for such fuels.

One of the objectives of this work was to compare our numerical simulations with experimental data by using a reaction scheme containing hydrocarbons up to C_4 in order to provide a more accurate evaluation of the mechanism. Another objective was to develop a kinetic reaction scheme by using the latest kinetic information published by Baulch et al. 2005 [2].

Further validation of the reaction mechanism is provided by systematic comparison of computed ignition-delay times with corresponding experimental results from shock tube studies at high temperature. Ignition-delay times are strongly affected by fuel-specific reactions. Because of the radical-poor situation the rate-limiting reactions tend to be chain-branching and chain-terminating ones, whose competitions are displayed in

sensitivity analises. Generalizations are difficult, because the experiments have been done at different conditions of pressure, equivalence ratio, and diluation with noble gas. In any case, the calculated results were found to be satisfactorily close to the experimental data. The only substantial disagreement was for the C_2H_2-O_2-Ar mixture, for which the calculated ignition-delay times were considerably longer than the measured ones.

Further insight into the high-temperature reaction mechanism governing the flame propagation is provided by sensitivity analysis with respect to the flame speed of laminar premixed methane and propane-air flames at atmospheric pressure. It clearly shows the dominating influence of the reactions of H atoms with O_2 and of CO with OH radicals. Nevertheless, for a detailed description of these flames, one can not neglect any of the reactions shown in the detailed mechanism (see Appendix).

Calculations of freely propagating one-dimensional flames have been performed. Because the stretch effects were neglected in the past in most experiments, simulations have a tendency to predict slightly higher burning velocities for some of the hydrocarbon fuels at comparable conditions.

The flame speed of C_2 fuel species does not seem to depend sensitively on details of the C_3 and C_4 sub-mechanisms. The flame simulations results are in a good agreement for all the fuels considered.

The comparison between flame speeds and ignition-delay times over a wide range of conditions (temperature, pressure and stoichiometry) provides a high degree of confidence in the usefulness of the present mechanism.

A H_2, CO, C_1, C_2, C_3 and C_4 hydrocarbons oxidation mechanism

Elementary reactions in the H_2-CO-C_1-C_2-C_3-C_4-O_2 system for high-temperature combustion (Heghes et al. 2005 [3], Warnatz and Heghes 2006 [4]); rate coefficients are presented in the modified Arrhenius form $k = AT^b \exp(-E_a/RT)$; only the forward reaction is considered; the reverse reaction may be calculated using thermodynamic data. The estimated uncertainty of the reaction rate is given. The collision efficiencies used are

$$\mathrm{M}(1) = [\mathrm{H_2}] + 6.5[\mathrm{H_2O}] + 0.4[\mathrm{O_2}] + 0.4[\mathrm{N_2}] + 0.75[\mathrm{CO}] + 1.5[\mathrm{CO_2}] + 3.0[\mathrm{CH_4}] + 0.35[\mathrm{Ar}]$$
$$\mathrm{M}(2) = [\mathrm{H_2}] + 2.5[\mathrm{H_2O}] + 0.4[\mathrm{O_2}] + 0.4[\mathrm{N_2}] + 0.75[\mathrm{CO}] + 1.5[\mathrm{CO_2}] + 3.0[\mathrm{CH_4}] + 0.15[\mathrm{Ar}]$$
$$\mathrm{M}(3) = [\mathrm{H_2}] + 6.5[\mathrm{H_2O}] + 0.4[\mathrm{O_2}] + 0.4[\mathrm{N_2}] + 0.75[\mathrm{CO}] + 1.5[\mathrm{CO_2}] + 3.0[\mathrm{CH_4}] + 0.29[\mathrm{Ar}]$$
$$\mathrm{M}(4) = [\mathrm{H_2}] + 6.5[\mathrm{H_2O}] + 0.4[\mathrm{O_2}] + 0.4[\mathrm{N_2}] + 0.75[\mathrm{CO}] + 1.5[\mathrm{CO_2}] + 0.7[\mathrm{CH_4}] + 0.35[\mathrm{Ar}]$$

The mechanism is presented in Table A.1.

The mechanism was developed on the basis of a previously available mechanism, see [49].

The rate parameters of the reactions follow the recommendations of the CODATA project [2].

The preexponential factor A is given in units of $(\mathrm{cm^3\ mol^{-1}})^{n-1}\ \mathrm{s^{-1}}$ and the activation energy E_a in kJ $\mathrm{mol^{-1}}$.

The double arrow, $\rightleftharpoons$, shows that the reverse reaction may be calculated using the thermodynamic data.

									A	n	E_a	no.
1. H_2–CO oxidation												
1.1. H_2–O_2 reactions (no HO_2, H_2O_2)												
O_2	+	H		⇌	OH	+	O		$2.06{\cdot}10^{14}$	−0.097	62.85	1
H_2	+	O		⇌	OH	+	H		$3.82{\cdot}10^{12}$	0.0	33.26	2
H_2	+	O		⇌	OH	+	H		$1.02{\cdot}10^{15}$	0.0	80.23	
H_2	+	OH		⇌	H_2O	+	H		$2.17{\cdot}10^{8}$	1.52	14.47	3
OH	+	OH		⇌	H_2O	+	O		$3.35{\cdot}10^{4}$	2.42	−8.06	4
H	+	H	+ M(1)	⇌	H_2	+	M(1)		$1.02{\cdot}10^{17}$	−0.6	0.0	5
O	+	O	+ M(1)	⇌	O_2	+	M(1)		$5.40{\cdot}10^{13}$	0.0	−7.4	6
H	+	OH	+ M(2)	⇌	H_2O	+	M(2)		$5.56{\cdot}10^{22}$	−2.0	0.0	7
1.2. HO_2 formation/consumption												
H	+	O_2	+ M(3)	⇌	HO_2	+	M(3)		$1.30{\cdot}10^{12}$	0.56	0.0	8
								LOW	$2.37{\cdot}10^{19}$	−1.2	0.0	
								TROE	0.5 0.0	0.0	0.0	
H	+	O_2	+ M(3)	⇌	HO_2	+	M(3)		$1.75{\cdot}10^{17}$	0.0	0.0	
								LOW	$2.37{\cdot}10^{19}$	−1.2	0.0	
								TROE	0.5 0.0	0.0	0.0	
HO_2	+	H		⇌	OH	+	OH		$4.46{\cdot}10^{14}$	0.0	5.82	9
HO_2	+	H		⇌	H_2	+	O_2		$1.05{\cdot}10^{14}$	0.0	8.56	10
HO_2	+	H		⇌	H_2O	+	O		$1.44{\cdot}10^{12}$	0.0	0.0	11
HO_2	+	O		⇌	OH	+	O_2		$1.63{\cdot}10^{13}$	0.0	−1.86	12
HO_2	+	OH		⇌	H_2O	+	O_2		$9.28{\cdot}10^{15}$	0.0	73.25	13
1.3. H_2O_2 formation/consumption												
HO_2	+	HO_2		⇌	H_2O_2	+	O_2		$4.22{\cdot}10^{14}$	0.0	50.14	14
HO_2	+	HO_2		⇌	H_2O_2	+	O_2		$1.32{\cdot}10^{11}$	0.0	−6.82	
OH	+	OH	+ M(1)	⇌	H_2O_2	+	M(1)		$1.57{\cdot}10^{13}$	0.0	0.0	15
								LOW	$5.98{\cdot}10^{19}$	−0.8	0.0	
								TROE	0.5 0.0	0.0	0.0	
H_2O_2	+	H		⇌	H_2	+	HO_2		$1.69{\cdot}10^{12}$	0.0	15.71	16
H_2O_2	+	H		⇌	H_2O	+	OH		$1.02{\cdot}10^{13}$	0.0	14.97	17
H_2O_2	+	O		⇌	OH	+	HO_2		$4.22{\cdot}10^{11}$	0.0	16.63	18
H_2O_2	+	O		⇌	H_2O	+	O_2		$4.22{\cdot}10^{11}$	0.0	16.63	19
H_2O_2	+	OH		⇌	H_2O	+	HO_2		$1.64{\cdot}10^{18}$	0.0	123.05	20
H_2O_2	+	OH		⇌	H_2O	+	HO_2		$1.92{\cdot}10^{12}$	0.0	1.79	

continues on next page

												A	n	E_a	no.

continued from previous page

1.4. CO reactions

CO	+	O	+ M(1)	⇌	CO_2	+	M(1)					$1.54{\cdot}10^{15}$	0.0	12.56	21
CO	+	OH		⇌	CO_2	+	H					$1.00{\cdot}10^{13}$	0.0	66.93	22
CO	+	OH		⇌	CO_2	+	H					$9.03{\cdot}10^{11}$	0.0	19.12	
CO	+	OH		⇌	CO_2	+	H					$1.01{\cdot}10^{11}$	0.0	0.25	
CO	+	HO_2		⇌	CO_2	+	OH					$1.50{\cdot}10^{14}$	0.0	98.7	23
CO	+	O_2		⇌	CO_2	+	O					$2.50{\cdot}10^{12}$	0.0	200.0	24

2. C_1–hydrocarbons oxidation

2.1. C reactions

CH	+	H		⇌	C	+	H_2					$1.20{\cdot}10^{14}$	0.0	0.0	25
C	+	O_2		⇌	CO	+	O					$6.02{\cdot}10^{13}$	0.0	2.66	26

2.2. CH reactions

CH	+	O		⇌	CO	+	H					$4.00{\cdot}10^{13}$	0.0	0.0	27
CH	+	OH		⇌	CHO	+	H					$3.00{\cdot}10^{13}$	0.0	0.0	28
CH	+	O_2		⇌	CHO	+	O					$1.69{\cdot}10^{13}$	0.0	0.0	29
CH	+	CO		⇌	HCCO							$2.80{\cdot}10^{11}$	0.0	−7.1	30
CH	+	CO_2		⇌	CHO	+	CO					$6.38{\cdot}10^{7}$	1.51	−2.99	31
CH	+	H_2O		⇌	CH_2O	+	H					$4.58{\cdot}10^{16}$	−1.42	0.0	32
CH	+	H_2O		⇌	$^3CH_2$	+	OH					$4.58{\cdot}10^{16}$	−1.42	0.0	33

2.3. CHO reactions

CHO	+	M(1)		⇌	CO	+	H	+	M(1)			$1.14{\cdot}10^{14}$	0.0	65.02	34
CHO	+	H		⇌	CO	+	H_2					$9.03{\cdot}10^{13}$	0.0	0.0	35
CHO	+	O		⇌	CO	+	OH					$3.01{\cdot}10^{13}$	0.0	0.0	36
CHO	+	O		⇌	CO_2	+	H					$3.01{\cdot}10^{13}$	0.0	0.0	37
CHO	+	OH		⇌	CO	+	H_2O					$1.08{\cdot}10^{14}$	0.0	0.0	38
CHO	+	O_2		⇌	CO	+	HO_2					$7.59{\cdot}10^{12}$	0.0	1.7	39
CHO	+	CHO		⇌	CH_2O	+	CO					$3.00{\cdot}10^{13}$	0.0	0.0	40

2.4. CH_2 reactions

$^3CH_2$	+	H		⇌	CH	+	H_2					$1.20{\cdot}10^{14}$	0.0	0.0	41
$^3CH_2$	+	O		→	CO	+	H	+	H			$1.23{\cdot}10^{14}$	0.0	2.24	42
$^3CH_2$	+	O		⇌	CO	+	H_2					$8.19{\cdot}10^{13}$	0.0	2.24	43
$^3CH_2$	+	O_2		⇌	CO	+	OH	+	H			$1.81{\cdot}10^{12}$	0.0	0.0	44
$^3CH_2$	+	O_2		⇌	CO_2	+	H_2					$1.81{\cdot}10^{12}$	0.0	0.0	45

continues on next page

								A	n	E_a	no.
continued from previous page											
$^3CH_2$	+	$^3CH_2$	⇌	C_2H_2	+	H_2		$1.81{\cdot}10^{14}$	0.0	49.88	46
$^3CH_2$	+	$^3CH_2$	⇌	C_2H_2	+	H	+ H	$1.63{\cdot}10^{15}$	0.0	49.88	47
$^3CH_2$	+	CH_3	⇌	C_2H_4	+	H		$7.23{\cdot}10^{13}$	0.0	0.0	48
$^1CH_2$	+	M(1)	⇌	$^3CH_2$	+	M(1)		$6.02{\cdot}10^{12}$	0.0	0.0	49
$^1CH_2$	+	H_2	⇌	CH_3	+	H		$1.26{\cdot}10^{16}$	−0.56	66.5	50
$^1CH_2$	+	O_2	⇌	CO	+	OH	+ H	$3.10{\cdot}10^{13}$	0.0	0.0	51
		2.5. CH_2O reactions									
CH_2O	+	M(1)	⇌	CHO	+	H	+ M(1)	$4.87{\cdot}10^{15}$	0.0	316.35	52
CH_2O	+	M(1)	⇌	CO	+	H_2	+ M(1)	$2.83{\cdot}10^{15}$	0.0	266.96	53
CH_2O	+	H	⇌	CHO	+	H_2		$4.10{\cdot}10^{8}$	1.47	10.23	54
CH_2O	+	O	⇌	CHO	+	OH		$4.16{\cdot}10^{11}$	0.57	11.56	55
CH_2O	+	OH	⇌	CHO	+	H_2O		$1.39{\cdot}10^{13}$	0.0	2.53	56
CH_2O	+	HO_2	⇌	CHO	+	H_2O_2		$4.10{\cdot}10^{4}$	2.5	42.73	57
CH_2O	+	O_2	⇌	CHO	+	HO_2		$2.44{\cdot}10^{5}$	2.5	152.56	58
CH_2O	+	CH_3	⇌	CHO	+	CH_4		$3.19{\cdot}10^{1}$	3.36	18.04	59
		2.6. CH_2OH reactions									
CH_2OH	+	M(1)	⇌	CH_2O	+	H	+ M(1)	$2.80{\cdot}10^{14}$	−0.73	137.31	60
							LOW	$1.50{\cdot}10^{34}$	−5.39	151.46	
							TROE	0.96 67.2	1855.0	7543.0	
CH_2OH	+	H	⇌	CH_2O	+	H_2		$2.44{\cdot}10^{13}$	0.0	0.0	61
CH_2OH	+	H	⇌	CH_3	+	OH		$1.05{\cdot}10^{13}$	0.0	0.0	62
CH_2OH	+	O_2	⇌	CH_2O	+	HO_2		$2.89{\cdot}10^{16}$	−1.5	0.0	63
CH_2OH	+	O_2	⇌	CH_2O	+	HO_2		$7.23{\cdot}10^{13}$	0.0	15.63	
		2.7. CH_3 reactions									
CH_3	+	M(1)	⇌	$^3CH_2$	+	H	+ M(1)	$2.92{\cdot}10^{16}$	0.0	379.0	64
CH_3	+	M(1)	⇌	CH	+	H_2	+ M(1)	$1.89{\cdot}10^{16}$	0.0	355.84	65
CH_3	+	O	⇌	CH_2O	+	H		$6.74{\cdot}10^{13}$	0.0	0.0	66
CH_3	+	OH	→	CH_3O	+	H		$1.20{\cdot}10^{10}$	0.0	58.11	67
CH_3	+	OH	⇌	$^1CH_2$	+	H_2O		$3.00{\cdot}10^{13}$	0.0	11.64	68
CH_3	+	OH	+ M(1) ⇌	CH_3OH	+	M(1)		$4.34{\cdot}10^{15}$	−0.79	0.0	69
							LOW	$1.10{\cdot}10^{38}$	−6.21	5.58	
							TROE	0.25 210.0	1434.0	0.0	
CH_3	+	HO_2	⇌	CH_3O	+	OH		$1.60{\cdot}10^{13}$	0.0	0.0	70
CH_3	+	O_2	⇌	CH_2O	+	OH		$6.86{\cdot}10^{1}$	2.86	40.87	71
CH_3	+	O_2	→	O	+	CH_3O		$6.08{\cdot}10^{7}$	1.54	116.44	72
CH_3	+	O_2	+ M(1) ⇌	CH_3O_2	+	M(1)		$7.83{\cdot}10^{8}$	1.2	0.0	73
							LOW	$1.55{\cdot}10^{26}$	−3.3	0.0	
							TROE	0.36 0.0	0.0	0.0	

continues on next page

								A	n	E_a	no.
continued from previous page											
CH_3	+	CO	+ M(1) ⇌	CH_3CO	+	M(1)		$5.06{\cdot}10^{11}$	0.0	28.77	74
							LOW	$3.11{\cdot}10^{14}$	0.0	15.88	
							TROE	0.5 0.0	0.0	0.0	
CH_3	+	$^1CH_2$	⇌	C_2H_4	+	H		$7.23{\cdot}10^{13}$	0.0	0.0	75
CH_3	+	CH_3	+ M(1) ⇌	C_2H_6	+	M(1)		$3.61{\cdot}10^{13}$	0.0	0.0	76
							LOW	$3.63{\cdot}10^{41}$	−7.0	11.6	
							TROE	0.62 73.0	1180.0	0.0	
	2.8. CH_3O reactions										
CH_3O	+	M(1)	⇌	CH_2O	+	H	+ M(1)	$6.80{\cdot}10^{13}$	0.0	109.49	77
							LOW	$4.66{\cdot}10^{25}$	−3.0	101.68	
							TROE	0.45 0.0	0.0	0.0	
CH_3O	+	H	→	CH_3	+	OH		$1.63{\cdot}10^{13}$	0.0	2.49	78
CH_3O	+	H	⇌	CH_2O	+	H_2		$3.79{\cdot}10^{13}$	0.0	2.49	79
CH_3O	+	O	→	O_2	+	CH_3		$1.13{\cdot}10^{13}$	0.0	0.0	80
CH_3O	+	O	⇌	OH	+	CH_2O		$3.76{\cdot}10^{12}$	0.0	0.0	81
CH_3O	+	OH	⇌	CH_2O	+	H_2O		$1.81{\cdot}10^{13}$	0.0	0.0	82
CH_3O	+	O_2	⇌	CH_2O	+	HO_2		$2.17{\cdot}10^{10}$	0.0	7.3	83
CH_3O	+	CH_2O	⇌	CH_3OH	+	CHO		$1.15{\cdot}10^{11}$	0.0	5.2	84
	2.9. CH_3O_2 reactions										
CH_3O_2	+	HO_2	⇌	CH_3O_2H	+	O_2		$2.28{\cdot}10^{11}$	0.0	−6.24	85
CH_3O_2	+	CH_3	⇌	CH_3O	+	CH_3O		$1.50{\cdot}10^{13}$	0.0	−5.0	86
CH_3O_2	+	CH_3O_2	→	CH_2O	+	CH_3OH	+ O_2	$3.43{\cdot}10^{10}$	0.0	−3.24	87
CH_3O_2	+	CH_3O_2	→	CH_3O	+	CH_3O	+ O_2	$2.29{\cdot}10^{10}$	0.0	−3.24	88
CH_3O_2	+	H_2O_2	⇌	CH_3O_2H	+	HO_2		$2.40{\cdot}10^{12}$	0.0	41.8	89
CH_3O_2	+	CH_2O	⇌	CH_3O_2H	+	CHO		$1.30{\cdot}10^{11}$	0.0	37.7	90
CH_3O_2	+	CH_4	⇌	CH_3O_2H	+	CH_3		$1.81{\cdot}10^{11}$	0.0	77.8	91
CH_3O_2	+	CH_3OH	⇌	CH_3O_2H	+	CH_2OH		$1.81{\cdot}10^{11}$	0.0	57.7	92
	2.10. CH_4 reactions										
CH_4	+	M(4)	⇌	CH_3	+	H	+ M(4)	$2.46{\cdot}10^{16}$	0.0	439.0	93
							LOW	$4.70{\cdot}10^{47}$	−8.2	492.18	
							TROE	0.0 1350.0	1.0	7834.0	
CH_4	+	H	⇌	H_2	+	CH_3		$6.14{\cdot}10^{5}$	2.5	40.12	94
CH_4	+	O	⇌	OH	+	CH_3		$4.40{\cdot}10^{5}$	2.5	27.52	95
CH_4	+	OH	⇌	H_2O	+	CH_3		$1.37{\cdot}10^{6}$	2.18	11.22	96
CH_4	+	HO_2	⇌	H_2O_2	+	CH_3		$4.70{\cdot}10^{4}$	2.5	87.88	97
CH_4	+	O_2	⇌	CH_3	+	HO_2		$4.88{\cdot}10^{5}$	2.5	219.24	98
CH_4	+	CH	⇌	C_2H_4	+	H		$1.32{\cdot}10^{16}$	−0.94	0.24	99
CH_4	+	$^3CH_2$	⇌	CH_3	+	CH_3		$8.40{\cdot}10^{12}$	0.0	−2.08	100

continues on next page

												A	n	E_a	no.

continued from previous page

2.11. CH_3OH reactions

CH_3OH	+	H	⇌	CH_2OH	+	H_2						$2.75{\cdot}10^{9}$	1.24	18.79	101
CH_3OH	+	H	⇌	CH_3O	+	H_2						$6.87{\cdot}10^{8}$	1.24	18.79	102
CH_3OH	+	O	⇌	CH_2OH	+	OH						$1.98{\cdot}10^{13}$	0.0	22.2	103
CH_3OH	+	O	⇌	CH_3O	+	OH						$4.94{\cdot}10^{12}$	0.0	22.2	104
CH_3OH	+	OH	⇌	CH_2OH	+	H_2O						$5.27{\cdot}10^{6}$	1.92	−1.2	105
CH_3OH	+	OH	⇌	CH_3O	+	H_2O						$9.30{\cdot}10^{5}$	1.92	−1.2	106
CH_3OH	+	HO_2	⇌	CH_2OH	+	H_2O_2						$6.20{\cdot}10^{12}$	0.0	81.1	107
CH_3OH	+	O_2	⇌	HO_2	+	CH_2OH						$2.05{\cdot}10^{13}$	0.0	189.1	108
CH_3OH	+	CH_3	⇌	CH_4	+	CH_2OH						$9.94{\cdot}10^{0}$	3.45	33.42	109
CH_3OH	+	CH_3	⇌	CH_4	+	CH_3O						$2.02{\cdot}10^{1}$	3.45	33.42	110
CH_3OH	+	CH_3O	⇌	CH_2OH	+	CH_3OH						$1.50{\cdot}10^{12}$	0.0	29.3	111
CH_3OH	+	CH_2O	→	CH_3O	+	CH_3O						$1.53{\cdot}10^{12}$	0.0	333.2	112

2.12. CH_3O_2H reactions

CH_3O_2H			⇌	CH_3O	+	OH						$6.00{\cdot}10^{14}$	0.0	177.1	113
CH_3O_2H	+	O	⇌	OH	+	CH_3O_2						$2.47{\cdot}10^{13}$	0.0	19.95	114
CH_3O_2H	+	OH	⇌	H_2O	+	CH_3O_2						$1.08{\cdot}10^{12}$	0.0	−1.83	115

3. C_2–hydrocarbons oxidation

3.1. C_2H reactions

C_2H	+	O	⇌	CO	+	CH						$5.96{\cdot}10^{13}$	0.0	0.0	116
C_2H	+	O_2	⇌	HCCO	+	O						$3.25{\cdot}10^{14}$	−0.35	0.0	117
C_2H	+	O_2	⇌	CO_2	+	CH						$2.92{\cdot}10^{15}$	−0.35	0.0	118
C_2H	+	CH_4	⇌	C_2H_2	+	CH_3						$2.17{\cdot}10^{10}$	0.94	2.73	119

3.2. HCCO reactions

HCCO	+	H	⇌	$^3CH_2$	+	CO						$1.06{\cdot}10^{13}$	0.0	0.0	120
HCCO	+	O	→	CO	+	CO	+	H				$1.53{\cdot}10^{14}$	0.0	0.0	121
HCCO	+	$^3CH_2$	⇌	C_2H_3	+	CO						$3.00{\cdot}10^{13}$	0.0	0.0	122

3.3. C_2H_2 reactions

C_2H_2	+	M(1)	⇌	C_2H	+	H	+	M(1)				$3.60{\cdot}10^{16}$	0.0	446.0	123
C_2H_2	+	H	⇌	C_2H	+	H_2						$2.01{\cdot}10^{9}$	1.64	126.79	124
C_2H_2	+	O	⇌	$^3CH_2$	+	CO						$1.48{\cdot}10^{8}$	1.4	9.23	125
C_2H_2	+	O	⇌	HCCO	+	H						$9.40{\cdot}10^{8}$	1.4	9.23	126

continues on next page

								A	n	E_a	no.
continued from previous page											
C_2H_2	+	OH	⇌	H_2O	+	C_2H		$6.42{\cdot}10^{14}$	0.0	56.54	127
C_2H_2	+	O_2	⇌	HCCO	+	OH		$2.00{\cdot}10^{8}$	1.5	126.0	128
C_2H_2	+	C_2H	⇌	C_4H_2	+	H		$7.83{\cdot}10^{13}$	0.0	0.0	129
		3.4. CH_2CO reactions									
CH_2CO	+	M(1)	⇌	$^3CH_2$	+	CO	+ M(1)	$1.00{\cdot}10^{16}$	0.0	248.0	130
CH_2CO	+	H	⇌	CH_3	+	CO		$3.25{\cdot}10^{10}$	0.85	11.89	131
CH_2CO	+	O	⇌	CH_2O	+	CO		$3.61{\cdot}10^{11}$	0.0	5.65	132
CH_2CO	+	O	→	CHO	+	H	+ CO	$1.81{\cdot}10^{11}$	0.0	5.65	133
CH_2CO	+	O	⇌	CHO	+	CHO		$1.81{\cdot}10^{11}$	0.0	5.65	134
CH_2CO	+	OH	⇌	CH_3	+	CO_2		$6.24{\cdot}10^{11}$	0.0	4.24	135
CH_2CO	+	OH	⇌	CH_2O	+	CHO		$3.37{\cdot}10^{10}$	0.0	4.24	136
		3.5. C_2H_3 reactions									
C_2H_3	+	M(1)	⇌	C_2H_2	+	H	+ M(1)	$7.80{\cdot}10^{8}$	1.62	155.06	137
							LOW	$3.24{\cdot}10^{27}$	−3.4	149.82	
							TROE	0.35 0.0	0.0	0.0	
C_2H_3	+	H	⇌	C_2H_2	+	H_2		$4.22{\cdot}10^{13}$	0.0	0.0	138
C_2H_3	+	O	⇌	C_2H_2	+	OH		$3.01{\cdot}10^{13}$	0.0	0.0	139
C_2H_3	+	O	⇌	CH_3	+	CO		$3.01{\cdot}10^{13}$	0.0	0.0	140
C_2H_3	+	O	⇌	CHO	+	$^3CH_2$		$3.01{\cdot}10^{13}$	0.0	0.0	141
C_2H_3	+	OH	⇌	C_2H_2	+	H_2O		$5.00{\cdot}10^{12}$	0.0	0.0	142
C_2H_3	+	O_2	⇌	CH_2O	+	CHO		$7.71{\cdot}10^{12}$	0.0	−1.0	143
C_2H_3	+	O_2	⇌	CH_2CHO	+	O		$8.15{\cdot}10^{12}$	0.0	−1.04	144
C_2H_3	+	O_2	⇌	C_2H_2	+	HO_2		$4.65{\cdot}10^{11}$	0.0	−1.04	145
		3.6. CH_3CO reactions									
CH_3CO	+	H	⇌	CH_2CO	+	H_2		$2.00{\cdot}10^{13}$	0.0	0.0	146
		3.7. CH_2CHO reactions									
CH_2CHO	+	H	⇌	CH_2CO	+	H_2		$2.00{\cdot}10^{13}$	0.0	0.0	147
		3.8. C_2H_4 reactions									
C_2H_4	+	M(1)	⇌	C_2H_2	+	H_2	+ M(1)	$2.92{\cdot}10^{17}$	1.0	327.49	148
C_2H_4	+	M(1)	⇌	C_2H_3	+	H	+ M(1)	$7.40{\cdot}10^{17}$	0.0	404.06	149
C_2H_4	+	H	+ M(1) →	C_2H_5	+	M(1)		$3.98{\cdot}10^{9}$	1.28	5.4	150
							LOW	$1.18{\cdot}10^{19}$	0.0	3.2	
							TROE	0.76 40.0	1025.0	0.0	
C_2H_4	+	H	⇌	C_2H_3	+	H_2		$2.35{\cdot}10^{2}$	3.62	47.14	151

continues on next page

								A	n	E_a	no.
continued from previous page											
C_2H_4	+	O	⇌	CH_2CHO	+	H		$4.74{\cdot}10^{6}$	1.88	0.76	152
C_2H_4	+	O	⇌	CHO	+	CH_3		$8.13{\cdot}10^{6}$	1.88	0.76	153
C_2H_4	+	O	⇌	CH_2CO	+	H_2		$6.77{\cdot}10^{5}$	1.88	0.76	154
C_2H_4	+	OH	⇌	C_2H_3	+	H_2O		$6.48{\cdot}10^{12}$	0.0	24.9	155
C_2H_4	+	CH	⇌	C_3H_4	+	H		$1.32{\cdot}10^{14}$	0.0	−1.44	156
C_2H_4	+	$^1CH_2$	⇌	C_3H_6				$7.24{\cdot}10^{13}$	0.0	0.0	157
C_2H_4	+	CH_3	⇌	C_2H_3	+	CH_4		$6.02{\cdot}10^{7}$	1.56	69.6	158
		3.9. CH_3CHO reactions									
CH_3CHO	+	M(1)	⇌	CH_3	+	CHO	+ M(1)	$2.10{\cdot}10^{16}$	0.0	342.0	159
							LOW	$7.83{\cdot}10^{17}$	0.0	342.0	
							TROE	0.5 0.0	0.0	0.0	
CH_3CHO	+	H	⇌	CH_3CO	+	H_2		$2.05{\cdot}10^{9}$	1.16	10.06	160
CH_3CHO	+	H	⇌	CH_2CHO	+	H_2		$2.05{\cdot}10^{9}$	1.16	10.06	161
CH_3CHO	+	O	⇌	CH_3CO	+	OH		$5.26{\cdot}10^{12}$	0.0	7.6	162
CH_3CHO	+	O	⇌	CH_2CHO	+	OH		$5.84{\cdot}10^{11}$	0.0	7.6	163
CH_3CHO	+	OH	⇌	CH_3CO	+	H_2O		$2.69{\cdot}10^{8}$	1.35	−6.58	164
CH_3CHO	+	OH	⇌	CH_2CHO	+	H_2O		$2.02{\cdot}10^{7}$	1.35	−6.58	165
CH_3CHO	+	HO_2	⇌	CH_3CO	+	H_2O_2		$4.10{\cdot}10^{4}$	2.5	42.69	166
CH_3CHO	+	O_2	⇌	CH_3CO	+	HO_2		$1.20{\cdot}10^{5}$	2.5	157.14	167
CH_3CHO	+	$^3CH_2$	⇌	CH_3CO	+	CH_3		$2.50{\cdot}10^{12}$	0.0	15.9	168
CH_3CHO	+	CH_3	⇌	CH_3CO	+	CH_4		$3.49{\cdot}10^{-10}$	6.21	6.82	169
		3.10. C_2H_5 reactions									
C_2H_5	+	M(1)	→	C_2H_4	+	H	+ M(1)	$4.10{\cdot}10^{13}$	0.0	166.8	170
							LOW	$3.65{\cdot}10^{18}$	0.0	139.68	
							TROE	0.75 97.0	1379.0	0.0	
C_2H_5	+	H	⇌	CH_3	+	CH_3		$4.22{\cdot}10^{13}$	0.0	0.0	171
C_2H_5	+	O	⇌	CH_3CHO	+	H		$5.32{\cdot}10^{13}$	0.0	0.0	172
C_2H_5	+	O	⇌	CH_2O	+	CH_3		$3.98{\cdot}10^{13}$	0.0	0.0	173
C_2H_5	+	O_2	⇌	C_2H_4	+	HO_2		$2.41{\cdot}10^{10}$	0.0	0.0	174
C_2H_5	+	CH_3	⇌	C_2H_4	+	CH_4		$9.03{\cdot}10^{11}$	0.0	0.0	175
C_2H_5	+	C_2H_5	⇌	C_2H_4	+	C_2H_6		$1.40{\cdot}10^{12}$	0.0	0.0	176
		3.11. C_2H_5O reactions									
C_2H_5O			⇌	CH_3CHO	+	H		$2.00{\cdot}10^{14}$	0.0	97.0	177
C_2H_5O			⇌	CH_2O	+	CH_3		$8.00{\cdot}10^{13}$	0.0	90.0	178
C_2H_5O	+	H	⇌	CH_3CHO	+	H_2		$1.00{\cdot}10^{14}$	0.0	0.0	179
C_2H_5O	+	O	⇌	CH_3CHO	+	OH		$1.21{\cdot}10^{14}$	0.0	0.0	180
C_2H_5O	+	OH	⇌	CH_3CHO	+	H_2O		$1.00{\cdot}10^{14}$	0.0	0.0	181
C_2H_5O	+	O_2	⇌	CH_3CHO	+	HO_2		$6.00{\cdot}10^{10}$	0.0	7.0	182

continues on next page

												A	n	E_a	no.

continued from previous page

3.12. CH_3CHOH reactions

CH_3CHOH			$\rightleftharpoons$	CH_3CHO	+	H						$1.00{\cdot}10^{14}$	0.0	105.0	183
CH_3CHOH	+	H	$\rightleftharpoons$	CH_3CHO	+	H_2						$3.00{\cdot}10^{13}$	0.0	0.0	184
CH_3CHOH	+	O	$\rightleftharpoons$	CH_3CHO	+	OH						$1.20{\cdot}10^{14}$	0.0	0.0	185
CH_3CHOH	+	OH	$\rightleftharpoons$	CH_3CHO	+	H_2O						$1.51{\cdot}10^{13}$	0.0	0.0	186
CH_3CHOH	+	O_2	$\rightleftharpoons$	CH_3CHO	+	HO_2						$8.43{\cdot}10^{15}$	−1.2	0.0	187
CH_3CHOH	+	O_2	$\rightleftharpoons$	CH_3CHO	+	HO_2						$4.82{\cdot}10^{14}$	0.0	20.1	

3.13. CH_2CH_2OH reactions

CH_2CH_2OH			$\rightleftharpoons$	C_2H_4	+	OH						$1.00{\cdot}10^{14}$	0.0	140.0	188
CH_2CH_2OH	+	H	$\rightleftharpoons$	CH_3CHO	+	H_2						$5.00{\cdot}10^{13}$	0.0	0.0	189

3.14. C_2H_5OH reactions

C_2H_5OH			$\rightleftharpoons$	CH_3	+	CH_2OH						$3.10{\cdot}10^{15}$	0.0	337.2	190
C_2H_5OH			$\rightleftharpoons$	C_2H_5	+	OH						$5.00{\cdot}10^{16}$	0.0	381.6	191
C_2H_5OH			$\rightleftharpoons$	C_2H_4	+	H_2O						$1.00{\cdot}10^{14}$	0.0	320.9	192
C_2H_5OH	+	H	$\rightleftharpoons$	CH_3CHOH	+	H_2						$4.40{\cdot}10^{12}$	0.0	19.1	193
C_2H_5OH	+	H	$\rightleftharpoons$	C_2H_5	+	H_2O						$5.90{\cdot}10^{11}$	0.0	14.4	194
C_2H_5OH	+	O	$\rightleftharpoons$	CH_3CHOH	+	OH						$5.42{\cdot}10^{5}$	2.5	7.73	195
C_2H_5OH	+	O	$\rightleftharpoons$	C_2H_5O	+	OH						$3.01{\cdot}10^{4}$	2.5	7.73	196
C_2H_5OH	+	O	$\rightleftharpoons$	CH_2CH_2OH	+	OH						$3.01{\cdot}10^{4}$	2.5	7.73	197
C_2H_5OH	+	OH	$\rightleftharpoons$	CH_3CHOH	+	H_2O						$2.14{\cdot}10^{7}$	1.78	−3.53	198
C_2H_5OH	+	OH	$\rightleftharpoons$	C_2H_5O	+	H_2O						$9.03{\cdot}10^{5}$	1.78	−3.53	199
C_2H_5OH	+	OH	$\rightleftharpoons$	CH_2CH_2OH	+	H_2O						$1.13{\cdot}10^{6}$	1.78	−3.53	200
C_2H_5OH	+	HO_2	$\rightleftharpoons$	CH_3CHOH	+	H_2O_2						$6.30{\cdot}10^{12}$	0.0	81.1	201
C_2H_5OH	+	CH_3	$\rightleftharpoons$	CH_3CHOH	+	CH_4						$4.70{\cdot}10^{11}$	0.0	40.57	202
C_2H_5OH	+	CH_3	$\rightleftharpoons$	CH_2CH_2OH	+	CH_4						$3.61{\cdot}10^{10}$	0.0	39.91	203
C_2H_5OH	+	CH_3	$\rightleftharpoons$	C_2H_5O	+	CH_4						$9.03{\cdot}10^{10}$	0.0	39.32	204
C_2H_5OH	+	CH_3O	$\rightleftharpoons$	CH_3CHOH	+	CH_3OH						$2.00{\cdot}10^{11}$	0.0	29.3	205
C_2H_5OH	+	CH_2O	$\rightleftharpoons$	C_2H_5O	+	CH_3O						$1.53{\cdot}10^{12}$	0.0	333.2	206
C_2H_5OH	+	C_2H_5O	$\rightleftharpoons$	C_2H_5OH	+	CH_3CHOH						$2.00{\cdot}10^{11}$	0.0	29.3	207

3.15. C_2H_6 reactions

C_2H_6	+	H	$\rightleftharpoons$	C_2H_5	+	H_2						$9.82{\cdot}10^{13}$	0.0	38.58	208
C_2H_6	+	O	$\rightleftharpoons$	C_2H_5	+	OH						$1.00{\cdot}10^{9}$	1.5	24.4	209
C_2H_6	+	OH	$\rightleftharpoons$	C_2H_5	+	H_2O						$9.15{\cdot}10^{6}$	2.0	4.16	210
C_2H_6	+	HO_2	$\rightleftharpoons$	C_2H_5	+	H_2O_2						$1.10{\cdot}10^{5}$	2.5	70.5	211
C_2H_6	+	O_2	$\rightleftharpoons$	C_2H_5	+	HO_2						$7.29{\cdot}10^{5}$	2.5	205.69	212

continues on next page

								A	n	E_a	no.
continued from previous page											
C_2H_6	+	$^3CH_2$	⇌	C_2H_5	+	CH_3		$2.20{\cdot}10^{13}$	0.0	36.3	213
C_2H_6	+	CH_3	⇌	C_2H_5	+	CH_4		$5.60{\cdot}10^{10}$	0.0	39.41	214
C_2H_6	+	CH_3	⇌	C_2H_5	+	CH_4		$8.43{\cdot}10^{14}$	0.0	93.12	
C_2H_6	+	CH	⇌	C_2H_4	+	CH_3		$1.08{\cdot}10^{14}$	0.0	−1.1	215
4. C_3–hydrocarbons oxidation											
4.1. C_3H_2 reactions											
C_3H_2	+	O_2	⇌	CHO	+	HCCO		$1.00{\cdot}10^{13}$	0.0	0.0	216
C_3H_3	+	OH	⇌	C_3H_2	+	H_2O		$2.00{\cdot}10^{13}$	0.0	0.0	217
4.2. C_3H_3 reactions											
C_3H_3	+	O	→	CO	+	C_2H_3		$3.80{\cdot}10^{13}$	0.0	0.0	218
C_3H_3	+	O_2	→	HCCO	+	CH_2O		$6.00{\cdot}10^{12}$	0.0	0.0	219
4.3. C_3H_4 reactions											
C_3H_4	+	O	⇌	CH_2O	+	C_2H_2		$1.00{\cdot}10^{12}$	0.0	0.0	220
C_3H_4	+	O	⇌	CHO	+	C_2H_3		$1.00{\cdot}10^{12}$	0.0	0.0	221
C_3H_4	+	OH	⇌	CH_2O	+	C_2H_3		$1.00{\cdot}10^{12}$	0.0	0.0	222
C_3H_4	+	OH	⇌	CHO	+	C_2H_4		$1.00{\cdot}10^{12}$	0.0	0.0	223
C_3H_4	+	M(1)	⇌	H	+	C_3H_3	+ M(1)	$1.00{\cdot}10^{17}$	0.0	293.0	224
C_3H_4	+	H	⇌	CH_3	+	C_2H_2		$2.00{\cdot}10^{13}$	0.0	10.0	225
C_3H_4	+	H	⇌	H_2	+	C_3H_3		$1.00{\cdot}10^{12}$	0.0	6.3	226
C_3H_4	+	C_2H	⇌	C_2H_2	+	C_3H_3		$1.00{\cdot}10^{13}$	0.0	0.0	227
C_3H_4	+	CH_3	⇌	C_3H_3	+	CH_4		$2.00{\cdot}10^{12}$	0.0	32.2	228
4.4. C_3H_5 reactions											
C_3H_5			⇌	C_3H_4	+	H		$3.98{\cdot}10^{13}$	0.0	293.1	229
C_3H_5	+	H	⇌	C_3H_4	+	H_2		$1.81{\cdot}10^{13}$	0.0	0.0	230
C_3H_5	+	O_2	⇌	C_3H_4	+	HO_2		$1.02{\cdot}10^{12}$	0.0	94.78	231
C_3H_5	+	OH	⇌	C_3H_4	+	H_2O		$6.02{\cdot}10^{12}$	0.0	0.0	232
C_3H_6	+	O_2	⇌	C_3H_5	+	HO_2		$1.90{\cdot}10^{12}$	0.0	163.8	233
C_3H_5	+	CH_3	⇌	C_3H_4	+	CH_4		$3.61{\cdot}10^{11}$	0.0	0.0	234
C_3H_5	+	C_3H_5	⇌	C_3H_6	+	C_3H_4		$6.02{\cdot}10^{10}$	0.0	0.0	235
CH_3	+	C_2H_2	⇌	C_3H_5				$6.00{\cdot}10^{11}$	0.0	32.4	236
4.5. C_3H_6 reactions											
C_3H_6			⇌	C_3H_5	+	H		$1.00{\cdot}10^{13}$	0.0	326.0	237
C_3H_6			⇌	C_2H_3	+	CH_3		$1.10{\cdot}10^{21}$	−1.2	408.8	238
C_3H_6	+	H	⇌	C_3H_5	+	H_2		$5.00{\cdot}10^{12}$	0.0	6.3	239

continues on next page

								A	n	E_a	no.
continued from previous page											
C_3H_6	+	O	⇌	C_2H_4	+	CH_2O		$5.90{\cdot}10^{13}$	0.0	21.0	240
C_3H_6	+	O	⇌	C_2H_5	+	CHO		$3.60{\cdot}10^{12}$	0.0	0.0	241
C_3H_6	+	O	⇌	CH_3	+	CH_3CO		$5.00{\cdot}10^{12}$	0.0	2.5	242
C_3H_6	+	OH	⇌	C_2H_5	+	CH_2O		$7.90{\cdot}10^{12}$	0.0	0.0	243
C_3H_6	+	OH	⇌	CH_3	+	CH_3CHO		$5.10{\cdot}10^{12}$	0.0	0.0	244
C_3H_6	+	OH	⇌	C_3H_5	+	H_2O		$4.00{\cdot}10^{12}$	0.0	0.0	245
C_3H_6	+	CH_3	⇌	CH_4	+	C_3H_5		$8.91{\cdot}10^{10}$	0.0	35.6	246
C_3H_6	+	C_2H_5	⇌	C_3H_5	+	C_2H_6		$1.00{\cdot}10^{11}$	0.0	38.5	247
		4.6. n-C_3H_7 reactions									
n-C_3H_7			⇌	CH_3	+	C_2H_4		$9.60{\cdot}10^{13}$	0.0	129.8	248
n-C_3H_7			⇌	H	+	C_3H_6		$1.25{\cdot}10^{14}$	0.0	154.9	249
n-C_3H_7	+	O_2	⇌	C_3H_6	+	HO_2		$1.00{\cdot}10^{12}$	0.0	20.9	250
		4.7. i-C_3H_7 reactions									
i-C_3H_7			⇌	H	+	C_3H_6		$6.30{\cdot}10^{13}$	0.0	154.5	251
i-C_3H_7			⇌	CH_3	+	C_2H_4		$2.00{\cdot}10^{10}$	0.0	123.5	252
i-C_3H_7	+	O_2	⇌	C_3H_6	+	HO_2		$1.99{\cdot}10^{10}$	0.0	−10.72	253
		4.8. C_3H_8 reactions									
C_3H_8	+	M(1)	⇌	CH_3	+	C_2H_5	+ M(1)	$4.00{\cdot}10^{23}$	−1.87	377.41	254
							LOW	$2.24{\cdot}10^{19}$	0.0	271.87	
							TROE	0.76 1946.0	38.0	0.0	
C_3H_8	+	H	⇌	H_2	+	n-C_3H_7		$1.30{\cdot}10^{14}$	0.0	40.6	255
C_3H_8	+	H	⇌	H_2	+	i-C_3H_7		$1.00{\cdot}10^{14}$	0.0	34.9	256
C_3H_8	+	O	⇌	n-C_3H_7	+	OH		$3.00{\cdot}10^{13}$	0.0	24.1	257
C_3H_8	+	O	⇌	i-C_3H_7	+	OH		$2.60{\cdot}10^{13}$	0.0	18.7	258
C_3H_8	+	OH	⇌	n-C_3H_7	+	H_2O		$3.70{\cdot}10^{12}$	0.0	6.9	259
C_3H_8	+	OH	⇌	i-C_3H_7	+	H_2O		$2.80{\cdot}10^{12}$	0.0	3.6	260
C_3H_8	+	HO_2	→	n-C_3H_7	+	H_2O_2		$1.14{\cdot}10^{13}$	0.0	81.2	261
n-C_3H_7	+	H_2O_2	→	C_3H_8	+	HO_2		$2.33{\cdot}10^{12}$	0.0	41.1	262
C_3H_8	+	HO_2	→	i-C_3H_7	+	H_2O_2		$3.40{\cdot}10^{12}$	0.0	71.2	263
i-C_3H_7	+	H_2O_2	→	C_3H_8	+	HO_2		$4.16{\cdot}10^{11}$	0.0	31.1	264
C_3H_8	+	CH_3	→	CH_4	+	n-C_3H_7		$4.00{\cdot}10^{11}$	0.0	39.8	265
n-C_3H_7	+	CH_4	→	CH_3	+	C_3H_8		$3.12{\cdot}10^{12}$	0.0	68.9	266
C_3H_8	+	CH_3	→	CH_4	+	i-C_3H_7		$1.30{\cdot}10^{12}$	0.0	48.6	267
i-C_3H_7	+	CH_4	→	CH_3	+	C_3H_8		$1.01{\cdot}10^{13}$	0.0	77.7	268
C_3H_8	+	O_2	→	n-C_3H_7	+	HO_2		$2.52{\cdot}10^{13}$	0.0	205.2	269
n-C_3H_7	+	HO_2	→	C_3H_8	+	O_2		$2.08{\cdot}10^{12}$	0.0	0.0	270
C_3H_8	+	O_2	→	i-C_3H_7	+	HO_2		$2.00{\cdot}10^{13}$	0.0	199.3	271

continues on next page

							A	n	E_a	no.
continued from previous page										
i-C_3H_7	+	HO_2	→	C_3H_8	+	O_2	$2.08{\cdot}10^{12}$	0.0	0.0	272
C_3H_8	+	CH_3O	→	n-C_3H_7	+	CH_3OH	$3.00{\cdot}10^{11}$	0.0	29.3	273
n-C_3H_7	+	CH_3OH	→	C_3H_8	+	CH_3O	$1.22{\cdot}10^{10}$	0.0	38.5	274
C_3H_8	+	CH_3O	→	i-C_3H_7	+	CH_3OH	$3.00{\cdot}10^{11}$	0.0	29.3	275
i-C_3H_7	+	CH_3OH	→	C_3H_8	+	CH_3O	$1.22{\cdot}10^{10}$	0.0	38.5	276

5. C_4–hydrocarbons oxidation

5.1. C_4H_2 reactions

C_4H_2	+	O	⇌	C_3H_2	+	CO	$7.89{\cdot}10^{12}$	0.0	5.64	277
C_4H_2	+	OH	⇌	C_3H_2	+	CHO	$6.68{\cdot}10^{12}$	0.0	−1.71	278

5.2. C_4H_6 reactions

C_4H_6			⇌	C_2H_3	+	C_2H_3	$4.03{\cdot}10^{19}$	−1.0	411.0	279
C_2H_3	+	C_2H_4	⇌	C_4H_6	+	H	$7.83{\cdot}10^{10}$	0.0	0.0	280
C_4H_6	+	O	⇌	C_2H_4	+	CH_2CO	$1.00{\cdot}10^{12}$	0.0	0.0	281
C_4H_6	+	O	⇌	CH_2O	+	C_3H_4	$1.00{\cdot}10^{12}$	0.0	0.0	282
C_4H_6	+	OH	⇌	C_2H_5	+	CH_2CO	$1.00{\cdot}10^{12}$	0.0	0.0	283
C_4H_6	+	OH	⇌	CH_2O	+	C_3H_5	$2.00{\cdot}10^{12}$	0.0	0.0	284
C_4H_6	+	OH	⇌	C_2H_3	+	CH_3CHO	$5.00{\cdot}10^{12}$	0.0	0.0	285

5.3. C_4H_7 reactions

C_4H_7			⇌	C_4H_6	+	H	$1.20{\cdot}10^{14}$	0.0	206.4	286
C_4H_7			⇌	C_2H_4	+	C_2H_3	$1.00{\cdot}10^{11}$	0.0	154.9	287
C_4H_7	+	H	⇌	C_4H_6	+	H_2	$3.16{\cdot}10^{12}$	0.0	0.0	288
C_4H_7	+	O_2	⇌	C_4H_6	+	HO_2	$1.00{\cdot}10^{11}$	0.0	0.0	289
C_4H_7	+	C_4H_7	⇌	C_4H_6	+	1-C_4H_8	$3.16{\cdot}10^{12}$	0.0	0.0	290
C_4H_7	+	CH_3	⇌	C_4H_6	+	CH_4	$1.00{\cdot}10^{13}$	0.0	0.0	291
C_4H_7	+	C_2H_3	⇌	C_4H_6	+	C_2H_4	$4.00{\cdot}10^{12}$	0.0	0.0	292
C_4H_7	+	C_2H_5	⇌	C_4H_6	+	C_2H_6	$4.00{\cdot}10^{12}$	0.0	0.0	293
C_4H_7	+	C_2H_5	⇌	1-C_4H_8	+	C_2H_4	$5.00{\cdot}10^{11}$	0.0	0.0	294
C_4H_7	+	C_2H_5	⇌	trans-2-C_4H_8	+	C_2H_4	$5.00{\cdot}10^{11}$	0.0	0.0	295
C_4H_7	+	C_2H_5	⇌	cis-2-C_4H_8	+	C_2H_4	$5.00{\cdot}10^{11}$	0.0	0.0	296
C_4H_7	+	C_3H_5	⇌	C_4H_6	+	C_3H_6	$4.00{\cdot}10^{13}$	0.0	0.0	297

5.4. 1-C_4H_8 reactions

1-C_4H_8			⇌	trans-2-C_4H_8			$4.00{\cdot}10^{11}$	0.0	251.0	298
1-C_4H_8			⇌	cis-2-C_4H_8			$4.00{\cdot}10^{11}$	0.0	251.0	299
1-C_4H_8			⇌	C_3H_5	+	CH_3	$8.00{\cdot}10^{16}$	0.0	307.4	300
1-C_4H_8			⇌	C_2H_3	+	C_2H_5	$2.00{\cdot}10^{18}$	−1.0	405.2	301
1-C_4H_8			⇌	H	+	C_4H_7	$4.11{\cdot}10^{18}$	−1.0	407.7	302

continues on next page

										A	n	E_a	no.
continued from previous page													
1-C_4H_8	+	H	⇌	C_4H_7	+	H_2				$5.00{\cdot}10^{13}$	0.0	16.3	303
1-C_4H_8	+	O	⇌	CH_3CHO	+	C_2H_4				$1.26{\cdot}10^{12}$	0.0	3.6	304
1-C_4H_8	+	O	⇌	CH_3	+	C_2H_5	+	CO		$1.62{\cdot}10^{13}$	0.0	3.6	305
1-C_4H_8	+	O	⇌	C_3H_6	+	CH_2O				$2.50{\cdot}10^{12}$	0.0	0.0	306
1-C_4H_8	+	O	⇌	C_4H_7	+	OH				$1.30{\cdot}10^{13}$	0.0	18.8	307
1-C_4H_8	+	OH	⇌	CH_3CHO	+	C_2H_5				$1.00{\cdot}10^{11}$	0.0	0.0	308
1-C_4H_8	+	OH	⇌	CH_3	+	C_2H_6	+	CO		$1.00{\cdot}10^{10}$	0.0	0.0	309
1-C_4H_8	+	OH	⇌	n-C_3H_7	+	CH_2O				$6.50{\cdot}10^{12}$	0.0	0.0	310
1-C_4H_8	+	OH	⇌	C_4H_7	+	H_2O				$1.75{\cdot}10^{13}$	0.0	29.1	311
1-C_4H_8	+	CH_3	⇌	C_4H_7	+	CH_4				$1.00{\cdot}10^{11}$	0.0	30.6	312
1-C_4H_8	+	O_2	⇌	C_4H_7	+	HO_2				$4.00{\cdot}10^{12}$	0.0	167.4	313
1-C_4H_8	+	HO_2	⇌	C_4H_7	+	H_2O_2				$1.00{\cdot}10^{11}$	0.0	71.4	314
1-C_4H_8	+	C_2H_5	⇌	C_4H_7	+	C_2H_6				$1.00{\cdot}10^{11}$	0.0	33.5	315
1-C_4H_8	+	C_3H_5	⇌	C_4H_7	+	C_3H_6				$8.00{\cdot}10^{10}$	0.0	51.9	316
1-C_4H_8	+	C_4H_7	⇌	C_4H_7	+	trans-2-C_4H_8				$3.98{\cdot}10^{10}$	0.0	51.9	317
1-C_4H_8	+	C_4H_7	⇌	C_4H_7	+	cis-2-C_4H_8				$3.98{\cdot}10^{10}$	0.0	51.9	318
				5.5. trans-2-C_4H_8 reactions									
trans-2-C_4H_8			⇌	H	+	C_4H_7				$4.11{\cdot}10^{18}$	−1.0	407.7	319
trans-2-C_4H_8			⇌	CH_3	+	C_3H_5				$6.50{\cdot}10^{14}$	0.0	298.3	320
trans-2-C_4H_8	+	H	⇌	C_4H_7	+	H_2				$5.00{\cdot}10^{12}$	0.0	14.6	321
trans-2-C_4H_8	+	O	⇌	C_2H_4	+	CH_3CHO				$1.00{\cdot}10^{12}$	0.0	0.0	322
trans-2-C_4H_8	+	O	⇌	i-C_3H_7	+	CHO				$6.03{\cdot}10^{12}$	0.0	0.0	323
trans-2-C_4H_8	+	OH	⇌	C_4H_7	+	H_2O				$1.01{\cdot}10^{14}$	0.0	12.8	324
trans-2-C_4H_8	+	OH	⇌	C_2H_5	+	CH_3CHO				$1.51{\cdot}10^{13}$	0.0	0.0	325
trans-2-C_4H_8	+	CH_3	⇌	C_4H_7	+	CH_4				$1.00{\cdot}10^{11}$	0.0	34.3	326
				5.6. c-2-C_4H_8 reactions									
cis-2-C_4H_8			⇌	trans-2-C_4H_8						$1.00{\cdot}10^{13}$	0.0	259.4	327
cis-2-C_4H_8			⇌	C_4H_6	+	H_2				$1.00{\cdot}10^{13}$	0.0	274.1	328
cis-2-C_4H_8			⇌	C_4H_7	+	H				$4.07{\cdot}10^{18}$	−1.0	407.3	329
cis-2-C_4H_8			⇌	C_3H_5	+	CH_3				$1.25{\cdot}10^{15}$	0.0	298.3	330
cis-2-C_4H_8	+	H	⇌	C_4H_7	+	H_2				$1.00{\cdot}10^{12}$	0.0	14.6	331
cis-2-C_4H_8	+	OH	⇌	C_4H_7	+	H_2O				$1.26{\cdot}10^{14}$	0.0	12.8	332
cis-2-C_4H_8	+	OH	⇌	C_2H_5	+	CH_3CHO				$1.40{\cdot}10^{13}$	0.0	0.0	333
cis-2-C_4H_8	+	O	⇌	i-C_3H_7	+	CHO				$6.03{\cdot}10^{12}$	0.0	0.0	334
cis-2-C_4H_8	+	O	⇌	C_2H_4	+	CH_3CHO				$1.00{\cdot}10^{12}$	0.0	0.0	335
cis-2-C_4H_8	+	CH_3	⇌	C_4H_7	+	CH_4				$1.00{\cdot}10^{11}$	0.0	34.3	336

continues on next page

											A	n	E_a	no.
continued from previous page														
			5.7. p-C_4H_9 reactions											
p-C_4H_9			$\rightleftharpoons$	C_2H_5	+	C_2H_4					$2.50{\cdot}10^{13}$	0.0	120.6	337
p-C_4H_9			$\rightleftharpoons$	1-C_4H_8	+	H					$1.26{\cdot}10^{13}$	0.0	161.6	338
p-C_4H_9	+	O_2	$\rightleftharpoons$	1-C_4H_8	+	HO_2					$1.00{\cdot}10^{12}$	0.0	8.4	339
			5.8. s-C_4H_9 reactions											
s-C_4H_9			$\rightleftharpoons$	1-C_4H_8	+	H					$2.00{\cdot}10^{13}$	0.0	169.2	340
s-C_4H_9			$\rightleftharpoons$	trans-2-C_4H_8	+	H					$5.00{\cdot}10^{13}$	0.0	158.7	341
s-C_4H_9			$\rightleftharpoons$	cis-2-C_4H_8	+	H					$5.00{\cdot}10^{13}$	0.0	158.7	342
s-C_4H_9			$\rightleftharpoons$	C_3H_6	+	CH_3					$4.00{\cdot}10^{14}$	0.0	139.0	343
s-C_4H_9	+	O_2	$\rightleftharpoons$	1-C_4H_8	+	HO_2					$2.00{\cdot}10^{12}$	0.0	18.8	344
s-C_4H_9	+	O_2	$\rightleftharpoons$	trans-2-C_4H_8	+	HO_2					$2.00{\cdot}10^{13}$	0.0	17.8	345
s-C_4H_9	+	O_2	$\rightleftharpoons$	cis-2-C_4H_8	+	HO_2					$2.00{\cdot}10^{13}$	0.0	17.8	346
			5.9. C_4H_{10} reactions											
C_2H_5	+	C_2H_5	$\rightleftharpoons$	C_4H_{10}							$8.00{\cdot}10^{12}$	0.0	0.0	347
C_4H_{10}			$\rightarrow$	n-C_3H_7	+	CH_3					$1.00{\cdot}10^{17}$	0.0	357.6	348
n-C_3H_7	+	CH_3	$\rightarrow$	C_4H_{10}							$2.00{\cdot}10^{13}$	0.0	0.0	349
C_4H_{10}	+	H	$\rightarrow$	p-C_4H_9	+	H_2					$5.63{\cdot}10^{7}$	2.0	32.2	350
p-C_4H_9	+	H_2	$\rightarrow$	C_4H_{10}	+	H					$9.12{\cdot}10^{12}$	0.0	60.6	351
C_4H_{10}	+	H	$\rightarrow$	s-C_4H_9	+	H_2					$1.75{\cdot}10^{7}$	2.0	20.9	352
s-C_4H_9	+	H_2	$\rightarrow$	C_4H_{10}	+	H					$1.54{\cdot}10^{13}$	0.0	66.5	353
C_4H_{10}	+	O	$\rightarrow$	p-C_4H_9	+	OH					$1.13{\cdot}10^{14}$	0.0	32.9	354
p-C_4H_9	+	OH	$\rightarrow$	C_4H_{10}	+	O					$1.48{\cdot}10^{13}$	0.0	51.3	355
C_4H_{10}	+	O	$\rightarrow$	s-C_4H_9	+	OH					$5.62{\cdot}10^{13}$	0.0	21.8	356
s-C_4H_9	+	OH	$\rightarrow$	C_4H_{10}	+	O					$7.35{\cdot}10^{12}$	0.0	40.2	357
C_4H_{10}	+	OH	$\rightarrow$	p-C_4H_9	+	H_2O					$4.13{\cdot}10^{7}$	1.7	3.2	358
p-C_4H_9	+	H_2O	$\rightarrow$	C_4H_{10}	+	OH					$7.17{\cdot}10^{7}$	1.7	93.3	359
C_4H_{10}	+	OH	$\rightarrow$	s-C_4H_9	+	H_2O					$7.23{\cdot}10^{7}$	1.6	−1.0	360
s-C_4H_9	+	H_2O	$\rightarrow$	C_4H_{10}	+	OH					$1.28{\cdot}10^{8}$	1.6	89.1	361
C_4H_{10}	+	HO_2	$\rightarrow$	p-C_4H_9	+	H_2O_2					$1.14{\cdot}10^{13}$	0.0	81.2	362
p-C_4H_9	+	H_2O_2	$\rightarrow$	C_4H_{10}	+	HO_2					$4.58{\cdot}10^{12}$	0.0	41.1	363
C_4H_{10}	+	HO_2	$\rightarrow$	s-C_4H_9	+	H_2O_2					$6.80{\cdot}10^{12}$	0.0	71.2	364
s-C_4H_9	+	H_2O_2	$\rightarrow$	C_4H_{10}	+	HO_2					$1.63{\cdot}10^{12}$	0.0	31.0	365
C_4H_{10}	+	CH_3	$\rightarrow$	p-C_4H_9	+	CH_4					$1.30{\cdot}10^{12}$	0.0	48.6	366
p-C_4H_9	+	CH_4	$\rightarrow$	C_4H_{10}	+	CH_3					$1.01{\cdot}10^{13}$	0.0	77.7	367
C_4H_{10}	+	CH_3	$\rightarrow$	s-C_4H_9	+	CH_4					$8.00{\cdot}10^{11}$	0.0	39.8	368
s-C_4H_9	+	CH_4	$\rightarrow$	C_4H_{10}	+	CH_3					$6.24{\cdot}10^{12}$	0.0	68.9	369

continues on next page

						A	n	E_a	no.
continued from previous page									
C_4H_{10}	+ O_2	→	p-C_4H_9	+	HO_2	$2.50{\cdot}10^{13}$	0.0	205.2	370
p-C_4H_9	+ HO_2	→	C_4H_{10}	+	O_2	$2.50{\cdot}10^{12}$	0.0	−9.2	371
C_4H_{10}	+ O_2	→	s-C_4H_9	+	HO_2	$4.00{\cdot}10^{13}$	0.0	199.3	372
s-C_4H_9	+ HO_2	→	C_4H_{10}	+	O_2	$4.07{\cdot}10^{12}$	0.0	−15.2	373
C_4H_{10}	+ CH_3O	→	p-C_4H_9	+	CH_3OH	$3.00{\cdot}10^{11}$	0.0	29.3	374
p-C_4H_9	+ CH_3OH	→	C_4H_{10}	+	CH_3O	$1.22{\cdot}10^{10}$	0.0	209.4	375
C_4H_{10}	+ CH_3O	→	s-C_4H_9	+	CH_3OH	$6.00{\cdot}10^{11}$	0.0	29.3	376
s-C_4H_9	+ CH_3OH	→	C_4H_{10}	+	CH_3O	$2.44{\cdot}10^{10}$	0.0	209.4	377
6. Iso mechanism									
	6.1. i-C_4H_7 reactions								
i-C_4H_7		⇌	C_3H_4	+	CH_3	$1.00{\cdot}10^{13}$	0.0	213.6	380
	6.2. i-C_4H_8 reactions								
i-C_4H_8		⇌	C_3H_5	+	CH_3	$5.00{\cdot}10^{18}$	−1.0	307.4	381
i-C_4H_8		⇌	i-C_4H_7	+	H	$1.00{\cdot}10^{17}$	0.0	368.5	382
i-C_4H_8	+ H	⇌	i-C_4H_7	+	H_2	$1.00{\cdot}10^{13}$	0.0	15.9	383
i-C_4H_8	+ O	⇌	i-C_4H_7	+	OH	$2.50{\cdot}10^{5}$	2.6	−4.7	384
i-C_4H_8	+ O	⇌	i-C_3H_7	+	CHO	$7.23{\cdot}10^{5}$	2.3	−4.4	385
i-C_4H_8	+ OH	⇌	i-C_4H_7	+	H_2O	$9.60{\cdot}10^{12}$	0.0	5.2	386
i-C_4H_8	+ OH	⇌	i-C_3H_7	+	CH_2O	$1.50{\cdot}10^{12}$	0.0	0.0	387
i-C_4H_8	+ CH_3	⇌	i-C_4H_7	+	CH_4	$6.03{\cdot}10^{11}$	0.0	37.23	388
	6.3. i-C_4H_9 reactions								
i-C_4H_9		⇌	C_3H_6	+	CH_3	$2.00{\cdot}10^{13}$	0.0	125.34	389
i-C_4H_9		⇌	i-C_4H_8	+	H	$1.00{\cdot}10^{14}$	0.0	151.88	390
i-C_4H_9	+ O_2	⇌	i-C_4H_8	+	HO_2	$2.41{\cdot}10^{10}$	0.0	0.0	391
	6.4. t-C_4H_9 reactions								
t-C_4H_9		⇌	H	+	i-C_4H_8	$8.30{\cdot}10^{13}$	0.0	159.63	392
t-C_4H_9		⇌	C_3H_6	+	CH_3	$1.00{\cdot}10^{16}$	0.0	193.0	393
t-C_4H_9	+ O_2	⇌	i-C_4H_8	+	HO_2	$6.02{\cdot}10^{10}$	0.0	−13.22	394
t-C_4H_9	+ t-C_4H_9	⇌	i-C_4H_{10}	+	i-C_4H_8	$7.23{\cdot}10^{16}$	−1.73	0.0	395
	6.5. i-C_4H_{10} reactions								
i-C_4H_{10}		⇌	CH_3	+	i-C_3H_7	$1.10{\cdot}10^{26}$	−2.61	377.98	396
i-C_4H_{10}		⇌	t-C_4H_9	+	H	$1.00{\cdot}10^{15}$	0.0	390.7	397
i-C_4H_{10}		⇌	i-C_4H_9	+	H	$1.00{\cdot}10^{15}$	0.0	410.4	398

continues on next page

										A	n	E_a	no.
continued from previous page													
$i\text{-}C_4H_{10}$	+	H	$\rightleftharpoons$	$t\text{-}C_4H_9$	+	H_2				$6.02 \cdot 10^{5}$	2.4	10.81	399
$i\text{-}C_4H_{10}$	+	H	$\rightleftharpoons$	$i\text{-}C_4H_9$	+	H_2				$1.81 \cdot 10^{6}$	2.54	28.27	400
$i\text{-}C_4H_{10}$	+	O	$\rightleftharpoons$	$t\text{-}C_4H_9$	+	OH				$1.56 \cdot 10^{5}$	2.5	4.66	401
$i\text{-}C_4H_{10}$	+	O	$\rightleftharpoons$	$i\text{-}C_4H_9$	+	OH				$4.28 \cdot 10^{5}$	2.5	15.25	402
$i\text{-}C_4H_{10}$	+	OH	$\rightleftharpoons$	$t\text{-}C_4H_9$	+	H_2O				$5.73 \cdot 10^{10}$	0.51	0.27	403
$i\text{-}C_4H_{10}$	+	OH	$\rightleftharpoons$	$i\text{-}C_4H_9$	+	H_2O				$2.29 \cdot 10^{8}$	1.53	3.24	404
$i\text{-}C_4H_{10}$	+	HO_2	$\rightleftharpoons$	$i\text{-}C_4H_9$	+	H_2O_2				$3.01 \cdot 10^{4}$	2.55	64.85	405
$i\text{-}C_4H_{10}$	+	HO_2	$\rightleftharpoons$	$t\text{-}C_4H_9$	+	H_2O_2				$3.61 \cdot 10^{3}$	2.55	44.07	406
$i\text{-}C_4H_{10}$	+	CH_3	$\rightleftharpoons$	$t\text{-}C_4H_9$	+	CH_4				$9.04 \cdot 10^{-1}$	3.46	19.24	407
$i\text{-}C_4H_{10}$	+	CH_3	$\rightleftharpoons$	$i\text{-}C_4H_9$	+	CH_4				$1.36 \cdot 10^{0}$	3.65	29.9	408
$i\text{-}C_4H_{10}$	+	O_2	$\rightleftharpoons$	$i\text{-}C_4H_9$	+	HO_2				$4.04 \cdot 10^{13}$	0.0	213.1	409
$i\text{-}C_4H_{10}$	+	O_2	$\rightleftharpoons$	$t\text{-}C_4H_9$	+	HO_2				$3.97 \cdot 10^{13}$	0.0	184.08	410
$i\text{-}C_4H_{10}$	+	CH_3O_2	$\rightleftharpoons$	$i\text{-}C_4H_9$	+	CH_3O_2H				$3.01 \cdot 10^{4}$	2.55	64.85	411
$i\text{-}C_4H_{10}$	+	CH_3O_2	$\rightleftharpoons$	$t\text{-}C_4H_9$	+	CH_3O_2H				$3.61 \cdot 10^{3}$	2.55	44.07	412

Table A.1.: Small hydrocarbons mechanism.

Reaction	Ref.	Reaction	Ref.	Reaction	Ref.	Reaction	Ref.	Reaction	Ref.
6	[107]	206	[178]	268	[179]	317	[180]	365	[179]
21	[107]	207	[178]	269	[179]	318	[180]	366	[179]
23	[11]	213	[179]	270	[179]	319	[180]	367	[179]
24	[11]	216	[131]	271	[179]	320	[180]	368	[179]
28	[131]	217	[131]	272	[179]	321	[180]	369	[179]
30	[89]	218	[179]	273	[179]	322	[180]	370	[179]
70	[89]	219	[179]	274	[179]	323	[180]	371	[179]
74	[89]	220	[179]	275	[179]	324	[180]	372	[179]
82	[107]	221	[179]	276	[179]	325	[180]	373	[179]
84	[107]	222	[179]	277	[181]	326	[180]	374	[179]
86	[107]	223	[179]	278	[182]	327	[180]	375	[179]
89	[107]	224	[179]	279	[180]	328	[180]	376	[179]
90	[179]	225	[179]	281	[180]	329	[180]	377	[179]
91	[107]	226	[179]	282	[180]	330	[180]	380	[183]
92	[184]	227	[179]	283	[180]	331	[180]	381	[183]
107	[11]	228	[179]	284	[180]	332	[180]	382	[183]
108	[179]	229	[179]	285	[180]	333	[180]	383	[183]
111	[107]	233	[89]	286	[180]	334	[180]	384	[183]
112	[179]	236	[89]	287	[180]	335	[180]	385	[183]

Reaction	Ref.	Reaction	Ref.	Reaction	Ref.	Reaction	Ref.	Reaction	Ref.
113	[89]	237	[36]	288	[180]	336	[180]	386	[183]
122	[92]	238	[185]	289	[180]	337	[180]	387	[183]
123	[11]	239	[36]	290	[180]	338	[180]	388	[186]
128	[92]	240	[36]	291	[180]	339	[180]	389	[187]
130	[11]	241	[36]	292	[180]	340	[180]	390	[188]
142	[131]	242	[36]	293	[180]	341	[180]	391	[187]
146	[11]	243	[36]	294	[180]	342	[180]	392	[187]
147	[89]	244	[36]	295	[180]	343	[180]	393	[11]
157	[89]	245	[36]	296	[180]	344	[180]	396	[187]
168	[11]	246	[36]	297	[180]	345	[180]	397	[183]
177	[189]	247	[36]	298	[180]	346	[180]	398	[183]
178	[89]	248	[179]	299	[180]	347	[89]	399	[187]
179	[190]	249	[179]	300	[180]	348	[179]	400	[187]
180	[190]	250	[179]	301	[180]	349	[179]	401	[187]
181	[190]	251	[179]	302	[180]	350	[179]	402	[187]
182	[89]	252	[179]	303	[180]	351	[179]	403	[187]
183	[178]	255	[11]	304	[180]	352	[179]	404	[187]
184	[178]	256	[11]	305	[180]	353	[179]	405	[187]
185	[191]	257	[11]	306	[180]	354	[179]	406	[187]
186	[191]	258	[11]	307	[180]	355	[179]	407	[187]
188	[178]	259	[11]	308	[180]	356	[179]	408	[187]
189	[192]	260	[11]	309	[180]	357	[179]	409	[187]
190	[193]	261	[179]	310	[180]	358	[179]	410	[187]
191	[109]	262	[179]	311	[180]	359	[179]	411	[187]
192	[193]	263	[179]	312	[180]	360	[179]	412	[187]
193	[194]	264	[179]	313	[180]	361	[179]		
194	[194]	265	[179]	314	[180]	362	[179]		
201	[178]	266	[179]	315	[180]	363	[179]		
205	[178]	267	[179]	316	[180]	364	[179]		

Table A.2: Non-CODATA references table.

Bibliography

[1] Kuo Kenneth K. *Principles of Combustion.* John Wiley & Sons, Inc., Hoboken, New Jersey, 2nd Edition, 2005.

[2] D.L. Baulch, C.T. Bowman, C.J. Cobos, R.A. Cox, Th. Just, J.A. Kerr, M.J. Pilling, D. Stocker, J. Troe, W. Tsang, R.W. Walker, J. Warnatz. *Evaluated Kinetic Data for Combustion Modelling: Supplement II.* J. Phys. Chem. Ref. Data **34**, 2005.

[3] C. Heghes, V. Karbach, J. Warnatz. *Evaluation of New Data for Hydrocarbon Kinetics.* Proc. of Europ. Combust. Meeting, 176, Louvain-la-Neuve, Belgium. 2005.

[4] J. Warnatz, C. Heghes. *Combustion Chemistry, Ed. Gardiner, W. C., Jr.*, Chapter Survey of the C/H/O Reactions. To be published. Springer-Verlag, New York, 2006.

[5] D.A. McQuarrie, J.D. Simon. *Physical Chemistry: A Molecular Approach.* University Science Books, Sausalito, California, 1997.

[6] F.A. Lindemann. *Discussion on The Radiation Theory of Chemical Action.* Trans. Faraday Soc. **17**, 598 1922.

[7] P.J. Robinson, K.A. Holbrook. *Unimolecular Reactions.* Wiley-Interscience, New York, 1972.

[8] P.W. Atkins. *Physical Chemistry.* Freeman, New York, 5th Edition, 1996.

[9] D.M. Golden. *Gas Phase Homogeneous Kinetics. In: Low-Temperature Chemistry of the Atmosphere.* Moortgat GK ed., Springer-Verlag, Berlin/Heidelberg, 1994.

[10] J. Warnatz. *The Mechanism of High Temperature Combustion of Propane and Butane.* Combust. Sci. Technol. **34**, 177 1983.

[11] J. Warnatz. *Combustion Chemistry*, Chapter Rate Coefficients in the C/H/O System., 197. Springer-Verlag, New York, 1984.

[12] J. Warnatz, U. Maas, R.W. Dibble. *Combustion, Physical and Chemical fundamentals, Modeling and Simulation, Experiments, Pollutant Formation.* Springer-Verlag, Berlin Heidelberg, New York, 2nd Edition, 1999.

[13] J. Warnatz, U. Maas, R.W. Dibble. *Combustion, Physical and Chemical fundamentals, Modeling and Simulation, Experiments, Pollutant Formation.* Springer-Verlag, Berlin Heidelberg, New York, 4th Edition, 2006.

[14] D.L. Baulch, C.J. Cobos, R.A. Cox, C. Esser, P. Frank, Th. Just, J.A. Kerr, M.J. Pilling, J. Troe, R.W. Walker, J. Warnatz. *Evaluated Kinetic Data for Combustion Modelling.* J. Phys. Chem. Ref. Data **21**(3), 411 1992.

[15] J. Troe. *Predictive Possibilities of Unimolecular Rate Theory.* J. Phys. Chem. **83**, 114 1979.

[16] J. Troe. *Theory of Thermal Unimolecular Reactions in the Fall-off Range. I.Strong Collision Rate Constants.* Ber. Bunsenges. Phys. Chem. **87**, 161 1983.

[17] R.G. Gilbert, K. Luther, J. Troe. *Theory of Thermal Unimolecular Reactions in the Fall-off Range. II. Weak Collision Rate Constants.* Ber. Bunsenges. Phys. Chem. **87**, 169 1983.

[18] D.R. Stull, H. Prophet. *JANAF Thermochemical Tables.* Department of Commerce, Washington DC Technical Report, 1971.

[19] R.J. Kee, F.M. Rupley, J.A. Miller. *Chemkin Thermodynamic Data Base.* Sandia Report 87-82153. UC-4, Sandia National Laboratories, Livermore CA Technical Report, 1987.

[20] A. Burcat. *Combustion Chemistry.*, Chapter Thermochemical Data for Combustion. Springer-Verlag, New York, 1984.

[21] P.W. Atkins. *Physical Chemistry.* Oxford University Press, New York, 7th Edition, 2002.

[22] M.J. Pilling, P.W. Seakins. *Reaction Kinetics.* Oxford University Press, 1995.

[23] M.A. Kramer, R.J. Kee, H. Rabitz. *CHEMSEN: A Computer Code for Sensitivity Analysis of Elementary Reaction Models.* Sandia Report SAND82-8230, Sandia National Laboratories, Livermore CA Technical Report, 1982.

[24] A.E. Lutz, R.J. Kee, J.A. Miller. *A FORTRAN Program to Predict Homogeneous Gas-Phase Chemical Kinetics Including Sensitivity Analysis.* Sandia Report SAND87-8248, Sandia National Laboratories, Livermore CA Technical Report, 1987.

[25] U. Nowak, J. Warnatz. *Sensitivity Analysis in Aliphatic Hydrocarbon Combustion.* Dynamics of Reactive Systems, Band 1, 87. AIAA, 1988.

[26] J. Warnatz. *Modelling of Chemical Reaction Systems.*, Chapter Chemistry of Stationary and Instationary Combustion Processes, 162. Springer, Heidelberg, 1981.

[27] K.A. Bhaskaran, P. Roth. *The Shock Tube as Wave Reactor for Kinetic Studies and Material Systems.* Prog. En. Combust. Sci. **28**, 151 2002.

[28] L.J. Spadaccini, M.B. Colket. *Ignition Delay Characteristics of Methane Fuels.* Prog. En. Combust. Sci. **20**, 431 1994.

[29] J. Warnatz. 18th Symp. (Int.) on Combust., 369 1981.

[30] H. Bockhorn, C. Chevalier, J. Warnatz, V. Weyrauch. *Bildung von Promptem NO in Kohlenwasserstoff-Luft-Flammen.* Number 6, TECFLAM, DLR Stuttgart. 1990.

[31] J. Warnatz. *Structure of Laminar Alkane, Alkene, and Acetylene Flames.* 18th Symp. (Int.) Combust., 369, 1981.

[32] J. Warnatz, H. Bockhorn, A. Moser, H.W. Wenz. *Experimental Investigations and Computational Simulation of Acetylene-Oxygen Flames from near Stoichiometric to Sooting Conditions.* 19th Symp. (Int.) on Combust., 197. The Combustion Institute, 1982.

[33] J. Warnatz. *Chemistry of High Temperature Combustion of Alkanes up to Octane.* 20th Symp. (Int.) on Combust., 845. The Combustion Institute, 1985.

[34] C.K. Westbrook, F.L. Dryer. *Prediction of Laminar Flame Properties of Methanol-Air Mixtures.* Combust. Flame **37**, 171 1980.

[35] C.K. Westbrook, F.L. Dryer. *Simplified Reaction Mechanisms for the Oxidation of Hydrocarbon Fuels in Flames.* Combust. Sci. Techn. **27**, 31 1981.

[36] C.K. Westbrook, F.L. Dryer. *Chemical Kinetic Modeling of Hydrocarbon Combustion.* Prog. En. Combust. Sci. **10**, 1 1984.

[37] M.D. Smooke, J.A. Miller, R.J. Kee. *Determination of Adiabatic Flame Speeds by Boundary Value Methods.* Comb. Sci. Technol. **34**, 79 1983.

[38] J.A. Miller, M.D. Smooke, R.M. Green, R.J. Kee. *Kinetic Modeling of the Oxidation of Ammonia in Flames.* Comb. Sci. Technol. **34**, 149 1983.

[39] J.A. Miller, R.E. Mitchell, M.D. Smooke, R.J. Kee. *Toward a Comprehensive Chemical Kinetic Mechanism for the Oxidation of Acetylene: Comparison of Model Predictions with Results from Flame and Shock Tube Experiments.* 19th Symp. (Int.) on Combust., 181. The Combustion Institute, 1982.

[40] G. Dixon-Lewis. *Flame Structure and Flame Reaction Kinetics. I. Solution of Conservation Equations and Application to Rich Hydrogen-Oxygen Flames.* Proc. Royal Soc. London **A298**, 495 1967.

[41] G. Dixon-Lewis. *Kinetic Mechanism, Structure and Properties of Premixed Flames in Hydrogen-Oxygen-Nitrogen Mixtures.* Philos. Trans. R. Soc. London **A292**, 45 1979.

[42] T.P. Coffee, A.J. Kotlar, M.S. Miller. *The Overall Reaction Concept in Premixed, Laminar, Steady-State Flames. I. Stoichiometries.* Combust. Flame **54**, 155 1983.

[43] T.P. Coffee. *Kinetic Mechanisms for Premixed, Laminar, Steady-State Methane/Air Flames.* Combust. Flame **55**, 161 1984.

[44] T.P. Coffee, A.J. Kotlar, M.S. Miller. *The Overall Reaction Concept in Premixed, Laminar, Steady-State Flames. II. Initial Temperatures and Pressures.* Combust. Flame **58**, 59 1984.

[45] J. Warnatz. *Calculation of the Structure of Laminar Flat Flames I: Flame Velocity of Freely Propagating Ozone Decomposition Flames.* Ber. Bunsenges. Phys. Chem. **82**, 193 1978.

[46] J. Warnatz. *Calculation of the Structure of Laminar Flat Flames II: Flame Velocity and Structure of Freely Propagating Hydrogen-Oxygen and Hydrogen-Air-Flames.* Ber. Bunsenges. Phys. Chem. **82**, 643 1978.

[47] J. Warnatz. *Calculation of the Structure of Laminar Flat Flames III: Structure of Burner-Stabilized Hydrogen-Oxygen and Hydrogen-Fluorine-Flames.* Ber. Bunsenges. Phys. Chem. **82**, 834 1978.

[48] R. Aglave. *CFD Simulations using Automatically Reduced Reaction Mechanisms.* Ph.d thesis, Universität Heidelberg, 2006.

[49] V. Karbach. *Entwicklung detaillierter Reaktionsmechanismen zur Modellierung der Verbrennungsprozesse aliphatischer und aromatischer Kohlenwasserstoffe.* Dissertation, Universität Heidelberg, 2006.

[50] J. Troe. *Theory of Thermal Unimolecular Reactions at Low Pressures. II. Strong Collision Rate Constants. Applications of the Master Equation.* J. Chem. Phys. **66**, 4758 1977.

[51] V.V. Lissianski, V.M. Zamansky, Jr. Gardiner, W.C. *Gas-Phase Combustion Chemistry.*, Chapter Combustion Chemistry Modeling. Springer-Verlag, Ed. Gardiner, W.C.,Jr., New York, 2000.

[52] S.W. Benson. *Thermochemical Kinetics.* Wiley, New York Technical Report, 1976.

[53] C. Vinckier, M. Schaekers, J. Peeters. *The Ketyl Radical in the Oxidation of Ethyne by Atomic Oxygen at* 300-600 *K.* J. Phys. Chem. **89**, 508 1985.

[54] P. Frank, K.A. Bhaskaran, Th. Just. *Acetylene Oxidation: the Reaction* $C_2H_2 + O$ *at High Temperatures.* 21st Symp. (Int.) Combust., 885, 1986.

[55] D.R. Lander, K.G. Unfried, G.P. Glass, R.F. Curl. *Rate Constant Measurements of* C_2H *with* CH_4, C_2H_6, C_2H_4, D_2, *and CO.* J. Phys. Chem. **94**, 7759 1990.

[56] B.J. Opansky, P.W. Seakins, J.O.P. Pedersen, S.R. Leone. *Kinetics of the Reaction* $C_2H + O_2$ *from* 193 *to* 350 *K using Laser Flash Kinetic Infrared Absorption Spectroscopy.* J. Phys. Chem. **97**, 8583 1993.

[57] H. Van Look, J. Peeters. *Rate Coefficients of the Reactions of* C_2H *with* O_2, C_2H_2, *and* H_2O *between* 295 *and* 450 *K.* J. Phys. Chem. **99**, 16284 1995.

[58] H. Thiesemann, C.A. Taatjes. *Temperature Dependence of the Reaction* C_2H *(*C_2D*)* $+ O_2$ *between* 295 *and* 700 *K.* Chem. Phys. Lett. **270**, 580 1997.

[59] D. Chastaing, P.L. James, I.R. Sims, I.W.M. Smith. *Neutral-Neutral Reactions at the Temperatures of Interstellar Clouds Rate Coefficients for Reactions of* C_2H *Radicals with* O_2, C_2H_2, C_2H_4 *and* C_3H_6 *down to* 15 *K.* Faraday Discuss. **109**, 165 1998.

[60] A.B. Vakhtin, D.E. Heard, I.W.M. Smith, S.R. Leone. *Kinetics of Reactions of* C_2H *Radical with Acetylene,* O_2*, Methylacetylene, and Allene in a Pulsed Laval Nozzle Apparatus at* $T = 103\,K$. Chem. Phys. Lett. **344**, 317 2001.

[61] C.A. Arrington, W. Brennen, G.P. Glass, H. Niki. *Reactions of Atomic Oxygen with Acetylene. I. Kinetics and Mechanisms.* J. Chem. Phys. **43**, 525 1965.

[62] J.O. Sullivan, P. Warneck. *Rate Constant for the Reaction of Oxygen Atoms with Acetylene.* J. Phys. Chem. **69**, 1749 1965.

[63] J.M. Brown, B.A. Thrush. *E.S.R. Studies of the Reactions of Atomic Oxygen and Hydrogen with Simple Hydrocarbons.* Trans. Faraday Soc. **63**, 630 1967.

[64] A.A. Westenberg, N. deHaas. *A Flash Photolysis-Resonance Fluorescence Study of the* $O + C_2H_2$ *and* $O + C_2H_3Cl$ *Reactions.* J. Chem. Phys. **66**, 4900 1977.

[65] F. Stuhl, H. Niki. *Determination of Rate Constants for Reactions of O Atoms with* C_2H_2, C_2D_2, C_2H_4, *and* C_3H_6 *using a Pulsed Vacuum-UV Photolysis-Chemiluminescent Method.* J. Chem. Phys. **55**, 3954 1971.

[66] C.P. Fenimore, G.P. Jones. *Destruction of Acetylene in Flames with Oxygen.* J. Chem. Phys. **39**, 1514 1963.

[67] D. Saunders, J. Heicklen. *Some Reactions of Oxygen Atoms. I. C_2F_4, C_3F_6, C_2H_2, C_2H_4, C_3H_6, 1-C_4H_8, C_2H_6, c-C_3H_6, and C_3H_8.* J. Phys. Chem. **70**, 1950 1966.

[68] K. Hoyermann, H.Gg. Wagner, J. Wolfrum. *Reactions of Acetylene with Hydrogen and Oxygen Atoms by Electron Spin Resonance.* Z. Phys. Chem. (Neue Folge) **55**, 72 1967.

[69] J.N. Bradley, R.S. Tse. *Electron Spin Resonance Study of the Reaction between Oxygen Atoms and Acetylene.* Trans. Faraday Soc. **65**, 2685 1969.

[70] I.T.N. Jones, K.D. Bayes. *Kinetics and Mechanism of the Reaction of Atomic Oxygen with Acetylene.* Proc. Royal Soc. London **A 335**, 547 1973.

[71] J. Peeters, G. Mahnen. *Structure of Ethylene-Oxygen Flames. Reaction Mechanism and Rate Constants of Elementary Reactions.* Proc. Combust. Inst. European Symp., 53 1973.

[72] J. Vandooren, P.J. Van Tiggelen. *Reaction mechanisms of Combustion in Low Pressure Acetylene-Oxygen Flames.* 16th Symp. (Int.) Combust., 1133, 1977.

[73] J.A. Miller, C.F. Melius. *A Theoretical Analysis of the Reaction between Hydroxyl and Acetylene.* 22nd Symp. (Int.) Combust., 1031, 1988.

[74] N.M. Marinov, P.C. Malte. *Ethylene Oxidation in a Well-Stirred Reactor.* Int. J. Chem. Kinet. **27**, 957 1995.

[75] Y. Hidaka, T. Nishimori, K. Sato, Y. Henmi, R. Okuda, K. Inami. *Shock-Tube and Modeling Study of Ethylene Pyrolysis and Oxidation.* Combust. Flame **117**, 755 1999.

[76] J.W. Bozzelli, A.N. Dean. *Hydrocarbon Radical Reactions with O_2: Comparison of Allyl, Formyl, and Vinyl to Ethyl.* J. Phys. Chem. **97**, 4427 1993.

[77] A.M. Mebel, E.W.G. Diau, M.C. Lin, K. Morokuma. *Ab Initio and RRKM Calculations for Multichannel Rate Constants of the C_2H_3 + O_2 Reaction.* J. Amer. Chem. Soc. **118**, 9759 1996.

[78] V.D. Knyazev, I.R. Slagle. *Experimental and Theoretical Study of the $C_2H_3 \rightleftharpoons H + C_2H_2$ Reaction. Tunneling and the Shape of Fall-off Curves.* J. Phys. Chem. **100**, 16899 1996.

[79] W.A. Payne, L.J. Stief. *Absolute Rate Constant for the Reaction of Atomic Hydrogen with Acetylene over an Extended Pressure and Temperature Range.* J. Chem. Phys. **64**, 1150 1976.

[80] D.G. Keil, K.P. Lynch, J.A. Cowfer, J.V. Michael. *An Investigation of Nonequilibrium Kinetic Isotope Effects in Chemically Activated Vinyl Radicals.* Int. J. Chem. Kinet. **8**, 825 1976.

[81] R. Ellul, P. Potzinger, R. Reimann, P. Camilleri. *Arrhenius Parameters for the System* $(CH_3)3Si + D_2 \rightleftharpoons (CH_3)3SiD + D$. *The* $(CH_3)3Si - D$ *bond dissociation energy.* Ber. Bunsenges. Phys. Chem. **85**, 407 1981.

[82] E.B. Gordon, A.P. Perminov, B.I. Ivanov, V.I. Matyushenko, A.N. Ponomarev, V.L. Tal'roze. *Variation of the Hyperfine State of the Hydrogen Atom in Collisions with Unsaturated Hydrocarbon Molecules in the Gaseous Phase.* Sov. Phys. JETP **36**, 212 1973.

[83] E.B. Gordon, B.I. Ivanov, A.P. Perminov, V.E. Balalaev. *A Measurement of Formation Rates and Lifetimes of Intermediate Complexes in Reversible Chemical Reactions involving Hydrogen Atoms.* Chem. Phys. **35**, 79 1978.

[84] P. Roth, Th. Just. *Measurement of the Homogeneous Thermal Decomposition of Ethylene.* Ber. Bunsenges. Phys. Chem. **77**, 1114 1973.

[85] T. Just, P. Roth, R. Damm. *Production of Hydrogen Atoms during the Thermal Dissociation of Ethylene between* 1700 *and* $2200 DegK$. 16th Symp. (Int.) Combust., 961, 1977.

[86] T. Tanzawa, Jr. Gardiner, W.C. *Thermal Decomposition of Ethylene.* Combust. Flame **39**, 241 1980.

[87] L.S. Zelson, D.F. Davidson, R.K. Hanson. *Vacuum Ultraviolet Absorption Diagnostic for Shock Tube Kinetics Studies of* C_2H_4. J. Quant. Spectros. Radiat. Transfer **52**, 31 1994.

[88] H. Hippler, B. Viskolcz. *Addition Complex Formation vs. Direct Abstraction in the* $OH + C_2H_4$ *Reaction.* Phys. Chem. Chem. Phys. **2**, 3591 2000.

[89] D.L. Baulch, C.J. Cobos, R.A. Cox, P. Frank, G. Haymann, Th. Just, J.A. Kerr, T. Murells, M.J. Pilling, J. Troe, R.W. Walker, J. Warnatz. *Evaluated Kinetic Data for Combustion Modelling: Supplement I.* J. Phys. Chem. Ref. Data **23**(6), 847 1994.

[90] I.R. Slagle, Q. Feng, D. Gutman. *Kinetics of the Reaction of Ethyl Radicals with Molecular Oxygen from* 294 *to* 1002 *K.* J. Phys. Chem. **88**, 3648 1984.

[91] A.F. Wagner, I.R. Slagle, D. Sarzynski, D. Gutman. *Experimental and Theoretical Studies of the* $C_2H_5 + O_2$ *Reaction Kinetics.* J. Phys. Chem. **94**, 1853 1990.

[92] J.A. Miller, R.E. Mitchell, M.D. Smooke, R.J. Kee. *Toward a Comprehensive Chemical Kinetic Mechanism for the Oxidation of Acetylene: Comparison of Model Predictions with Results from Flame and Shock Tube Experiments.* 19th Symp. (Int.) on Combust., 181, Pittsburgh. The Combustion Institute, 1982.

[93] L.F. Loucks, K. Laidler. *Thermal Decomposition of the Ethyl Radical.* Can. J. Chem. **45**, 2795 1967.

[94] P.D. Pacey, J.H. Wimalasena. *An Induction Period in the Pyrolysis of Ethane. Determination of Individual Rate Constants for Ethyl Radical Reactions.* Chem. Phys. Lett. **76**, 433 1980.

[95] P.D. Pacey, J.H. Wimalasena. *Relative Rates of Radical-Radical Processes in the Pyrolysis of Ethane.* Can. J. Chem. **62**, 293 1984.

[96] P.D. Pacey, J.H. Wimalasena. *Kinetics and Thermochemistry of the Ethyl Radical. The Induction Period in the Pyrolysis of Ethane.* J. Phys. Chem. **88**, 5657 1984.

[97] Y. Simon, J.F. Foucaut, G. Scacchi. *Experimental Study and Theoretical Model of the Decomposition of the Ethyl Radical.* Can. J. Chem. **66**, 2142 1988.

[98] Y. Feng, J.T. Niiranen, A. Bencsura, V.D. Knyazev, D. Gutman, W. Tsang. *Weak Collision Effects in the Reaction* $C_2H_5 \rightleftharpoons C_2H_4 + H$. J. Phys. Chem. **97**, 871 1993.

[99] U. Meier, H.H. Grotheer, G. Riekert, Th. Just. *Study of Hydroxyl Reactions with Methanol and Ethanol by Laser-Induced Fluorescence.* Ber. Bunsenges. Phys. Chem. **89**, 325 1985.

[100] U. Meier, H.H. Grotheer, G. Riekert, Th. Just. *Reactions in a Non-Uniform Flow Tube Temperature Profile: Effect on the Rate Coefficient for the Reaction* $C_2H_5OH + OH$. Chem. Phys. Lett. **133**, 162 1987.

[101] W.P. Hess, F.P. Tully. *Catalytic Conversion of Alcohols to Alkenes by OH.* Chem. Phys. Lett. **152**, 183 1988.

[102] U. Mass. *Mathematische Modellierung instationärer Verbrennungsprozesse unter Verwendung detaillierter Reaktionsmechanismen.* Dissertation, Universität Heidelberg, 1988.

[103] U. Mass, J. Warnatz. *Ignition Processes in Hydrogen-Oxygen Mixtures.* Combust. Flame **74**, 53 1988.

[104] G. Dixon-Lewis, D.J. Williams. *Comprehensive Chemical Kinetics.*, Band 17. Bamford, C.H. and Tipper, C.F.H., Ed Elsevier, Amsterdam, 1977.

[105] G. Dixon-Lewis. *Mechanism of Inhibition of Hydrogen-Air Flames by Hydrogen Bromide and its Relevance to the General Problem of Flame Inhibition.* Combust. Flame **36**, 1 1979.

[106] P. Glarborg, J.A. Miller, R.J. Kee. *Kinetic Modeling and Sensitivity Analysis of Nitrogen Oxide Formation in Well-Stirred Reactors.* Combust. Flame **65**, 177 1986.

[107] W. Tsang, R.F. Hampson. *Chemical Kinetic Data Base for Combustion Chemistry. Part I. Methane and Related Compounds.* J. Phys. Chem. Ref. Data **15**(3), 1087 1986.

[108] M. Frenklach, J. Warnatz. *Detailed Modeling of PAH Profiles in a Sooting Low-Pressure Acetylene Flame.* Combust. Sci. Technol. **51**, 265 1987.

[109] M. A. Mallard, F. Westley, J.T. Herron, R.F. Hampson, D.H. Frizzel. *NIST Chemical Kinetic Database: Version 6.0.* National Institute of Standards and Technology, Gaithersburg, MD, 1994.

[110] K.M. Pamidimukkala, G.B. Skinner. *Resonance Absorption Measurements of Atom Concentrations in Reacting Gas Mixtures. IX - Measurements of O Atoms in Oxidation of H_2 and D_2.* 13th Symp. (Int.) Shock Tubes and Waves, 585, 1982.

[111] J. Vandooren, F. Nelson da Cruz, P.J. Van Tiggelen. *The Inhibiting Effect of Trifluoromethane on the Structure of a Stoichiometric Hydrogen/Carbon Monoxide/Oxygen/Argon Flame.* 22nd Symp. (Int.) Combust., 1587, 1988.

[112] A.N. Pirraglia, J.V. Michael, J.W. Sutherland, R.B. Klemm. *A Flash Photolysis-Shock Tube Kinetic Study of the H Atom Reaction with O_2: $H + O_2 \rightleftharpoons OH + O$ ($962\ K \leq T \leq 1705\ K$) and $H + O_2 + Ar \rightarrow HO_2 + Ar$ ($746\ K \leq T \leq 987\ K$).* J. Phys. Chem. **93**, 282 1989.

[113] D.A. Masten, R.K. Hanson, C.T. Bowman. *Shock Tube Study of the Reaction $H + O_2 \rightarrow OH + O$ Using OH Laser Absorption,.* J. Phys. Chem. **94**, 7119 1990.

[114] T. Yuan, C. Wang, C.L. Yu, M. Frenklach, M.J. Rabinowitz. *Determination of the Rate Coefficient for the Reaction $H + O_2 \rightarrow OH + O$ by a Shock Tube/Laser Absorption/Detailed Modeling Study.* J. Phys. Chem. **95**, 1258 1991.

[115] K.S. Shin, J.V. Michael. *Rate Constants for the Reactions $H + O_2 \rightarrow OH + O$ and $D + O_2 \rightarrow OD + O$ Over the Temperature Range* 1085-2278 *K by the Laser Photolysis-Shock Tube Technique.* J. Phys. Chem. **95**, 262 1991.

[116] H. Du, J.P. Hessler. *Rate Coefficient for the Reaction $H + O_2 \rightarrow OH + O$: Results at High Temperatures,* 2000 *to* 5300 *K.* J. Chem. Phys. **96**, 1077 1992.

[117] C.-L. Yu, M. Frenklach, D.A. Masten, R.K. Hanson, C.T. Bowman. *Reexamination of Shock-Tube Measurements of the Rate Coefficient of $H+O_2 \rightarrow OH+O$.* J. Phys. Chem. **98**, 4770 1994.

[118] H. Yang, W.C. Gardiner, K.S. Shin, N. Fujii. *Shock Tube Study of the Rate Coefficient of $H+O_2 \rightarrow OH+O$.* Chem. Phys. Lett. **231**, 449 1994.

[119] S.-O. Ryu, S.M. Hwang, M.J. Rabinowitz. *Shock Tube and Modeling Study of the $H+0_2 = OH+0$ Reaction over a Wide Range of Composition, Pressure, and Temperature.* J. Phys. Chem. **99**, 13984 1995.

[120] G.B. Skinner, G.H. Ringrose. *Ignition Delays of a Hydrogen-Oxygen-Argon Mixture at Relatively Low Temperatures.* J. Chem. Phys. **42**, 2190 1965.

[121] J. Warnatz. *Calculation of the Structure of Laminar Flat Flames. II. Flame Velocity and Structure of Freely Propagating Hydrogen-Oxygen and Hydrogen-Air-Flames.* Ber. Bunsenges. Phys. Chem. **82**, 643 1978.

[122] J. Warnatz. *Resolution of Gas Phase and Surface Chemistry into Elementary Reaction.* 24th Symp. (Int.) Combust., 553, Pittsburgh. The Combustion Institute, 1993.

[123] J. Warnatz. *Structure of freely propagating and burner-stabilized flames in the H_2-CO-O_2 system.* Ber. Bunsenges. Phys. Chem. **83**, 950 1979.

[124] I.C. McLean, D.B. Smith, Taylor S.C. *The Use of Carbon Monoxide/Hydrogen Burning Velocities to Examine the Rate of the $CO+OH$ Reaction.* 25th Symp. (Int.) Combust., Band 25, 749. The Combustion Institute, 1994.

[125] T.G. Scholte, P.B. Vaags. *The Burning Velocity of Hydrogen-Air Mixtures and Mixtures of some Hydrocarbons with Air.* Combust. Flame **3**, 495 1959.

[126] A. Lifshitz, K. Scheller, A. Burcat, G.B. Skinner. *Shock-tube Investigation of Ignition in Methane-Oxygen-Argon Mixtures.* Combust. Flame **16**, 311 1971.

[127] R.W. Crossley, E.A. Dorko, K. Scheller, A. Burcat. **Effect of Higher Alkanes on the Ignition of Methane-Oxygen-Argon Mixtures in Shock Waves.* Combust. Flame **19**, 373 1972.

[128] D.B. Olson, Jr. Gardiner, W.C. *An Evaluation of Methane Combustion Mechanisms.* J. Phys. Chem. **81**, 2514 1977.

[129] C.T. Westbrook. *Analytical Study of the Shock Tube Ignition of Mixtures of Methane and Ethane.* Comb. Sci. Technol. **20**, 5 1979.

[130] A.A. Borisov, E.V. Dragalova, V.V. Lisyanskii, G.I. Skachkov, V.M. Zamanskii. *Kinetics and Mechanism of Methane Oxidation at High Temperatures.* Oxid. Commun. **4**, 45 1983.

[131] J.A. Miller, C.T. Bowman. *Mechanism and Modeling of Nitrogen Chemistry in Combustion.* Prog. En. Combust. Sci., Band 15, 287, 1989.

[132] T.M. Sloane. *Ignition and Flame Propagation Modeling with an Improved Methane Oxidation Mechanism.* Comb. Sci. Technol. **63**, 287 1989.

[133] C. Chevalier, W.J. Pitz, J. Warnatz, C.K. Westbrook, H. Melenk. *Hydrocarbon Ignition: Automatic Generation of Reaction Mechanisms and Applications to Modeling of Engine Knock.* 24th Symp. (Int.) on Combust., 93, 1992.

[134] C. Corre, F.L. Dryer, W.J. Pitz, C.K. Westbrook. *Two-Stage n-Butane Flame: a Comparison between Experimental Measurements and Modeling Results.* 24th Symp. (Int.) on Combust., 843, 1992.

[135] M. Frenklach, H. Wang, M.J. Rabinowitz. *Optimization and Analysis of Large Chemical Kinetic Mechanisms using the Solution Mapping Method - Combustion of Methane.* Prog. En. Combust. Sci. **18**, 47 1992.

[136] M. Frenklach, H. Wang, M. Goldenberg, G.P. Smith, D.M. Golden, C.T. Bowman, R.K. Hanson, Jr. Gardiner, W.C., V.V. Lissianski. *GRI-Mech- An Optimized Detailed Chemical Reaction Mechanism for Methane Combustion.* Gas Research Institute Topical Report GRI-95/0058 Technical Report, 1995.

[137] A.A. Konnov. *Detailed Reaction Mechanism for C_1-C_2 Hydrocarbon Combustion.* 26th Symp. (Int.) on Combust., 286, 1996.

[138] M.J̃. Pilling, T. Turanyi, K.J̃. Hughes, A.R̃. Clague. *The Leeds Methane Oxidation Mechanism.* http://chem.leeds.ac.uk/ Combustion/Combustion.html., 1996.

[139] K.J. Bosschaart. *Analysis of the Heat Flux Method for Measuring Burning Velocities.* Eindhoven University Press, Technische Universiteit Eindhoven, 2002.

[140] K.J. Bosschaart, L.P.H. de Goey. *The Laminar Burning Velocity of Flames Propagating in Mixtures of Hydrocarbons and Air Measured with the Heat Flux Method.* Combust. Flame **136**, 261 2004.

[141] G. Rozenchan, D.L. Zhu, Law C.K., S.D. Tse. *Outward Propagation, Burning Velocities, and Chemical Effects of Methane Flames up to* 60 *atm.* Proc. Combust. Inst., Band 29, 1461, 2002.

[142] C.M. Vagelopoulos, F.N. Egolfopoulos, Law C.K. *Further Considerations on the Determination of Laminar Flame Speeds with the Counterflow Twin-Flame Technique.* Proc. Combust. Inst., Band 25, 1341, 1994.

[143] C.M. Vagelopoulos, F.N. Egolfopoulos. *Direct Experimental Determination of Laminar Flame Speeds.* Proc. Combust. Inst., Band 27, 513, 1998.

[144] D.F. Cooke, M.G. Dondson, A. Williams. *A Shock Tube Study of the Ignition of Methanol and Ethanol with Oxygen.* Combust. Flame **16**, 233 1971.

[145] T.A. Brabbs, R.S. Brokaw. *Shock Tube Measurements of Specific Reaction Rates in the Branched Chain Methane-Carbon Monoxide-Oxygen System.* 15th Symp. (Int.) on Combust., 893, 1975.

[146] K.A. Bhaskaran, P. Frank, Th. Just. *High-Temperature Methyl Radical Reactions with Atomic and Molecular Oxygen.* Proc. 12th Symp. (Int.) on Shock Tubes and Waves, 503, Jerusalem. The Magnes Press, 1980.

[147] D.S.Y. Hsu, W.M. Shaub, T. Creamer, D. Gutman, M.C. Lin. *Kinetic Modeling of CO Production from the Reaction of CH_3 with O_2 in Shock Waves.* Ber. Bunsenges. Phys. Chem. **87**, 909 1983.

[148] K. Saito, R. Ito, T. Kakumoto, A. Imamura. *The Initial Process of the Oxidation of the Methyl Radical in Reflected Shock Waves.* J. Phys. Chem. **90**, 1422 1986.

[149] T.C. Clark, T.P.J. Izod, S. Matsuda. *Oxidation of Methyl Radicals Studied in Reflected Shock Waves using the Time-of-Flight Mass Spectrometer.* J. Chem. Phys. **55**, 4644 1971.

[150] C.J. Jachimowski. *Kinetics of Oxygen Atom Formation during the Oxidation of Methane behind Shock Waves.* Combust. Flame **23**, 233 1974.

[151] C.T. Bowman. *Non-Equilibrium Radical Concentrations in Shock-Initiated Methane Oxidation.* 15th Symp. (Int.) on Combust., 869, 1975.

[152] D.B. Olson, W.C. Gardiner. *Combustion of Methane in Fuel-Rich Mixtures.* Combust. Flame **32**, 151 1978.

[153] K. Tabayashi, S.H. Bauer. *The Early Stages of Pyrolysis and Oxidation of Methane.* Combust. Flame **34**, 63 1979.

[154] R. Zellner, F. Ewig. *Computational Study of the Methyl + Oxygen Chain Branching Reaction.* J. Phys. Chem. **92**, 2971 1988.

[155] W. Fraatz. *Untersuchung der Reaktion $CH_3 + O_2 \rightarrow$ Produkte in Stosswellen mit Hilfe der UV-Absorption.* Dissertation, Universität Göttingen, 1990.

[156] D.M. Golden, J.T. Herbon, R.K Hanson, C.T. Bowman. *The Reaction of CH_3 + O_2: Experimental Determination of the Rate Coefficients for the Product Channels at High Temperatures.* 18th Symp. (Int.) Gas Kinetics, 53, Bristol. 2004.

[157] J.B. Homer, G.B. Kistiakowsky. *Oxidation and Pyrolysis of Ethylene in Shock Waves.* J. Chem. Phys. **47**(12), 5290 1967.

[158] J. Warnatz. *Concentration-, Pressure-, and Temperature-Dependence of the Flame Velocity in Hydrogen-Oxygen-Nitrogen Mixtures.* Comb. Sci. Technol. **26**, 203 1981.

[159] H. Bockhorn, F. Fetting, H.W. Wenz. *Investigation of the Formation of High Molecular Hydrocarbons and Soot in Premixed Hydrocarbon-Oxygen Flames.* Ber. Bunsenges. Phys. Chem. **87**, 1067 1983.

[160] M. Frenklach, D.W. Clary, Jr. Gardiner, W.C., S.E. Stein. *Detailed Kinetic Modeling of Soot Formation in Shock-Tube Pyrolysis of Acetylene.* 20th Symp. (Int.) on Combust., 887, 1985.

[161] K.C. Smyth, J.H. Miller. *Chemistry of Molecular Growth Processes in Flames.* Science **236**, 1540 1987.

[162] F.N. Egolfopoulos, D.L. Zhu, C.K. Law. *Experimental and Numerical Determination of Laminar Flame Speeds: Mixtures of C_2 Hydrocarbons with Oxygen and Nitrogen.* 23rd Symp. (Int.) Combust., 471, Pittsburg. The Combustion Institute, 1990.

[163] J.A. Baker, G.B. Skinner. *Shock Tube Studies on the Ignition of Ethylene-Oxygen-Argon Mixtures.* Combust. Flame **19**, 347 1972.

[164] E. Bartholomé. *Zur Methodik der Messung von Flammengeschwindigkeiten.* Z. Elektrochem. **53**, 191 1949.

[165] F.N. Egolfopoulos, P. Cho, C.K. Law. *Laminar Flame Speeds of Methane-Air Mixtures under Reduced and Elevated Pressures.* Combust. Flame **76**, 375 1989.

[166] G.J. Gibbs, H.F. Calcote. *Effect of Molecular Structure on Burning Velocity.* J. Chem. Eng. Data **4(3)**, 226 1959.

[167] R. Guenther, G. Janisch. *Measurements of Burning Velocity in a Flat Flame Front.* Combust. Flame **19**, 49 1972.

[168] S.D. Raezer, H.L. Olsen. *Measurement of Laminar Flame Speeds of Ethylene-Air and Propane-Air Mixtures by the Double Kernel Method.* Combust. Flame **6**, 227 1962.

[169] F.A. Smith, S.F. Pickering. *Measurements of Flame Velocity by a Modified Burner Method.* J. Res. Nat. Bur. Standards **17**, 7 1936.

[170] R. Lindow. *Eine Verbesserte Brennermethode zur Bestimmung der Laminaren Flammengeschwindigkeiten von Brenngas/Luft Gemischen.* Brennst. Waerme Kraft **20(1)**, 8 1968.

[171] W.A. Chupka. *Mass-Spectrometric Study of the Photoionization of Methane.* J. Chem. Phys. **48**, 2337 1968.

[172] O. Dobis, S.W. Benson. *Analysis of Flow Dynamics in a New, very Low Pressure Reactor. Application to the Reaction: $Cl + CH_4 \rightleftharpoons HCl + CH_3$.* Int. J. Chem. Kinet. **19**, 691 1987.

[173] C.W. Bauschlicher, H. Partridge. *The Vibrational Frequencies of CH_2OH.* Chem. Phys. Lett. **215**, 451 1993.

[174] K.A. Peterson, Jr. Dunning, T.H. *Benchmark Calculations with Correlated Molecular Wave Functions. VIII. Bond Energies and Equilibrium Geometries of the CH_n and C_2H_n (n=1-4) Series.* J. Chem. Phys. **106**, 4119 1997.

[175] A. Burcat, A. Lifshitz, K. Scheller, G.B. Skinner. *Shock Tube Investigation of Ignition in Propane-Oxygen-Argon Mixtures.* 13th Symp. (Int.) on Combust., 745, 1971.

[176] M. Gerstein, O. Levine, E.L. Wong. *Flame Propagation. II. The Determination of Fundamental Burning Velocities of Hydrocarbons by a Revised Tube Method.* J. Am. Chem. Soc. **73**, 418 1951.

[177] A. Burcat, A. Lifshitz, K. Scheller. *Shock Tube Investigation of Comparative Ignition Delay Times for C_1-C_5 Alkanes.* Combust. Flame **16**, 29 1971.

[178] C. Chevalier. *Entwicklung eines detaillierten Reaktionsmechanismus zur Modellierung der Verbrennungsprozesse von Kohlenwasserstoffen bei Hoch- und Niedertemperaturbedingungen.* Dissertation, Universität Stuttgart, 1993.

[179] W.J. Pitz, C.K. Westbrook, W.M. Proscia, F.L. Dryer. *A Comprehensive Chemical Kinetic Reaction Mechanism for the Oxidation of n-Butane.* 20th Symp. (Int.) on Combust., 831, Pittsburgh. The Combustion Institute, 1984.

[180] A. Chakir, M. Cathonnet, J.C. Boettner, F. Gaillard. *Kinetic Study of n-Butane Oxidation.* Combust. Sci. Technol. **65**(4-6), 207 1989.

[181] M.B. Mitchell, D.F. Nava, L.J. Stief. *Rate Constant for the Reaction of $O(3P)$ with Diacetylene from 210 to 423 K.* J. Chem. Phys. **85**, 3300 1986.

[182] R.A. Perry. *Absolute Rate Measurements for the Reaction of the OH Radicals with Diacetylene over the Temperature Range of* 296-688 *K.* Combust. Flame **58**, 221 1984.

[183] C. Esser. *Simulation der Zündung und Verbrennung höherer Kohlenwasserstoffe.* Dissertation, Universität Heidelberg, 1990.

[184] W. Tsang. *Chemical Kinetic Data Base for Combustion Chemistry. Part II, Methanol.* J. Phys. Chem. Ref. Data **16**, 471 1987.

[185] W Tsang. *Chemical Kinetic Data Base for Combustion Chemistry. Part V. Propene.* J. Phys. Chem. Ref. Data **20**(2), 221 1991.

[186] T.J. Mitchell, S.W. Benson. *Modelling of the Homogeneously Catalyzed and Uncatalyzed Pyrolysis of Neopentane: Thermochemistry of the Neopentyl Radical.* Int. J. Chem. Kinet. **25**, 931 1993.

[187] W. Tsang. *Chemical Kinetic Data Base for Combustion Chemistry. Part IV, Isobutane.* J. Phys. Chem. Ref. Data **19**, 1 1990.

[188] M. Weismann, S.W. Benson. *Pyrolysis of Methyl Chloride, a Pathway in the Chlorine-Catalyzed Polymerization of Methane.* Int. J. Chem. Kinet. **16**, 307 1984.

[189] J. Heicklen. *The Decomposition of Alkyl Nitrites and the Reactions of Alkoxyl Radicals.* Advances in Photochem. **14**, 177 1988.

[190] Y. Tan, Ph. Dagaut, M. Cathonnet, J.C. Boettner. *Acetylene Oxidation in a JSR from* 1 *to* 10 *atm and Comprehensive Kinetic Modeling.* Combust. Sci. Technol. **102**, 21 1994.

[191] H.H. Grotheer, F.L. Nesbitt, R.B. Klemm. *Absolute Rate Constant for the Reaction of O (^3P) with Ethanol.* J. Phys. Chem. **90**, 2512 1986.

[192] W.J. Pitz, C.K. Westbrook, W.M. Proscia, F.L. Dryer. *Elementary Reactions in the Oxidation of Ethylene: The Reaction of OH Radicals with Ethylene and the Reaction of C_2H_4OH Radicals with H Atoms.* 19th Symp. (Int.) on Combust., 61, Pittsburgh. The Combustion Institute, 1982.

[193] A.A. Konnov. *Detailed Reaction Mechanism for Small Hydrocarbons Combustion. Release 0.3.* http://homepages.vub.ac.be/ akonnov/, 1997.

[194] W.K. Aders, H.Gg. Wagner. *Reactions of Hydrogen Atoms with Ethanol and Tert-Butyl Alcohol.* Ber. Bunsenges. Phys. Chem. **77**(9), 712 1973.